UNIVERSITÀ DEGLI STUDI DI NAPOLI FEDERICO II

Doctorate in Biology

XXXVII CYCLE

Arf at the crossroad between cancer and differentiation

ELENA DE MARINO

Supervisor	**PhD Coordinator**
Prof. Alessandra Pollice	Prof. Sergio Esposito

INDEX

Outline of the thesis

This PhD thesis reports the results of a research project focused on studying the role of the p19Arf oncosupressor in *in vitro* pancreatic differentiation. Specifically, the project investigates if and how ARF may influence pancreatic lineage commitment during *in vitro* differentiation. The focus was initially directed toward designing a comprehensive strategy to assess the involvement of p19Arf in the homeostasis of Stem Cells and Pancreatic Progenitor Cells. Therefore, after having established a CRISPR-Cas9 based technology to target the genomic Arf sequence in mouse Embryonic Stem Cells (mESCs), the efforts were concentrated on generating a molecular construct specifically designed to target exon 1β of p19Arf and on the generation of stably ESC mutated Arf clones to analyze alterations in the differentiative process toward PPCs (Pancreatic Progenitor Cells). This analysis provided insights into the role of ARF in lineage-specific differentiation, enabling a deeper understanding of its function in the regulation of stemness and differentiation pathways. Results of the research were presented in three congresses and are the object of a manuscript in preparation.

At the end of the thesis there is an **APPENDIX** containing two publications regarding research lines in which I was involved during my three years of PhD:

1- "Identification of Cdk8 and Cdkn2d as New Prame-Target Genes in 2C-like Embryonic Stem Cells". *Lucci V, De Marino E, Tagliaferri D, Amente S, Pollice A, Calabrò V, Vivo M, Falco G, Angrisano T.*
doi: 10.3390/genes13101745. PMID: 36292630; PMCID: PMC9601988".
This research aimed to explore the role of *Prame* in regulating pluripotency in embryonic stem cells (ESCs) and brought to the identification of Cdk8 and Cdkn2d as two targets of of Prame in 2C-like Embryonic Stem Cells Genes. My contribution in the publication was mainly in the data validation: cell treatment RNA extraction and Real-time PCR analysis.

2- "Integrated Bioinformatics Analysis Reveals Novel miRNA as Biomarkers Associated with Preeclampsia" *Brancaccio M, Giachino C, Iazzetta AM, Cordone A, De Marino E, Affinito O, Vivo M, Calabrò V, Pollice A, Angrisano T. doi: 10.3390/genes13101781. PMID: 36292666; PMCID: PMC9601722".*

This research aimed at identifying key microRNAs (miRNAs) associated with preeclampsia and explore their potential biological roles, focusing on their expression in plasma and placenta. Analyzing miRNA expression profiles by bioinformatics analysis it was possible to identify nine specific miRNAs as promising candidates for non-invasive biomarkers for preeclampsia. I was mainly involved in establishing a methodology for analyzing GEO dataset data, followed by conducting a formal analysis of bioinformatic data.

Abstract

The p14/p19ARF (Alternative Reading Frame), encoded by the Cdkn2A locus, is recognized as one of the most critical tumor suppressors due to its well-established role in cancer suppression. Recent findings, however, reveal an emerging role for ARF in development, differentiation, and in the regulation of stem cell self-renewal, positioning it at the crossroads between cancer biology and cellular differentiation. Progenitor cell homeostasis is crucial not only for physiological processes, such as organ development, but also for pathological events, including cancer. Progenitor cells (PCs), which arise from the asymmetric division of stem cells within cellular niches, are particularly essential for regenerating organs and tissues with high cellular turnover, such as the pancreas. Dysregulation of PC homeostasis is central to both healthy tissue function and disease, as disruptions can contribute to tumorigenesis. Notably, the multi-step molecular progression to pancreatic cancer frequently involves the inactivation of key tumor suppressor genes, including p14/p19ARF.

This PhD project focuses on studying ARF's role in balancing progenitor cell proliferation and quiescence during *in vitro* pancreatic differentiation. Previous findings from our laboratory indicated that p19ARF levels increase at both transcriptional and protein levels during *in vitro* pancreatic differentiation, suggesting its potential involvement in this process. Therefore, to explore ARF's role in progenitor cell homeostasis, by using the CRISPR-Cas9 technology, I introduced mutations in exon 1β of p19Arf in mESCs. I obtained several clones with biallelic and mono allelic mutations confirmed by sequencing. Remarkably, p19Arf mutated clones showed impairment in the differentiation process toward PPCs with a more prolonged expression of stemness factors, thus suggesting an important role of p19Arf in the regulation of the stemness phenotype and PPCs homeostasis. These observations could help to clarify p19Arf role in differentiation processes and cancer susceptibility.

INTRODUCTION

The CDKN2A locus

The CDKN2A locus, located on human chromosome 9p21 and mouse chromosome 4, is among the most commonly mutated regions in human cancers, second only to the p53 locus. This locus encodes two distinct tumor suppressor proteins, p16Ink4a and p19Arf, which play crucial roles in inhibiting tumor development. The way in which a single genetic locus encodes two distinct proteins is unique among mammals (Quelle, et al., 1995): p16Ink4a is transcribed from three closely associated exons (named 1α, 2, and 3), while p19Arf transcripts origins from a different first exon (1β), located 13–20 kb upstream in the genome of humans, mice, and rats, and contains exon 2 (Duro, et al., 1995; Mao, et al., 1995; Stone, et al., 1995; Swafford, et al., 1997). The start codon in exon 1β is not in frame with the sequences coding for p16Ink4a in exon 2, resulting in a completely different polypeptide. In mice, this 19-kDa protein includes 65 amino acids from exon 1β and 105 amino acids produced from the alternative reading frame (Arf) of exon 2 (Quelle., et al., 1995) (Figure 1). So, the β transcript produces mouse p19Arf (169 amino acids) or human p14ARF (132 amino acids), while mice, with only moderate conservation between species. Both mouse p19Arf and human p14ARF are highly basic nuclear proteins that can trigger cell cycle arrest at G1 and G2 phases in various cell types (Quelle, et al., 1995; Stott, et al., 1998).

In particular, the p16Ink4a protein is part of the INK4 family, which inhibits the cyclin-dependent kinases CDK4 and CDK6. This inhibition prevents cyclin D-CDK4/6 from advancing the cell cycle from G1 to S phase. As a result, the retinoblastoma protein (pRB) remains active in its hypo-phosphorylated form, binding E2F transcription factors and causing cell cycle arrest in G1. Conversely, the Arf protein stabilizes p53 by blocking Mdm2, activating p53 pathways (Russo, et al., 1998; Serrano, et al., 1993; Sharpless, et al., 1999). Cells lacking Ink4a are vulnerable to Arf-induced cell cycle arrest, indicating that p19Arf activity is independent from that of p16Ink4a. First observations underlined the importance of the amino-terminal region of Arf (amino acids 1–64), that is sufficient to trigger

cell cycle arrest when overexpressed (Quelle, et al., 1997; Zhang, et al., 1998). This Arf-Mdm2-p53 axis serves as a checkpoint against hyperproliferative signals, arresting cell growth and potentially inducing apoptosis in response to oncogenic stress (Sherr, et al., 1998)

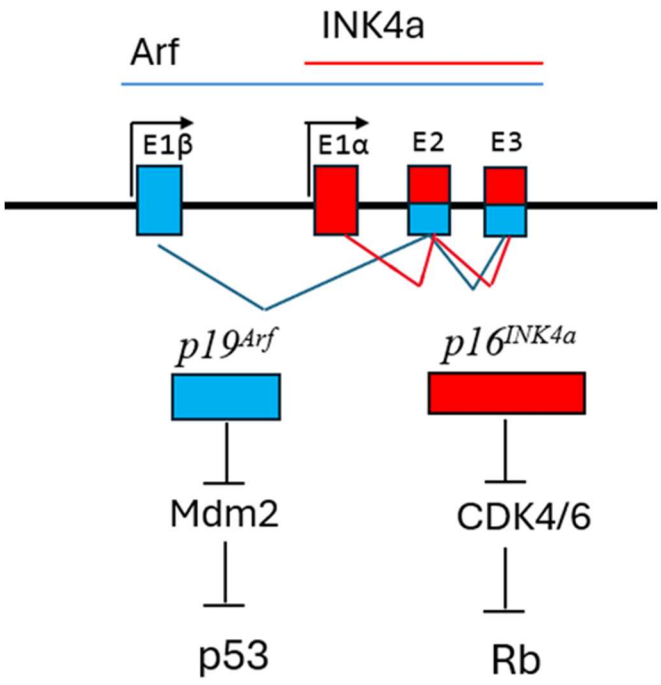

Figure 1. Representation of the INK4-ARF Locus.

The rectangles illustrate the coding exons for each of the two genes, separated by intronic regions (horizontal black line). Exons encoding p19Arf are in blue (blue rectangle), and those for p16Ink4a are in red (red rectangle). Exons 2 (E2) and 3 (E3) are shared by both the p16Ink4a and p19Arf proteins but are translated using different reading frames, resulting in no sequence similarity. It is noteworthy that, for p19Arf, the third exon is transcribed but remains untranslated (friendly adapted from Sharpless, et al., 2006).

p19Arf/p14 ARF protein

Both mouse p19Arf (169 amino acids) and human p14ARF (132 amino acids) proteins are highly basic due to a high arginine content (over 20%), giving them hydrophobic characteristics (Ozenne, et al., 2010). Interestingly, Arf is a recently evolved protein with the human and mouse proteins sharing only about 50% sequence similarity (Figure 2 shows the N-terminus of both mouse and human proteins). Due to the highly basic characteristic, the Arf protein lacks recognizable structural motifs both *in vitro* and *in vivo*, so it is likely that the proper folding requires the interactions with other molecules. Thus, the binding with its partners could be important to obtain stabilization at physiological pH, explaining the multitude of interactors described. Mammalian and avian ARF proteins lack identifiable structural motifs, and no NMR or crystallographic structures have been resolved, despite the protein's small size. With an isoelectric point above 12, ARF promiscuously binds to other molecules, and more than 25 binding partners have been described, some of which involved in p53-independent functions (Sherr et al., 2006). Mouse p19Arf and human p14ARF have limited lysine and methionine content, with only one internal methionine each (Met45 in mice, Met 48 in humans), which is absent in other species. Initiation from these methionines produces a shorter mitochondrial-localizing form (smARF), while full-length ARF generally localizes in nucleoli due to nucleolar localization signals (NoLS) in exon 1β (aa 26–37) of p19Arf (Weber, et al., 1999; Reef, et al., 2006).

Figure 2. Alignment of Human and Mouse Protein Sequences. Comparison of the amino acid sequence of the N-terminal region of mouse Arf (in bold) with the human protein. Conserved residues between the two species are highlighted. (DiGiammarino, et al., 2010).

The regulation of ARF

The intriguing behavior of ARF expression triggered by oncogenes has led researchers to explore its transcriptional regulators. Normally, ARF expression is kept at low levels, but oncogenic signals or DNA damage due to stressors significantly increase ARF expression, thus activating the cellular fail-safe mechanism. The precise regulation of ARF by different transcription factors suggests that its tumor-suppressive function can be adjusted depending on the specific stress signals present (Figure 3). Here, we highlight several critical transcription factors involved in modulating ARF mRNA expression. Notably, DMP1β interacts with DMP1α to prevent DMP1α binding to the ARF promoter. Additionally, the transforming growth factor beta 1 (TGFβ1) signaling pathway downregulates ARF transcription by suppressing E2F1 expression (Seo, et al., 2020).

Arf transcriptional regulation

Under oncogenic stress, ARF transcriptional levels are induced by MYC, an oncogenic protein that regulates many specific targets. In this context, MYC induces ARF transcription to trigger oncogene-induced senescence (OIS), which can proceed through p53-dependent or independent mechanisms. The transcriptional activation of ARF mediated by MYC on one hand depends on the stabilization of p53 by sequestering MDM2 (Conacci-Sorrell, et al., 2014; Zindy, et al., 1998; Kamijo, et al., 1998; Pomerantz, et al., 1998) on the other hand MYC-induced ARF expression occurs even in p53-null cells, indicating ARF's additional roles beyond p53 regulation. In the MYC-mediated ARF expression are also involved E2F transcription factors, particularly E2F1, E2F2 and E2F3 which bind to E2F-responsive elements in the ARF promoter to activate its transcription independently of RB (De Gregori, et al., 1997; Parisi, et al., 2002; Aslanian, et al., 2004). However, E2F3b acts as a negative ARF regulator, binding to the ARF

promoter to suppress its transcription, and its deletion can lead to ARF stabilization, p53 activation, and cell cycle arrest (Komori, et al., 2005; Humbert, et al., 2000).

DMP1, specifically the DMP1α isoform, can also increase ARF expression by binding to its promoter, promoting cell cycle arrest (Inoue, et al., 1999; Tschan, et al., 2015). Conversely, DMP1β sequesters DMP1α, reducing ARF transcription; this antagonistic role of DMP1β has been associated with oncogenic behavior in breast cancer (Maglic, et al., 2015).

FoxO transcription factors also contribute to the ARF expression, in fact there is FoxO-binding site within the ARF intron, activating its transcription and inhibiting MYC-driven lymphomagenesis (Bouchard, et al., 2007).

Interestingly, ARF is also regulated by members of the TGFβ family although in different ways. In fact, transcriptional levels increase during embryogenesis due to TGFβ2 that promotes chromatin remodeling at the ARF locus, while TGFβ1 negatively regulates ARF expression in B-cell lymphoma, highlighting the dual regulatory potential of ARF in tumor suppression and development (Bouchard, et al., 2007; Zheng, et al., 2010; Chen, et al., 2012).

ARF levels are downregulated by factors such as BMI-1 from the Polycomb group (PcG) and the transcription factor Twist-1 (a bHLH protein), both of which recruit Ezh2 to the ARF promoter region. Polycomb group proteins form two main complexes, PRC1 and PRC2, which modify histones, alter chromatin structure, and regulate gene expression. Specifically, BMI-1 and Twist-1 repress ARF transcription by promoting trimethylation of histone H3 at lysine 27 (H3K27me3), mediated by Ezh2, the catalytic component of PRC2 (Bracken, et al., 2007; Ding, et al., 2014) (Figure 3).

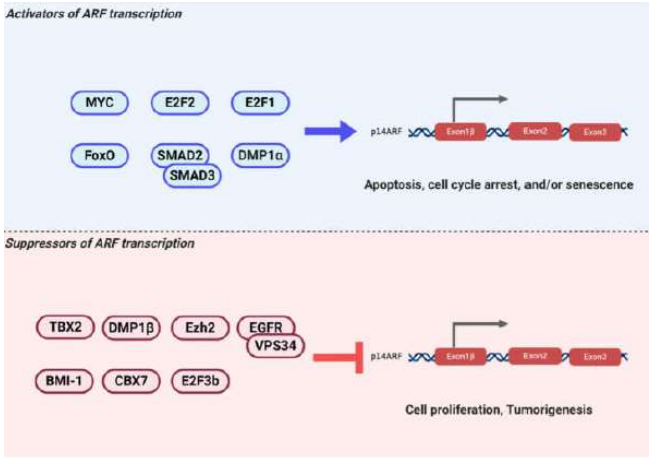

Figure 3. The transcriptional regulation of Arf: Activators and Suppressors.

This figure shows the transcriptional regulation of the ARF gene, highlighting its key activators and suppressors, which influence cell fate decisions. The activators of ARF transcription (top section, in blue): are proteins that upregulate ARF transcription such as MYC, E2F2, E2F1, FoxO, SMAD2, SMAD3, and DMP1α. This activation leads to cell cycle arrest, and/or senescence processes critical for tumor suppression and controlling abnormal cell proliferation. The suppressors of ARF transcription (bottom section, in red): are proteins that inhibit ARF expression such as BX2, DMP1β, Ezh2, EGFR, VPS34, BMI-1, CBX7, and E2F3 which supports cell proliferation and tumorigenesis. This suppression mechanism allows cells to bypass senescence and continue dividing, a common feature in cancer development. Overall, ARF acts as a checkpoint for cell growth control, where its transcriptional regulation is influenced by various factors that either promote or inhibit its function, balancing between tumor suppression and potential tumorigenesis (Seo, et al., 2020).

Arf post translational regulations

The regulation of ARF expression has been extensively characterized at the transcriptional level. However, recent studies indicate that post-translational mechanisms also play a critical role in controlling ARF in response to oncogenic stress. Alongside, post-translational modifications such as phosphorylation, ubiquitination, degradation pathways involving the proteasome and the lysosome, have been implicated in fine-tuning of ARF protein levels and functionality. These findings suggest that the stability and activity of ARF in cells may be tightly

regulated (Seo, et al., 2020). Phosphorylation, a key post-translational modification, modulates protein function across many cellular signaling pathways by targeting serine, threonine, or tyrosine residues. This modification, catalyzed by kinases, alters protein conformation due to changes in charge, which can lead to activation or deactivation, proteasome-mediated degradation, or modified protein–protein interactions. While phosphorylation is crucial in cellular signaling, ARF has only one identified phosphorylation site. In has been demonstrated that activation of protein kinase C alpha (PKCα) through TPA stabilizes ARF by phosphorylating it at threonine 8, thereby prolonging its half-life and shifting its localization from the nucleolus to the cytoplasm. This phosphorylation prevents ARF from regulating the MDM2/p53 axis and impairs its tumor-suppressive role (Vivo, et al., 2013).

Interestingly, during cell spreading, ARF expression is notably upregulated as a result of Protein Kinase C (PKC) activation. A mutant form of ARF, designed to mimic phosphorylation at the conserved threonine 8 (T8D), has been shown to enhance both cell spreading and the activation of Focal Adhesion Kinase (FAK). Moreover, cells expressing the ARF-T8D mutant demonstrated a proliferative advantage, indicating that phosphorylation at threonine 8 plays a critical role in promoting cell proliferation (Fontana, et al., 2018).

Ubiquitination is a critical cellular process that facilitates protein turnover by attaching ubiquitin molecules to lysine residues (or occasionally to methionine), on target proteins. This modification typically marks proteins for degradation by the proteasome, playing a vital role in regulating various cellular functions.

The rate limiting step is facilitated by over 1000 identified E3 ligases (Seo, et al., 2019) that direct proteins for different cellular fates: K48-linked chains target proteins for proteasome-dependent degradation, whereas K63- and M1-linked chains are involved in signaling cascades (Buetow, et al., 2016).

Although human ARF lacks lysine residues, research has been focused on its potential N-terminal ubiquitination and ULF E3 ubiquitin ligase has been identified as he enzyme of election (Chen, et al., 2010).

Depletion of ULF stabilizes p53 by increasing ARF protein levels, indicating a regulatory relationship. ULF-mediated ARF ubiquitination likely occurs in the nucleolus, as the interaction is inhibited when nucleophosmin (NPM) sequesters ARF in the nucleolus, thus protecting it from ULF mediated degradation. Other factors modulate ULF-mediated ARF degradation: MYC binds to ULF, inhibiting ARF-ULF interaction, independent of MYC's transcriptional activity, thereby controlling ARF levels through both transcriptional and post-translational mechanisms (Chen, et al., 2010; Chen, et al., 2013). Additionally, TNFR-associated death domain (TRADD) inhibits ARF ubiquitination via the TNFR pathway by disrupting the ARF-ULF interaction, stabilizing ARF and promoting oncogene-induced senescence (OIS) upon H-RasV12 expression. Finally, nucleostemin (NS), a nucleolar GTPase, also stabilizes ARF by preventing its degradation, supporting ARF's role in tumor suppression and cellular homeostasis. Nucleostemin (NS) stabilizes ARF through two mechanisms: enhancing the NPM-ARF complex in the nucleolus and preventing ARF interaction with ULF, an E3 ligase, thus reducing ARF ubiquitination and degradation. GLTSCR2, a nucleolar protein, relocates ARF to the nucleoplasm, where it increases ARF's interaction with ULF, leading to proteasome-dependent degradation of ARF (Lo, et al., 2015; Lee, et al., 2017).

Several E3 ligases further regulate ARF stability. MKRN1 tags ARF for degradation, reducing ARF levels and promoting cell proliferation; MKRN1 depletion in gastric cancer cells induces senescence, reversible by co-depleting ARF (Ko, et al., 2012). Similarly, Siva1 interacts with ARF, inducing its export from the nucleolus and promoting K48-linked ubiquitination, destabilizing ARF and leading to G1 cell cycle arrest upon Siva1 depletion (Wang, et al., 2013). β-TrCP2 specifically targets p19Arf for degradation in response to growth factor

signaling via mTOR-S6K1 phosphorylation, which is essential for cell proliferation control in mouse models (Nakagawa, et al., 2015).

Deubiquitinating enzymes (DUBs) counteract these E3 ligases. USP10 stabilizes ARF by removing ubiquitin tags, particularly under MYC-induced oncogenic stress, thereby sustaining ARF's tumor-suppressive function (Ko, et al., 2018). USP7 also indirectly modulates ARF by stabilizing ULF, promoting ARF degradation in hepatocellular carcinoma (HCC) cells, thus enhancing proliferation (Cai, et al., 2015). These findings illustrate a complex regulatory network where ARF levels are finely balanced by both ubiquitination and deubiquitination, influencing cell proliferation, senescence, and tumor suppression (Seo, et al., 2020).

Interestingly, ARF is protected from degradation by the proteasome by TBP-1 (Tat-Binding Protein 1), a multifunctional protein, component of the regulatory subunit of the proteasome (Pollice, et. al, 2004; Pollice, et al., 2007) and also by binding to NPM/B23 a multifunctional nucleolar phospho-protein (Bertwistle, et al., 2004).

Arf inactivation in cancer and role in pancreatic cancer

Molecular and cellular biology techniques, animal models, and genetic studies on cancers have demonstrated ARF's role in tumor suppression (Muniz, et al., 2011; Shimizu, et al., 2010). In murine models, Arf has been shown to be more critical than p16 in tumor suppression, as Arf-deficient mice develop a wide range of tumors, including lymphomas, sarcomas, and adenocarcinomas, with a median survival of approximately one year. Additionally, tumors arising in heterozygous mice frequently undergo loss of the remaining Arf allele, further emphasizing its crucial role in tumor suppression. This highlights the predominant role of ARF over p16 in mice (Kamijo, et al., 1999; Fontana, et al., 2018).

In the majority of human cancers, both ARF and p16 are inactive, complicating efforts to discern their specific roles in tumor suppression (del Arroyo, et al., 2005; Rizos, et al., 2001; Gardie, et al., 1998; Rutter, et al., 2003; Zhang, et al., 1998). Changes in the CDKN2a locus have been identified in approximately 30% of human tumors, including glioblastoma, melanoma, and pancreatic adenocarcinoma (Sharpless, et al., 1999; Maggi, et al., 2014). Germline mutations in CDKN2A have also been identified in pancreatic cancer patients and families (Lal, et al., 2000; Bartsch, et al., 2002; Gerdes, et al., 2000). Additionally, CDKN2A/B variants have been associated with increased susceptibility to type 2 diabetes, underscoring their potential role in beta-cell function and regeneration (Bao, et al., 2011).

Conversely, it has been shown that the loss of Arf markedly accelerates tumor development by promoting the angiogenic switch. This evidence highlights the p53-independent functions of Arf and suggests a novel role for Arf as a regulator of tumor angiogenesis (Ulanet, et al., 2010).

However, Arf-null mice typically die within a year from birth due to the onset of various types of cancers including sarcomas (43%), lymphoid malignancies (29%),

carcinomas (17%), and neurological tumors (11%). In heterozygous mice, tumors often show loss of the remaining allele (Kamijo, et al., 1999).

Despite the abnormal methylation of both p16INK4a and p14ARF promoters being linked to lymph node metastasis and higher tumor grade in colon cancer (Lee, et al., 2006), this alteration is also associated with poor prognosis in breast, colon, and bladder cancers (Dominguez, et al., 2003). Additionally, in squamous cell carcinoma of the anterior tongue, p14ARF expression independently predicts both relapse and survival outcomes (Kwong, et al., 2005).

Interestingly, promoter methylation in the ARF gene has been observed to occur independently of INK4a promoter methylation, suggesting this as a distinct alteration affecting ARF expression. In fact, methylation of p14ARF is correlated with a lower recurrence rate in oral cancer patients who have favorable clinical outcomes (Sailasree, et al., 2008). A CpG island within the promoter region of p14ARF has been found to be hypermethylated (Maggi, et al., 2014) across a range of human cancers, including colorectal (Esteller, et al., 2000), gastric (Tsujimoto, et al., 2002), and prostate carcinomas (Konishi, et al., 2002). Deletions and point mutations in exon 1β have been reported in familial melanoma syndromes and glioblastoma (Ozenne, et al., 2010; Rizos, et al., 2001; Rizos, et al., 2001; Hewitt, et al., 2002; Randerson-Moor, et al., 2001; Nakamura, et al., 2001). In breast cancer, various events such as homozygous deletion, loss of heterozygosity, and promoter hypermethylation have been documented (Silva, et al., 2001). In hepatocellular carcinoma, increased p14ARF mRNA expression is linked to a poorly differentiated cell type (Ito, et al., 2004).

p53 dependent pathways

Arf serves as a crucial activator of the p53 pathway. One of its most clearly defined roles is to prevent abnormal cell growth in response to oncogene activation by activating the transcription factor p53, which initiates the expression of various apoptosis-promoting and cell cycle-inhibiting genes (Sharpless, et al., 2005). Arfis thought to enhance and stabilize p53 activity by counteracting the effects of two specific ubiquitin ligases, Mdm2 and ARF-BP1/Mule (ARF-binding protein 1/Mcl1-ubiquitin ligase E3) (Figure 4). These ligases directly target p53 and can inhibit its tumor-suppressing functions. When Arf is overexpressed, it directly interacts with Mdm2, blocking Mdm2's ability to ubiquitinate, export from the nucleus, and degrade p53 via the proteasome (Sherr, et al., 2006). Additionally, Arf can move Mdm2 to the nucleoli, thereby preventing p53 ubiquitination and nuclear export. Some studies suggest that Arf can stabilize p53 and halt the cell cycle even without relocating endogenous Mdm2 to the nucleoli (Llanos, et al., 2001; Korgaonkar, et al., 2002). Furthermore, Arf also supports the p53 pathway by targeting the ARF-BP1 ubiquitin ligase. In response to oncogene overactivation, Arf is induced and inhibits ARF-BP1's proteasome-driven degradation of nuclear p53, thereby promoting p53-dependent cell cycle arrest or apoptosis (Chen, et al., 2005). Conversely, some propose that NPM's sequestration of ARF in the nucleolus could suppress Arf's growth-inhibitory functions, and its translocation to the nucleoplasm could facilitate p53 interaction and cell cycle arrest, primarily by inhibiting Mdm2. Interestingly, since Arf's nucleolar localization and Mdm2 binding are mediated by the same domains, it's suggested that Mdm2 and NPM may compete for binding with Arf. Thus, ARF may inhibit cell growth via interactions with NPM in the nucleolus while also modulating the p53 pathway through its interactions with Mdm2 and ARF-BP1 in the nucleoplasm (Ozenne, et al., 2010).

Other evidences of Arf involvement in p53 dependent pathways regard DNA damage in which the p53 pathway is activated. In this context the p53 induction coordinated by the protein kinases ATM (ataxia–telangiectasia mutated) and ATR (ataxia–telangiectasia and Rad3–related), which promote the rapid degradation of Mdm2. In irradiated Arf-null MEFs, sustained p53 induction requires p19ARF expression (Khan, et al., 200), and Arf's UV sensitization effect depends on coexpression with p53 (Lee, et al.,2005). Additional research demonstrates that ARF is involved in the p53 response to ionizing radiation, UV exposure, and genotoxic treatments (Meek, et al., 2009), underscoring Arf's contribution to p53-mediated DNA damage response. However, it has been demonstrated that p14ARF expression and the activated phospho-CHK2(Thr68) (a key player in the DNA damage response) are directly associated (Eymin, et al., 2006). Consistent with these findings, p14ARF is an essential component for initiating the ATM/CHK2 DNA damage signaling pathway, it seems that p14ARF is crucial for CHK2 activation in human lung tumors (Vonlanthen, et al., 1998).

Further research has clarified that Arf's inhibition of cell proliferation also utilizes p53-independent pathways, involving functional and molecular interactions with various proteins (Fontana, et al., 2019).

Arf's p53-independent pathways and roles

The Arf response is notably complex. Initially, Arf was primarily recognized for its role in suppressing abnormal cell growth by activating the p53 pathway, which mediates tumor suppression. However, while Arf is indeed a crucial component of the p53 pathway, evidences show that it can also restrict cell growth independently of p53 (Figure 4). These functions outside the p53 pathway are diverse and several potential regulators have been identified (Ozenne, et al., 2010).

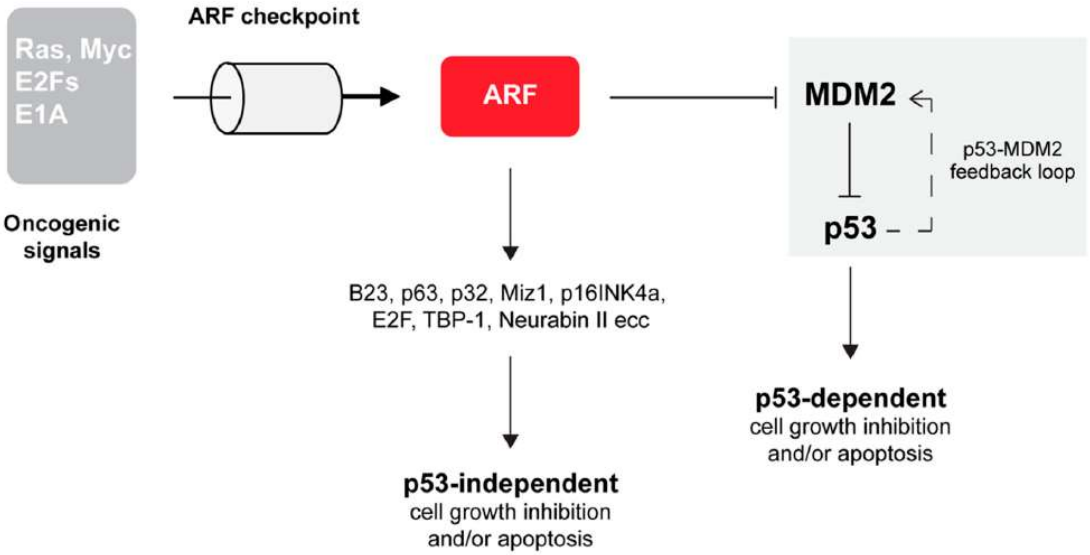

Figure 4. Arf's p53-dependent and independent pathways. The role of ARF in tumor suppression involves both p53-dependent and p53-independent pathways. When oncogenes such as E2F, Ras, E1A, and Myc are overexpressed, ARF levels within the cell rapidly increase, activating the ARF checkpoint. ARF inhibits MDM2 activity, disrupting the p53/MDM2 circuit (shown in grey), which results in p53 stabilization and subsequently induces cell cycle arrest and/or apoptosis. Additionally, ARF can inhibit cell growth independently of p53 by functionally interacting with various molecular players (Fontana, et al., 2019).

Interestingly, the overexpression of p19Arf can cause a G1 cell cycle arrest even in cells that lack p53 (Carnero, et al., 2000; Weber, et al., 2000). Additionally, human p14ARF can halt cells in the S phase or induce apoptosis through mechanisms that do not require wild-type p53 protein (Yarbrough, et al., 2002;

Hemmati, et al., 2002).

Several studies have also shown that p14ARF can suppress the growth of human lung tumor cells without p53 by inducing a G2 cell cycle arrest followed by apoptosis in both *in vitro* and *in vivo* models. In these cases, forced expression of p14ARF inhibits tumor growth and even leads to the regression of lung tumors in nude mice (Eymin, et al., 2001; Eymin, et al., 2006). In addition, mice lacking

Arf, p53, and Mdm2 have a higher tendency for tumor formation than those lacking only p53 and Mdm2 and Arf-null and heterozygous mice develop a broader range of tumors than p53-deficient animals alone (Kamijo, et al., 1999; Weber, et al., 200). Furthermore, multiple research groups have demonstrated that Arf interacts with and antagonizes the transcriptional functions of Myc and E2F1 independently of p53, both of which are potent oncogenes required for cell cycle progression (Sherr, et al., 2006). Rather than directly interfering with the DNA binding of these transcription factors at their target promoters, Arf instead causes their sequestration in the nucleolus and/or blocks the recruitment of coactivators.

These observations suggest that Arf plays a role in p53-independent tumor-suppressing functions and may act outside of the Mdm2-p53 axis in tumor control.

ARF primarily localizes in the nucleolus, where it binds with NPM, an abundant nucleolar protein whose expression correlates with cell proliferation levels (Itahana, et al., 2003; Bertwistle, et al., 2004).

NPM is involved in various cellular activities, including ribosome production. Under oncogenic stress, Arf moves to the nucleolus and forms stable complexes with NPM (Sherr, et al., 2006). The predominant view is that Arf exerts growth-inhibitory functions within the nucleolus; it slows down rRNA transcription and processing, disrupts NPM's nucleocytoplasmic shuttling, and blocks ribosome export from the nucleus to the cytoplasm.

Numerous studies have highlighted Arf's role in the DNA damage response. Arf-null mice exposed to ionizing radiation develop tumors more frequently than their wild-type counterparts (Kamijo, et al., 1999). Additionally, Arf has been shown to enhance DNA-damage–induced apoptosis (de Stanchina, et al., 1998) and is essential for certain types of DNA damage response (Khan, et al., 2000).

Interestingly, some studies indicate that Arf may influence ATM/ATR kinase activity through mechanisms that bypass the p53–Mdm2 axis. For example, overexpression of p14ARF has been reported to activate ATR/CHK1-dependent

NFκB phosphorylation, inhibiting NFκB's transactivation activity and leading to TNFα-dependent apoptosis (Rocha, et al., 2005).

Ozenne et al., 2010 also shows that p14ARF activates ATM/ATR/CHK signaling pathways in response to various genotoxic agents, inducing p53-independent cell cycle arrest and apoptosis (Eymin, et al., 2006). The activation of the ATM/CHK2 signaling cascade is mediated by p14ARF-stabilized Tip60, a histone acetyltransferase that activates ATM through acetylation (Sun, et al., 2005). These findings suggest that Arf functions as an upstream regulator of the ATM/ATR pathways, potentially acting as a sensor of cellular damage. Furthermore, p14ARF has been reported to maintain chromosomal stability in p53-null cells, with three critical residues outside p14ARF's known functional domains identified as essential for chromosomal stability (di Tommaso, et al., 2009). Together, these studies suggest that Arf activates pathways crucial for maintaining genomic integrity and plays an important role in genome stability.

Studies have revealed a role for p14ARF in adhesion and spreading processes within a specific temporal window, during which ARF relocates to adhesion sites and areas of active actin polymerization, where it interacts with phosphorylated focal adhesion kinases (pFAK). Decreasing ARF expression levels leads to defects in these processes (Vivo, et al., 2017; Fontana, R. et al., 2017).

Other interesting function of Arf are related to its small isoform, named **smArf** that is mainly involved in autophagy. In both mice and humans, translation initiation from an internal methionine produces a shorter, mitochondrial-targeted ARF variant (smARF) (Reef, et al., 2006). Although smARF is normally quickly degraded by the proteasome, it accumulates in mitochondria when cells are exposed to abnormal growth signals, disrupting mitochondrial membrane potential and triggering caspase-independent autophagic cell death (Type II) in response to nutrient stress, where cells self-digest to obtain energy. This can occur with or without p53 and Bcl-2, and recent findings indicate that full-length ARF can also promote autophagy, with an important role played by exon 2 that binds p32

mitochondrial protein, underscoring its role in cellular stress responses (Reef, et al., 2006; Abida, et al., 2008; Budina-Kolomets, et al., 2013; Itahana, et al., 2008). Interestingly, smARF can correct some p53-independent defects of development of Arf null mice, indicating a role of this form in developmental processes. However, the mechanisms through which this occurs are not clear (van Oosterwijk, et al., 2017).

Arf emergent roles

p19Arf is fundamental not only as a tumor suppressor but also as a regulator of cell differentiation and developmental processes by maintaining balanced cell proliferation, thereby contributing to the maturation of various cell types. For example, emerging studies have demonstrated that p19Arf can exacerbate cellular responses to chronic stressors, such as cigarette smoke. For instance, research has shown that cigarette smoke exposure in mice induces the expression of p19Arf in lung cells, enhancing cellular senescence markers and contributing to inflammation-related tissue damage. This suggests that p19Arf may play a dual role in both protecting cells from malignant transformation and, paradoxically, promoting inflammation and senescence under chronic stress conditions, potentially leading to age-related tissue dysfunction (Mikawa, et al., 2020).

Therefore, is well demonstrated that p19Arf expression can be even induced in response to differentiation signals, such as during neurogenesis and hematopoiesis, acting to avoid excessive cell proliferation, thus ensuring proper development and maturation of cells (Kamijo, et al., 1999; Sherr, et al., 1999). Furthermore, p19Arf can interact with other signaling molecules, modifying pathways that influence the fate of stem and progenitor cells, which are vital for development.

Arf involvement in differentiation and developmental processes

The Arf tumor suppressor is involved in many other processes, including differentiative programs. In fact, p19Arf is expressed in a precise time window during mice eye development and male germ cell line maturation. Initial evidence of Arf's developmental role comes from observations in Arf knock-out (KO) mice, which display eye developmental defects. These KO mice are born with smaller eyes than wild-type mice, due to retinal and lens abnormalities that result in blindness. The lack of p19Arf expression in KO mice allows for continued PDGF expression in the hyaloid vascular system (HVS), leading to abnormal perivascular cell proliferation. This forms a retrolental mass that eventually damages the posterior lens and retina. In contrast, Arf expression in wild-type mice during a specific time frame reduces PDGF receptor (PDGFR) levels, preventing abnormal perivascular cell growth and ensuring normal eye and retinal development. This action is p53-independent, as it involves Arf-induced microRNAs (miRNAs) that suppress PDGFR synthesis (Gromley, et al., 2009).

In addition, p19Arf is transiently expressed in spermatogonia, during the first synchronous wave of spermatogenesis disappearing in meiotic spermatocytes and their more advanced progeny. In older Arf-null males, testicular atrophy and germ cell apoptosis suggest Arf’s role in maintaining stem cell homeostasis by regulating the mitotic-to-meiotic transition, similarly to its role in hematopoietic stem cells (Schmidt, et al., 2000; de Rooij, et al., 2001; Akala, et al., 2008).While Arf expression in spermatogonia may signal the erasure of epigenetic silencing that occurs during chromatin remodeling in male germ cell development, aged Arf-null males show testicular atrophy, increased germ cell apoptosis, and reduced sperm counts. This suggests that Arf could regulate the transition from mitotic to meiotic divisions, crucial for maintaining the stability of stem cells over the reproductive life span. This role resembles the Ink4a-Arf locus's function in supporting long-term repopulating hematopoietic stem cells while promoting short-term amplification of multipotent progenitors (Akala, et al., 2008).

Overall, these findings suggest that the Ink4a-Arf locus plays a role in restraining normal cellular self-renewal as adult stem cells generate more differentiated progeny. These observations support an evolving view that stem cell self-renewal regulation through changes in Ink4a-Arf expression adjusts across life stages, with the maintenance of embryonic, fetal, young, and old stem cells being controlled by distinct transcriptional and silencing factors (Levi, et al., 2009).

In addition, the p19Arf protein, though not usually present in fetal or young adult mouse tissues, is expressed in the fetal yolk sac, indicating its role in late-stage differentiation of extraembryonic endoderm (ExEn) cells. Arf deficiency delays ExEn differentiation in embryoid bodies but doesn't affect other cell lineages. In ExEn development, Arf responds to Ras/Erk signaling and interacts with p53, supported by miR-205 to regulate cell adhesion and migration (Li, et al., 2013).

van Osterwijk, et al 2017 demonstrated that the smArf rescues the eye phenotype and fertility in Arf-null mice, although with a still unclear mechanism.

Interestingly, p19Arf plays key roles in mammary gland development. During pregnancy, p19Arf levels are regulated by progesterone, increasing its expression sixfold, and the protein levels are stabilized during lactation (Yi, et al., 2004).

Interestingly, Ink4a-Arf locus is epigenetically silenced in stem cell to maintain their ability of self-renewal (Li, et al., 2012). In addition, Li, et al., 2009 demonstrated that the Ink4/Arf tumor suppressor locus is fully silenced in induced pluripotent stem (iPS) and embryonic stem (ES) cells, acquiring a bivalent chromatin state that allows reactivation upon differentiation. This silencing is essential for successful reprogramming, by increasing the reprogramming efficiency by 7-fold. In mouse cells, Arf represents the main reprogramming barrier, while INK4a is more critical in human cells (Li, et al., 2009).

Mouse embryonic stem cells

Given the emergent role of Arf in developmental and differentiation processes, it can be interesting to study its role in embryonic stem cells.

Embryonic stem cells (ESCs), derived from the inner cell mass of the blastocyst, are a population of undifferentiated cells that exhibit two fundamental properties: self-renewal and pluripotency. Self-renewal refers to the ability of ESCs to divide symmetrically, producing identical undifferentiated daughter cells, while pluripotency confers the capacity to generate a broad range of cellular lineages (Jiang, et al., 2013). ESCs' unrestricted potential, known as "naïve" pluripotency, allows for the formation of all lineages, including germline cells (Boroviak, et al., 2014). Notably, mouse ESCs are highly resistant to cellular aging, able to undergo over 250 divisions without reaching senescence or undergoing transformation (Zalzman, et al., 2010). Various studies have shown that ESCs fluctuate among various potency levels within the same culture conditions due to paracrine signaling and cell-to-cell interactions (Cerulo, et al., 2014; Hisada, et al., 2012). Studies of gene expression in embryonic stem cells (ESCs) have pinpointed numerous transcription factors that collaboratively drive cell proliferation while inhibiting differentiation, making them potential markers for ESCs (Liu, et al., 2013). Among these, transcription factors like Oct4, Sox2, Klf4, and Nanog are essential regulators of self-renewal and pluripotency, actively suppressing pathways that lead to differentiation (Kallas, et al., 2014; Shi, et al., 2010; Rizzino, 2013). These factors are core components in maintaining the undifferentiated state and are integral to ESCs identity and stability.

Intriguingly, ESCs are able to maintain their pluripotent nature also in cultures (Hou, et al., 2016) using several factors in the culture medium that allows the self-renewal maintenance by preventing differentiation and promoting proliferation (Tamm, et al., 2013). In particular, ESCs cultured in serum with leukemia inhibitory factor (LIF) (a key factor that prevents *in vitro* differentiation) may

retain an undifferentiated state (Nakai, et al., 2013). Leukemia inhibitory factor (LIF) belongs to the interleukin-6 (IL-6) cytokine family and interacts with a heterodimeric receptor complex composed by the LIF receptor β subunit and the gp130 signal transducer. This receptor-ligand interaction is crucial for maintaining pluripotency in mouse embryonic stem cells as it activates signaling pathways that promote self-renewal and inhibit differentiation (Ohtsuka, et al., 2015). LIF-gp130 signaling is known to involve pathways such as STAT3, which plays a key role in sustaining an undifferentiated state in these cells.

Stem cells are distinct based on their differentiation potential, setting them apart from typical somatic cells and making them invaluable tools in cellular research. Mammalian stem cells are primarily divided into two groups: embryonic stem cells (ESCs), found within the inner cell mass (ICM) of blastocysts, and adult stem cells (ASCs), present in various tissues. These stem cell types vary in their properties and biological functions.

Early-stage embryonic cells can form both embryonic and extra-embryonic cell types, thus classified as **totipotent**. Totipotency describes a cell's capacity to generate a whole organism. During development, totipotent cells diverge into two lineages: the embryonic lineage (ICM) and the extra-embryonic lineage (trophoectoderm). ICM cells contribute to all embryonic lineages, including the three primary germ layers—endoderm, mesoderm, and ectoderm (Andrews, 2002), but not to extra-embryonic lineages (D'Angelo, et al., 2018; Chen, et al., 2013).

These cells recapitulate the expression patterns typical of the pre-implantation epiblast, including the expression of several transcription factors such as Nanog and Oct4 and are mostly **pluripotent** (Mitsui, et al., 2003; Chambers, et al., 2003; Schöler, et al., 1989). However, the stem cells in culture are highly heterogeneous, characterized by subpopulations of cells with varying expression levels in a dynamic equilibrium (Canham, et al., 2010; Torres-Padilla, et al., 2014). Much of this heterogeneity results in fluctuating expression of pluripotency-associated transcription factors which are part of a large regulatory "core network" within ESCs (Rodriguez-Terrones, et al., 2018). These fluctuations are thought to contribute to a dynamic balance between self-renewal and readiness for differentiation, allowing cells to retain flexibility in their fate decisions. For instance, Nanog expression oscillates in response to cellular signals, promoting transitions between more and less pluripotent states, which may reflect varying stages of commitment to specific lineage.

In contrast, Oct3/4 (Pou5f1), a core transcription factor for pluripotency, remains consistently expressed across pluripotent states, suggesting a fundamental role in maintaining the undifferentiated state. This stability highlights Oct3/4 as a master regulator of pluripotency, essential for the transcriptional network that sustains self-renewal and prevents differentiation. Studies by Nichols et al. 1998 and Niwa et al. 2000 demonstrated that fluctuations in Oct3/4 levels can disrupt this balance, leading to differentiation into specific lineages depending on its upregulation or downregulation. Together, these findings emphasize the complex regulatory network in pluripotent cells, where some factors fluctuate to modulate readiness for differentiation, while others like Oct3/4 remain constant to set pluripotency identity. This dynamic, yet stable, expression pattern enables embryonic stem cells to efficiently respond to developmental signals while preserving their fundamental self-renewing capacity (Nichols, et al., 1998; Niwa, et al., 2000).

Pluripotency markers

The most important factors primarily involved in pluripotency are: *Oct3/4, Sox2, Nanog and Dppa5a or Esg1*.

Oct3/4

The pluripotent state of ESCs is sustained by a complex gene regulatory network centered on the core pluripotency transcription factors (TFs) Oct4, Sox2, and Nanog (Li, et al., 2016). Oct4 the mammalian POU transcription factor (Nichols, et al., 1998) is a master regulator of pluripotency that works in concert with other transcription factors and coregulators to sustain this undifferentiated state. It is present in oocytes, blastomeres, inner cell mass (ICM), epiblast, and germ cells *in vivo*, as well as in pluripotent cells cultured *in vitro* (Schöler, et al., 1989; Rosner, et al., 1990).

A lack of Oct4 results in preimplantation lethality due to the embryo's inability to establish a pluripotent ICM. In embryonic stem cells (ESCs), a precise control of Oct4 expression is essential; either a reduction or an increase in Oct4 levels leads ESCs to initiate differentiation (Niwa, et al., 2000). Oct4 predominantly operates by activating genes linked to pluripotency and self-renewal while concurrently suppresses genes associated with differentiation (Boyer, et al., 2005). Genome-wide analyses of Oct4 and other ESC factors' binding sites have identified networks of co-regulated or co-bound targets, indicating that Oct4 likely collaborates with other transcription factors or coregulators to orchestrate transcriptional programs that maintain ESC pluripotency (Chen, et al., 2008; Loh, et al., 2006) (Figure 5). Oct4 contains a bipartite DNA-binding domain, with a POU-specific domain (POUS) and a POU homeodomain (POUHD), connected by a linker region. This linker not only tethers the two domains but also plays a crucial role in maintaining the structure necessary for Oct4 functions in pluripotency. The flexible linkers is structured as an α-helix and is essential for its biological role in sustaining the undifferentiated state of embryonic stem cells (ESCs) (Esch, et al.,

2013; Klemm, et al., 1994; Jauch, et al., 2011). Mutations in this linker impact Oct4's interactions and modify binding patterns (Chen, et al., 2014) indicating that Oct4 may rely on other factors in a multiprotein complex to maintain ESC pluripotency (Boyer, et al., 2005; Loh, et al., 2006).

Cross-linking techniques reveal an expanded Oct4 interactome, including known pluripotency-associated proteins like Sall4, Esrrb, and Smarca4, as well as newly identified interactors such as Cbx1 and Ctr9, which contribute to the regulation of histone modifications and gene expression. Disruptions in these interactions can lead to imbalanced epigenetic changes, with increased differentiation-related gene expression and suppressed self-renewal genes (Klockenbusch, et al., 2010; Mattout, et al., 2015; Ding, et al., 2009; Parisi, et al., 2008; Jiang, et al., 2008).

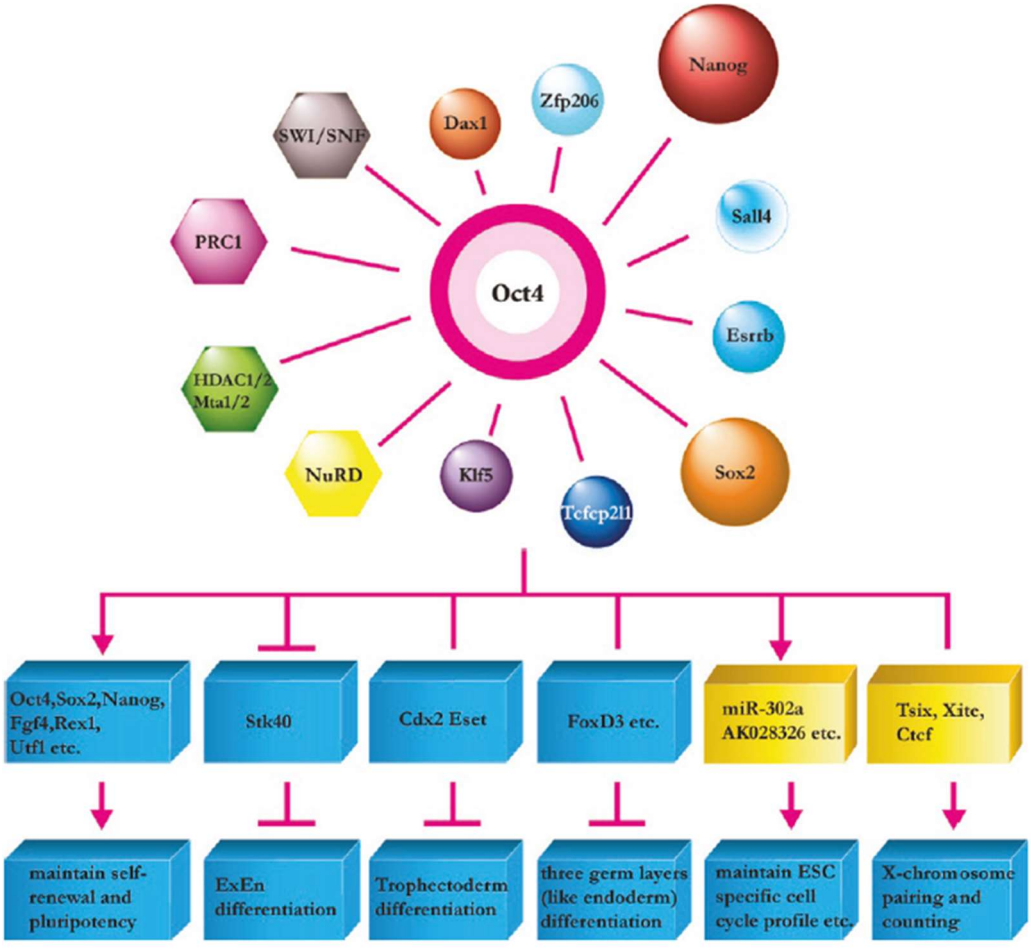

Figure 5. Oct4 interactome. Oct4 can either activate or repress target genes depending on its binding partners. When associated with factors like Sox2, Nanog, and Sall4, Oct4 generally promotes gene activation to support pluripotency. Conversely, it can repress developmental genes by interacting with repressor complexes such as NuRD and PRC1. Through these interactions, Oct4 not only activates key pluripotency factors but also prevents differentiation by repressing genes linked to development. Additionally, Oct4 influences other ESC functions, including cell cycle regulation and X-chromosome inactivation, through various effectors like miR-302a and Ctcf. This complex regulatory network allows Oct4 to effectively balance stem cell maintenance and suppression of differentiation (Shi, et al., 2010).

Nanog

Nanog is a pivotal homeobox transcription factor and a key downstream effector within pluripotency signaling pathways. In mouse ES cells, elevated Nanog levels enable self-renewal independent of LIF, and similarly, promote human ES cell growth without feeder cells. Beyond external signals, transcription factors like FoxD3, P53, and Oct4 regulate Nanog expression, situating it within a complex autoregulatory network in the core pluripotency network (CPN). Working alongside other core factors such as Oct4 and Sox2, Nanog helps stabilize pluripotency by regulating target genes and contributing to essential feedback loops within the CPN (Pan, et al., 2007; Papatsenko, et al., 2018) (Figure 6).

Nanog's self-regulatory mechanisms are varied: it engages in positive autoregulation by directly binding to its own enhancer regions, enhancing its own expression (Herberg, et al., 2015). Additionally, Nanog's negative autoregulation is indirect and is suggested to involve the factor Zfp281, which modulates Nanog expression levels (Fidalgo, et al., 2012). This dual regulation of Nanog exemplifies its nuanced control within the network, as it both promotes and attenuates its own activity depending on the cellular context.

In studies involving knockdown and knockout models, the removal of Oct4 leads to a rapid downregulation of Nanog (as well as Sox2 and Esrrb) within 12–24 hours (Martello, et al., 2012). However, Oct4 itself is less affected by the immediate absence of Nanog, highlighting Nanog's downstream positioning in the regulatory hierarchy relative to Oct4. This suggests that while Nanog is essential, it is more a responsive regulator rather than the primary initiator in the transcriptional hierarchy (Papatsenko, et al., 2015; Papatsenko, et al., 2013).

Given Nanog's role in autoregulation and its interconnection with other core factors, feedback mechanisms are crucial for maintaining pluripotency in embryonic stem cells (ESCs) by stabilizing the expression levels of key factors and preventing unwanted differentiation. This finely tuned balance emphasizes the

central function of Nanog in sustaining pluripotent states in ESCs, positioning it as a pivotal yet carefully modulated element within the pluripotency network (Papatsenko, et al., 2018).

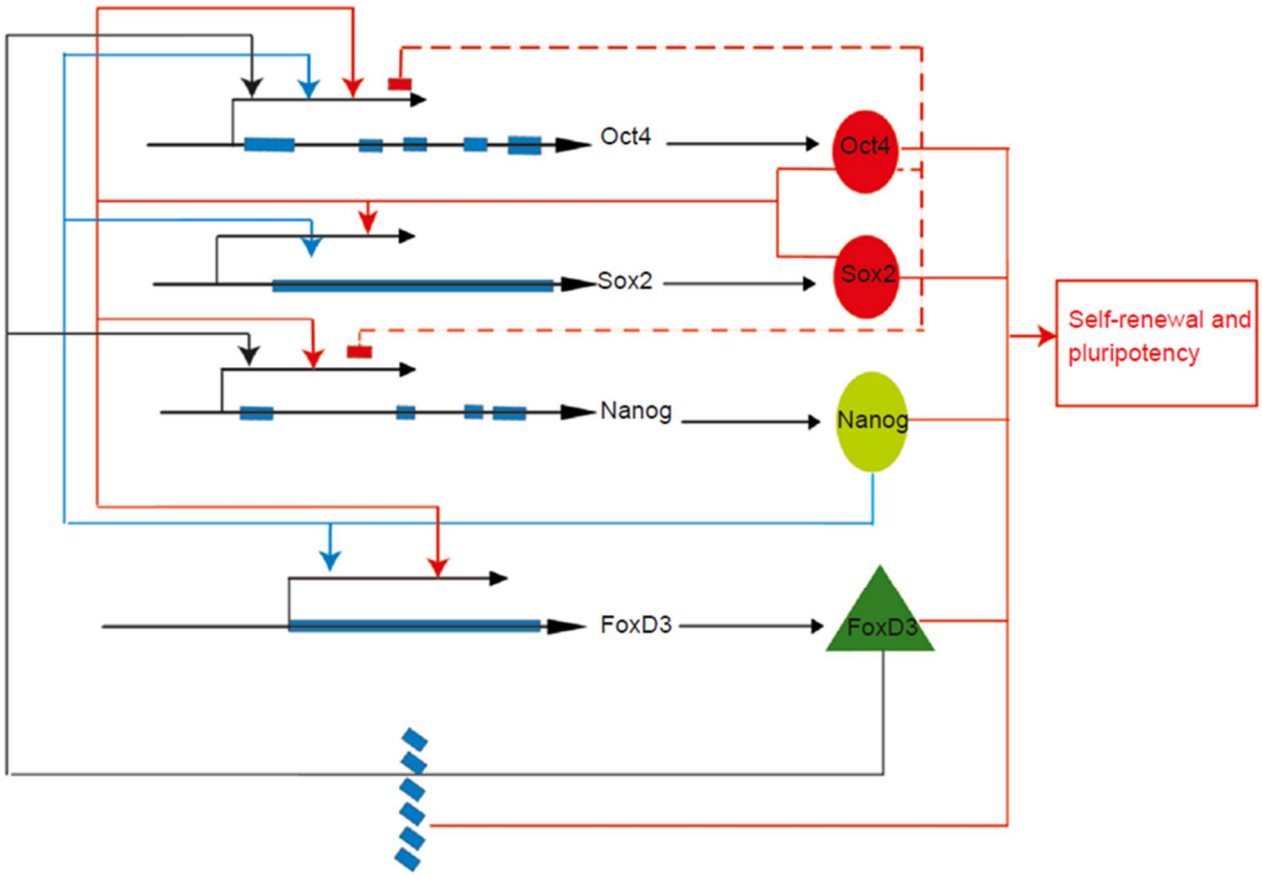

Figure 6. Regulatory network essential for ES cell pluripotency and self-renewal. The image shows the core pluripotency network involving transcription factors like Oct4, Nanog, Sox2, and FoxD3. These factors bind to each other's promoters, creating a tightly connected autoregulatory network. Solid arrows show positive regulation, where one factor enhances another's expression, while broken lines indicate negative regulation targeting Oct4. This balanced interplay supports the maintenance of pluripotency and self-renewal in ES cells (Pan, et al., 2007).

Sox2

SOX2 functions as a pioneering factor by binding nucleosomes and opening chromatin, recruiting additional chromatin-altering factors such as the ATP-dependent SWI/SNF complex components. This role enables it to subsequently

attract other transcription factors and initiate target gene transcription. In mouse (mESC) and human (hESC) embryonic stem cells, SOX2 is known to activate transcription of genes regulating stem cell maintenance and proliferation (Boyer, et al., 2005; Chen, et al., 2008). Specific degradation studies of Sox2 in mESCs during different cell cycle phases show that Sox2 is crucial for the M-to-G1 phase transition to maintain pluripotency (Hagey, et al., 2022). "Gain and loss of function" studies further demonstrate SOX2's key role in sustaining pluripotency in stem cells (Avilion, et al., 2003; Bylund, et al., 2003; Graham, et al., 2003). Additionally, SOX2 is implicated in cell cycle progression, lineage specification, and differentiation (Hagey, et al., 2014; Oosterveen, et al., 2013; Peterson, et al., 2012; Bergsland, et al., 2011; Bylund et al., 2003; Graham, et al., 2003).

In neural progenitor cells, SOX2 is critical for preserving progenitor identity and regulating proliferation in the brain, acting in a dose-dependent manner—both excessive and insufficient levels of SOX2 disrupt progenitor cell division rates. SOX2 deficiency in these cells leads to rapid loss of their progenitor identity, reduced proliferation, and premature differentiation. SOX2 expression helps maintain the progenitor state, ensuring a reserve of cells capable of differentiating into specific neural cell types as needed (Graham, et al., 2003; Hagey, et al.,2014).

SOX2 also influences progenitor differentiation by modulating the neural progenitors' response to Sonic Hedgehog (Shh) signaling. SOX2 enables selective responsiveness to Shh signals, maintaining neural identity, and collaborates with Gli proteins to activate neural-specific genes precisely. The combined action of Sox2 and differential-affinity Gli binding sites allows progenitor cells to form distinct cell types in response to the Shh gradient, ensuring accurate neural cell type formation (Peterson, et al., 2012).

Dppa5a or Esg1

Esg-1 appears to be a critical mediator within the pluripotency network, operating downstream of both Oct3/4 and LIF–Stat3 pathways, thus playing a unique role in sustaining the undifferentiated state of embryonic stem cells (ES cells). Stat3, a primary effector of LIF signaling, is sufficient to maintain ES cells in an undifferentiated state independently of LIF, and Esg-1 expression is strongly linked to this state, suggesting that Stat3 might regulate Esg-1 directly or through intermediary pathways. In the absence of active Stat3, Esg-1 expression declines significantly, indicating its dependence on this pathway for maintaining pluripotency (Matsuda, et al., 1999).

Furthermore, Esg-1 appears to promptly respond to changes in Oct3/4 levels, positioning it as an early-response gene within the pluripotency framework. The rapid downregulation of Esg-1 upon Oct3/4 suppression underscores its sensitivity to core pluripotency factors, highlighting it as an essential marker of the undifferentiated state that responds dynamically within the cellular regulatory network (Niwa, et al., 2000).

Interestingly, unlike other pluripotency factors that act mainly at the transcriptional level, Esg-1 contains an RNA-binding KH domain, indicating it may exert post-transcriptional control over certain genes critical for maintaining the pluripotent state. This RNA-binding capacity links Esg-1 to post-transcriptional regulation, positioning it uniquely within the Oct3/4 and Stat3 pathways, which are traditionally composed of transcription factors. Esg-1's RNA-binding function may allow for fine-tuning of gene expression, adding an additional regulatory layer to the pluripotency network (Adinolfi, et al., 1999). This unique role of Esg-1 could therefore provide stability and adaptability within the stem cell's regulatory landscape, distinguishing the pluripotent state from lineage-specific stem cells by endowing it with an added level of post-transcriptional control (Tanaka, et al., 2002).

Progenitor Cells (PPCs)

Progenitor Cells (PCs) serve as a vital regenerative reserve for both the maintenance and repair of organs and tissues. Their homeostasis is crucial not only for normal organ development but also for responses to pathological challenges. They play an especially important role in sustaining and regenerating organs and tissues with high cell turnover like Pancreas. The existence and role of progenitor cells in the adult mammalian pancreas (PPCs Pancreatic Progenitor Cells) are increasingly recognized as crucial to understanding pancreatic regeneration (Tanase, et al., 2014). While pancreatic embryonic progenitors are well-characterized, identifying similar regenerative populations in adults has proven difficult due to inconsistent findings on regenerative capacity following injury or disease in mice. Recent technological advances, however, are challenging these previous uncertainties and revealing that certain adult pancreatic cells may indeed possess progenitor-like properties.

Under specific conditions such as inflammation, tissue injury, or oncogenic stress these progenitor-like cells appear capable of activating regenerative processes. This potential for progenitors to contribute both to routine maintenance (homeostasis) and to repair in response to damage underscores the functional versatility of the adult pancreas. Notably, recent single-cell transcriptomics have exposed a remarkable cellular diversity within the pancreas, with certain subpopulations displaying gene expression signatures indicative of progenitor potential. These findings suggest that rather than being absent, progenitor-like cells may remain latent within the adult pancreas, poised to activate under the right physiological triggers.

High-resolution single-cell RNA sequencing (scRNA-seq) and emerging *in vitro* culture models became essential tools to explore how a single progenitor population generates the three differentiated cell types within the adult pancreas: acinar, ductal, and endocrine cells (Alvarez, et al.,2021). These technologies have

enabled researchers to dissect the cellular heterogeneity of these progenitors, providing insights into their specific characteristics and regenerative potential (Edlund 2002; Alvarez, et al., 2021) (Figure 7). These advancements are redefining our understanding of the pancreas not as a static organ but as a dynamic system with a capacity for renewal, especially under stress. This growing knowledge opens promising therapeutic avenues, particularly in regenerative medicine, for treating diseases that compromise pancreatic structure and function by potentially harnessing or enhancing progenitor-mediated repair mechanisms (Alvarez, et al., 2021).

Emerging evidence on the stem-like features within tumoral cells has led to a compelling debate, particularly emphasizing the role of de-differentiation in tumorigenesis. Rather than tumors originating solely from dedicated stem cells or progenitors, it is increasingly hypothesized that differentiated cells might revert to a stem-like state, thus gaining tumorigenic potential. This de-differentiation process is supported by the high differentiation observed in some low-aggressive tumors, which might indicate that these tumors arise from cells that initially differentiated and later reverted to a more progenitor-like, stem-capable state. Additionally, normal differentiated cells have been shown to adopt stem-like characteristics under specific conditions, further suggesting that de-differentiation could be a fundamental mechanism by which cells acquire the ability to drive tumor formation (Carvalho, 2020; Gabbert, et al., 1985; Zhou, et al., 2019).

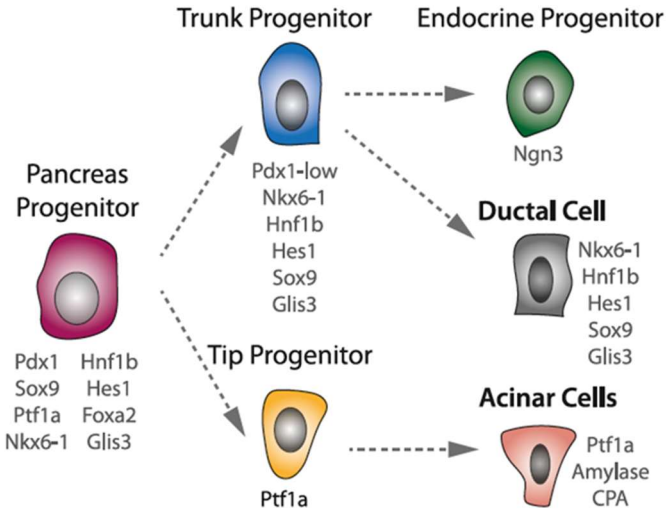

Figure 7. Schematic representation of pancreatic progenitor cells and the three mature cell types derived from them. During pancreatic development, multipotent Pdx1+ progenitors differentiate into the three main cell types of the adult pancreas: acinar, ductal, and endocrine cells. These progenitors express key transcription factors such as Sox9, Ptf1a, Foxa2, Nkx6-1, Hnf1b, Hes1, and Glis3. Two primary lineages emerge from this progenitor population: tip progenitors, which retain Ptf1a expression and differentiate into acinar cells characterized by the production of digestive enzymes and trunk progenitors, which maintain Nkx6.1 expression (Alvarez, et al., 2021).

PPCs markers

Pdx1

The three main types of adult pancreatic cells originate from a common progenitor marked by the transcription factor Pancreatic and duodenal homeobox 1 (Pdx1) during embryonic development (Edlund 2002). PDX1 encodes a critical transcription factor that regulates both the development and function of pancreatic β-cells (Jennings, et al., 2015; Bastidas-Ponce, et al., 2017). In mice, Pdx1 expression begins at embryonic days E8.5–9.0 and later localizes specifically to β- and δ-cells within adult islets (Ahlgren, et al., 1996; Guz, et al., 1995; Offield, et

al., 1996; Ahlgren, et al., 1998). Mice with homozygous Pdx1 knockout form initial pancreatic buds but do not develop a fully formed pancreas (Jonsson, et al., 1994). In contrast, heterozygous Pdx1 knockout mice develop a normal pancreas but become diabetic as adults with β-cells undergoing increased apoptosis over time (Brissova, et al., 2002; Johnson, et al., 2003; Holland, et al., 2005).

The critical role of Pdx1 is evident, as its ablation leads to pancreatic agenesis (Offield, et al., 1996; Stoffers, et al., 1997), underscoring its necessity for both exocrine and endocrine cell formation. In mice, $Pdx1^{+}$ progenitors that also express Sox9 and Ptf1a emerge in the posterior foregut endoderm at embryonic day E8.5. These progenitors then progress into the pancreatic bud, transitioning between E12 and E15 into specific cell types—ductal, acinar, or endocrine—guided by a finely regulated signaling network (Edlund 2002) (Alvarez, et al., 2021).

PDX1 binds to regions associated with 5,664 genes, with its binding sites located within 20 kb of their transcription start sites (TSS) or within the gene body. These target genes include PDX1 itself and other important pancreatic genes such as RFX6, MEIS1, and HNF1B (associated with MODY). PDX1 binding is accompanied by the active histone modification marker H3K27ac, which is notably present at PDX1-bound regions, especially in intergenic (44.2%) and intronic (40.4%) regions, while a smaller proportion (11.3%) is found in promoter regions. This concentration near TSS highlights PDX1's influence on activating transcription for its target genes (Wang, et al., 2018).

Nkx6.1

NKX6.1, an important homeobox protein, functions as a transcription factor essential for the performance and growth of pancreatic β cells. Alongside PDX1, NKX6.1 is prominently expressed in both multipotent pancreatic progenitor cells (MPCs) and mature β cells, underscoring its role across various developmental stages. During pancreatic development, NKX6.1 is found in three main cell types:

pancreatic progenitors (PDX1+/NKX6.1+), endocrine progenitors (NGN3+/NKX6.1+), and fully differentiated insulin-producing β cells (insulin+/PDX1+/NKX6.1+) (Aigha, et al., 2020; Villasenor, et al., 2008). Throughout pancreatic development, NKX6.1 expression becomes more concentrated in the trunk region of the pancreatic epithelium, which will later give rise to endocrine lineages responsible for hormone production（Al-Khawaga, et al., 2017). Within human pancreatic islets, NKX6.1 is exclusively expressed in β cells and is not detectable in other islet cell types. Conversely, MPCs without NKX6.1 expression (PDX1+/NKX6.1−) tend to differentiate into non-functional polyhormonal β cells, which is an undesirable outcome. In mice, Nkx6.1 appears as early as embryonic day 9.5 (E9.5), with its role becoming more defined over time. By E10.5, Nkx6.1 coexists with Ptf1a in numerous MPCs, indicating a shared potential for endocrine and exocrine fates. However, by E12.5, Nkx6.1 and Ptf1a diverge in function: Nkx6.1 restricts itself to the trunk domain, guiding cells towards the endocrine lineage, while Ptf1a localizes to the tip domain, leading cells toward exocrine differentiation （Zhou, et al., 2007). In addition, it has also been demonstrated that forced expression of NKX6.1 in PDX1+ MPCs can restore pancreatic β cell development in NKX6.1-deficient progenitors （Nelson, et al., 2007). The progressive restriction of NKX6.1 to the trunk domain highlights its central function in endocrine differentiation, establishing NKX6.1 as indispensable for the formation and function of β cell populations (Aigha, et al., 2020) (Figure 8).

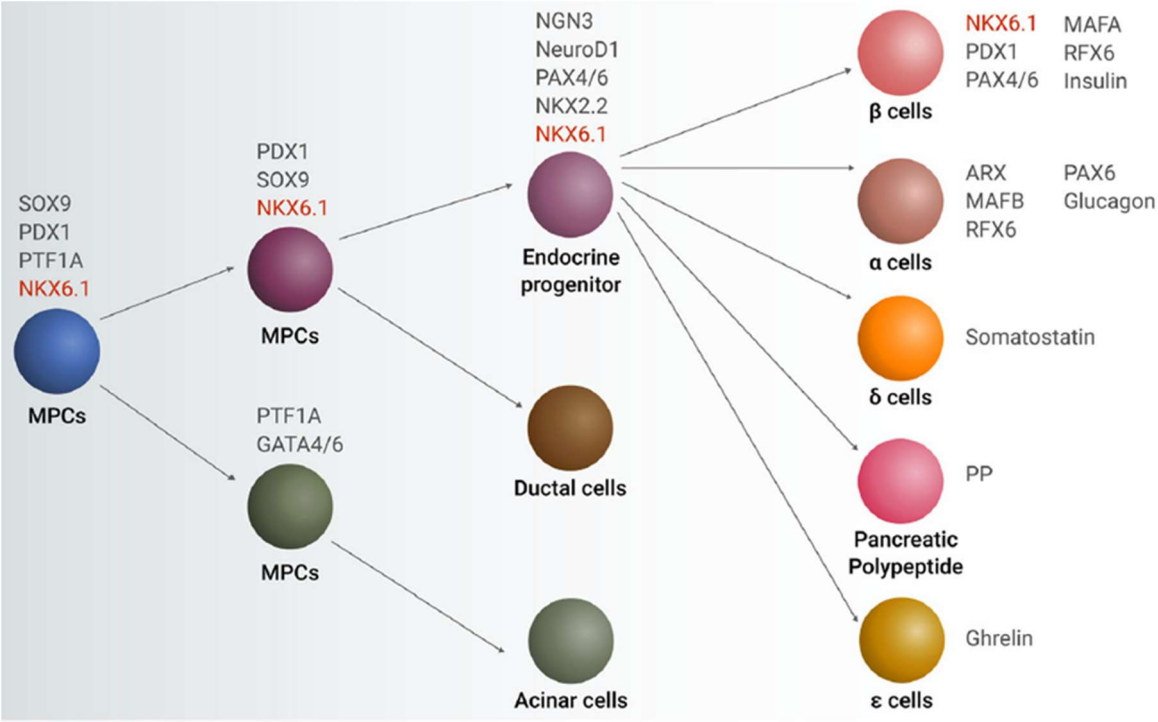

Figure 8. An overview of the transcription factors that marks each stage of pancreatic differentiation. The expression of essential transcription factors (TFs) varies throughout the stages of multipotent pancreatic progenitor (MPC) differentiation into distinct pancreatic cell lineages. NKX6.1 expression begins at the MPC stage, persists within the endocrine lineage, and ultimately becomes confined to β cells (Aigha, et al., 2020)

Gata4

The GATA transcription factors family to which Gata4 belong is a subfamily, expressed in the definitive endoderm that forms the pancreas and other gastrointestinal organs. In particular, GATA4 is a transcriptional regulatory factor involved in the development of endoderm-derived organs such as the heart and gut (Gong, et al., 2018). Detailed RNA in situ hybridization analysis of GATA factors in the mouse pancreas has revealed that only Gata4 and Gata6 are expressed in the embryonic pancreas （Decker, et al., 2006). Both Gata4 and Gata6 are present in the early pancreatic endoderm and remain active throughout pancreatic development although early studies reported conflicting data on Gata expression

during pancreas formation（Decker, et al., 2006; Nemer, et al., 2003; Ritz-Laser, et al., 2005; Ketola, et al., 2004). Recent immunohistochemistry studies have clarified these patterns, showing that Gata4 expression gradually becomes limited to the acinar compartment. These expression patterns have been further confirmed in transgenic mouse reporter assays （Rojas, et al., 200; Freyer, et al., 2015), although a study noted low levels of Gata4 expression in mouse islets, detected via RT-PCR (Sartori, et al., 2014). GATA4 together with GATA6 are essential for the expansion and maintenance of MPCs (multipotent pancreatic progenitors) during the early stages of mouse pancreas development（Xuan., et al., 2012; Carrasco., et al., 2012). Interestingly, while GATA factors are not required for pancreas specification within the foregut endoderm, they are crucial for maintaining pancreatic identity in MPCs. The absence of both GATA4 and GATA6 leads to the conversion of pancreatic tissue into intestinal and gastric cell types in the dorsal and ventral pancreas, respectively（Xuan, et al., 2016). This transformation is partly attributed to the inappropriate activation of the Shh (Sonic hedgehog) pathway in pancreatic progenitors. GATA4 and GATA6 contribute to sustaining pancreatic identity by repressing Shh expression in the pancreatic endoderm through binding to the foregut endoderm enhance（Xuan, et al., 2016). However, Gata4 may function as a potential tumor suppressor gene. Notably, high levels of GATA4 expression have been observed in pancreatic cancer tissues, where its expression correlates with the grade of pathological differentiation. When the GATA4 gene is ectopically expressed, it reduces cell viability, while interference with GATA4 expression significantly enhances the colony-forming ability of pancreatic cancer cells. Additionally, GATA4 has been shown to inhibit tumor growth in xenograft mouse models. Moreover, re-expression of GATA4 was found to up-regulate P53 expression. Collectively, these findings suggest that GATA4 may influence cell proliferation and differentiation in the progression of pancreatic cancer (Gong, et al., 2018).

Sox9

SOX9 acts as a critical "molecular gatekeeper" in preserving the pluripotency of pancreatic progenitors during early pancreatic development, similar to its role in other tissues such as the nervous system, hair follicle, testis, and notochord (Bylund, et al., 2003; Blache, et al., 2014; Vidal, et al., 2005; Akiyama, et al., 2005; Cheung, et al., 2005; Barrionuevo, et al., 2006). Within the developing pancreas, SOX9 is selectively expressed in a subset of $PDX1^+$ progenitors that are mitotically active and responsive to Notch signaling, absent from differentiated cells (Bylund, et al., 2003; Graham, et al., 2003). It supports progenitor maintenance by promoting their proliferation, survival, and undifferentiated state. The reduced expression of the Notch effector HES1 in SOX9-deficient cells suggests that SOX9 may regulate pancreatic progenitors via the Notch pathway, mirroring its role in neurogenesis, where SOX factors prevent premature differentiation by inducing Notch effectors (Bylund, et al., 2003; Bani-Yaghoub, et al., 2006).

SOX9/HES1 co-expressing cells in the pancreas appear interspersed with NGN3/SOX9-negative cells, consistent with a SOX/Notch-mediated mechanism of lateral inhibition during pancreatic development. However, SOX9-deficient pancreas shows more pronounced hypoplasia and increased apoptosis than Hes1 mutants, indicating that SOX9 has additional Notch-independent roles (Jensen , et al., 2000). Although SOX9 deficiency in mice leads to a relative increase in $glucagon^+$ cells, this is likely due to delayed SOX9 inactivation compared to Hes1-null models, where $glucagon^+$ cells drastically increase. During early organogenesis, SOX9 colocalizes with PDX1 within the pancreatic bud region, starting from embryonic day (E) 9.0, with nearly complete overlap in expression until E12.5, marking SOX9 as a definitive marker of pluripotent pancreatic progenitors. As differentiation intensifies post-E14, SOX9 expression becomes restricted to a subset of PDX1+ cells, underscoring its role in maintaining undifferentiated progenitors and preventing premature differentiation. Lineage-tracing studies further affirm SOX9's function in progenitor cell maintenance,

showing that SOX9+ cells contribute to all pancreatic cell types (Lioubinski, et al., 2003; Akiyama, et al., 2005).

p21

p21, encoded by the gene CDKN1A, is the first discovered member of cyclin-dependent kinase inhibitors (CKIs), crucial regulators of the cell cycle that help maintain genomic stability and are frequently deregulated in human cancers (Xiong, et al., 1993; Abbas, et al., 2009; Kreis, et al., 2015, Roninson, et al., 2002). Identified through cDNA isolation, p21 was associated with differentiation, initially recognized for its elevated expression in differentiating human melanoma cells, thus named melanoma differentiation-associated gene 6 (mda6) (Jiang, et al., 1995). As cell proliferation and differentiation are inversely related, their coordination is essential for growth, development, and tissue homeostasis (Ruijtenberg, et al., 2016). p21-induced cell cycle arrest is often required for cells to enter terminal differentiation, quiescence, or senescence, typically marked by increased p21 levels. Activated by p53, the primary transcriptional regulator of p21 (el-Deiry, et al., 1993), it initiates cell cycle arrest by repressing cell cycle genes through the DREAM complex (Engeland, et al., 2017). Besides p53, p21 expression is also promoted during differentiation by p53-independent mechanisms, influenced by factors like vitamin D3, TNF-β, nerve growth factor, and others (Gartel, et al., 1999).

Research indicates that p21's role in differentiation varies by cell type and differentiation stage, acting positively or negatively depending on the context (Dutto, et al., 2014). Overexpression of p21 induces differentiation in both normal and cancer cells by triggering cell cycle exit (Warfel, et al., 2013). In support of its positive role, p21 promotes differentiation in various cell types, including murine oligodendrocytes, human monocytes, megakaryocytes, erythroid progenitors, and skeletal muscle cells (Asada, et al., 1999; Zezula, et al., 2001;

Baccini, et al., 2001; Papetti, et al., 2010; Guo, et al., 1995; Wang, et al., 1996; Mercer, et al., 2005). In p21-knockout mice, muscular differentiation is disrupted, and p21 expression correlates with terminal differentiation across multiple cell types—muscle, cartilage, skin, and nasal epithelium—during embryogenesis and in adult tissues, independent of p53 (Chinzei, et al., 2015; Parker, et al., 1995).

AIM OF THE THESIS

Although p14/p19Arf is best characterized as one of the most relevant oncosuppressor (Weber, et al., 2002; Sherr, et al., 2000; Fontana, et al., 2018), recent evidences underline its emerging role in the context of differentiation and control of stem cells self-renewal. In fact, p19Arf has been shown to be transiently expressed in a precise time window during mouse male germ cell and eye development as well as during *in vitro* keratinocytes differentiation (Li, et al., 2013; Gromley, et al., 2009; van Oosterwijk, et al., 2017). Furthermore, p14/p19Arf must be silenced to generate induced Pluripotent Stem Cells and to maintain the self-renewal capacity of stem cells in physiological conditions (Li, et al., 2009) (See Introduction). In line with these observations, our research group explored Arf's relevance during *in vitro* pancreatic differentiation: mouse Embryonic Stem cells were induced to differentiate through definitive endoderm toward Pancreatic Progenitor cells by using an *in vitro* differentiation protocol already set up in the laboratory (De Angelis, et al., 2014, Figure 9) and it was demonstrated that p19Arf intracellular levels increase during differentiation, starting at Day 4 (when definitive endoderm is formed) and continuing to rise up until Day 8 of differentiation both at the RNA and protein level (Figure 10 and Montano, et al., 2021).

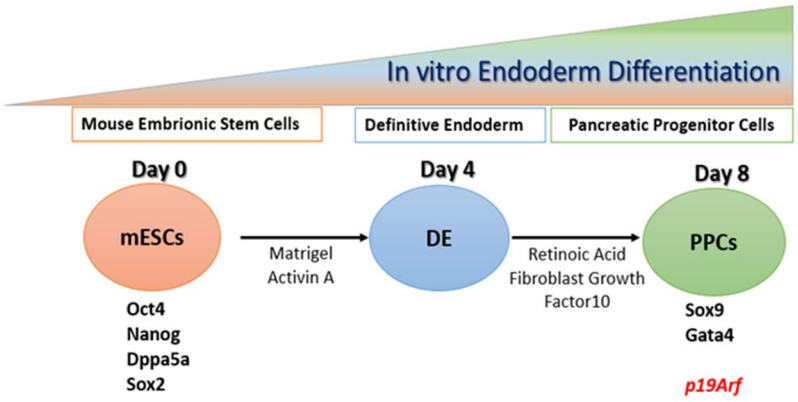

Figure 9. Schematic of the differentiation protocol used to differentiate mouse embryonic stem cells (mESC) toward Pancreatic Progenitor Cells (PPCs).

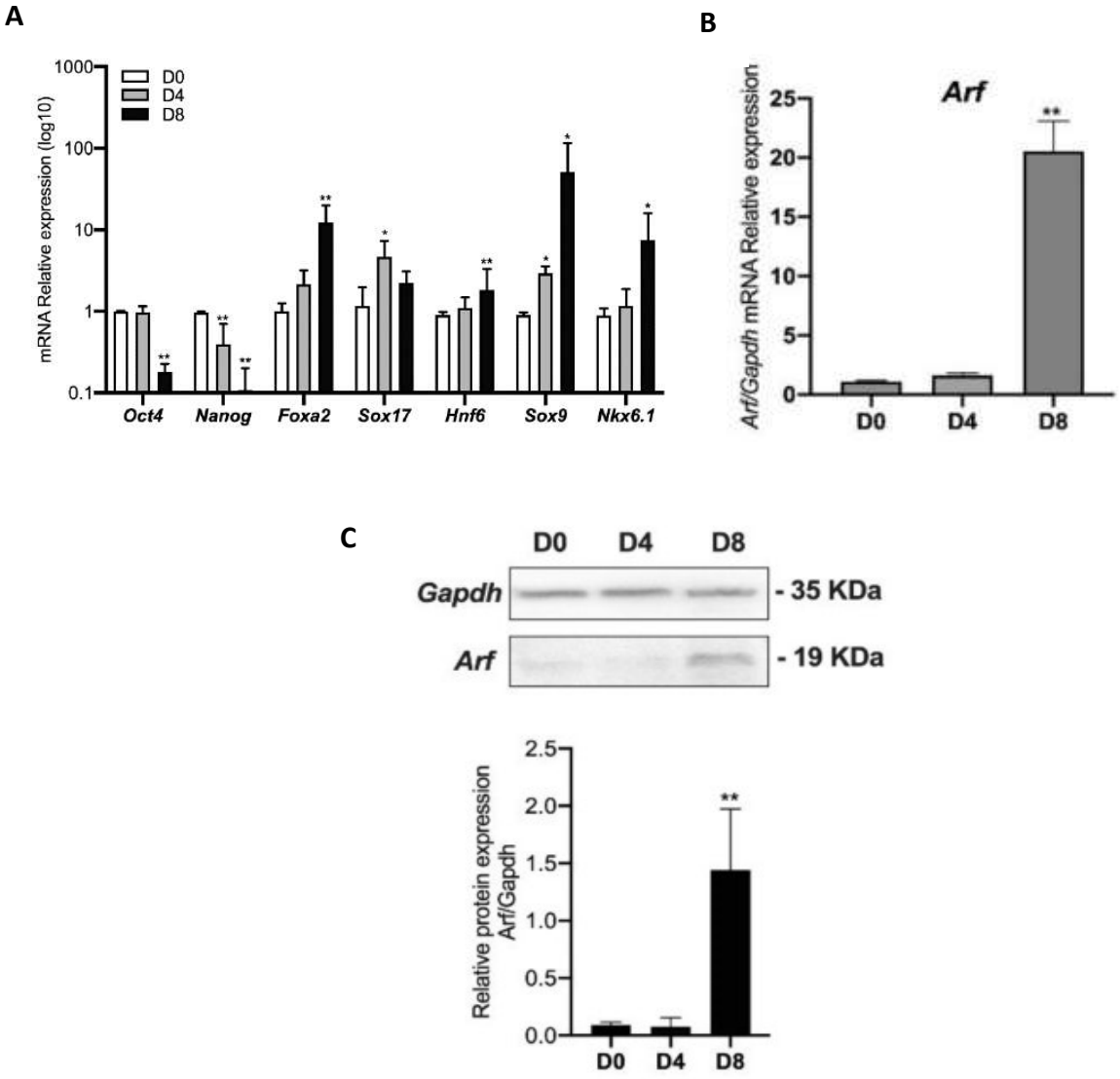

Figure 10. Mouse embryonic stem cells were treated to differentiate toward Pancreatic Progenitor cells. Cells were collected at 3 different time points (D0, D4, D8). Differentiation process was analyzed by qRT-PCR (**A**) by using stemness markers (Oct4 and Nanog), definitive endoderm markers (FoxA2 and Sox17), Posterior Foregut markers (Hnf6) and Pancreatic Progenitor cell's markers (Sox9 and Nkx6.1). (**B**) p19Arf gene expression was analyzed by qPCR vs. Gapdh is reported as folds increase. Data points represent the average of triplicate determinations ± SD. Similar results were obtained in 3 independent experiments. *, $p < 0.05$; **, $p < 0.01$. **(C)** p19Arf protein levels were also evaluated by Western Blot and densitometric analysis relative to Gapdh. The data are expressed as average of three independent experiments ± SD,* $p < 0.05$; **, $p < 0.01$.

p19Arf levels increase during pancreatic differentiation toward the pancreatic lineage is suggestive of its potential involvement in the differentiative process.
This is the starting point of my PhD project, the main objective of which is to explore the potential role of ARF in *in vitro* pancreatic differentiation.
Therefore, a direct genetic approach was employed to analyze whether alterations in p19Arf interfere with proper *in vitro* pancreatic differentiation toward pancreatic progenitor cells (PPCs). To this end, CRISPR-Cas9 technology was adopted to target the genomic exon 1β of p19Arf and phenotyping of cellular clones displaying mutations in p19Arf.

RESULTS

Application of the Crispr-Cas9 technology to target Exon 1β of p19Arf

In order to investigate the potential role of p19Arf during pancreatic differentiation we decided to use the CRISPR-Cas9 technology to target the INK4a/Arf locus of mESCs. This versatile technology for genome editing consists of two components: a single guide RNA (sgRNA) and the Cas9 nuclease. The specificity of CRISPR-Cas9 is determined by the recognition of the target DNA through base pairing with a 20-base sgRNA. Thus, the interaction between the target DNA and the sgRNA makes it highly precise.

To apply this technology to our system, it has to be taken into account the peculiarity of the Ink4a/Arf locus (Cdkn2a) that codes two important oncosuppressors, Ink4a and Arf that are mostly intertwined with each other (Figure 11 and see Introduction). The two proteins encoded by the locus are translated from two different transcripts, an α-transcript and a β-transcript which share DNA sequences in exon 2 and 3 but not in their amminoacidic sequence. Thus, the resulting INK4a and ARF tumor suppressors display completely different amino acid sequences with distinctive functions due to the alternative reading frames (Ko, et al., 2016; Ko, et al., 2018; Seo, et al., 2020)

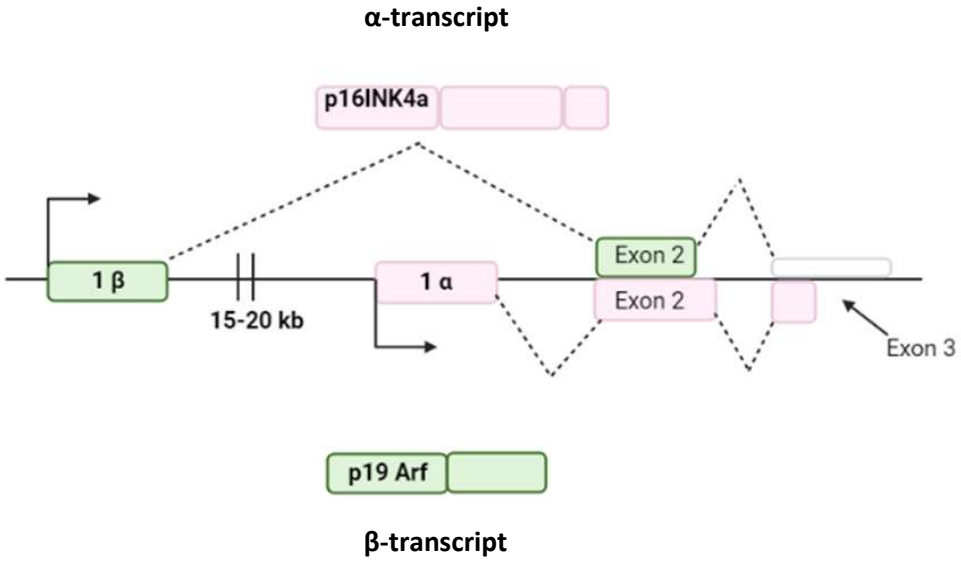

Figure 11. Genomic structure of the Ink4a/Arf locus (*Cdkn2a)* This locus encodes two oncusuppressor transcribed from two different transcription start site: α-transcript, encoding INK4a (pink) and β-transcript, encoding ARF (green). Although these two transcripts share exon 2 and 3 sequences, they are translated following alternative reading frames, thus resulting into two completely different proteins (freely adapted from Seo, at al., 2020).

Therefore, given the structure of the CDKN2a locus, we decided to target exon 1β to exclusively mutate Arf. In fact, exon 1β is fundamental for p19Arf tumor suppressor activity and for the control of cell cycle functions as well as in several developmental and differentiation context (see Introduction).
It has to be noted that the Arf sequence is highly repetitive rendering very difficult to design specific oligos. Therefore, we decided to use a single guide RNA already successfully used (Weber, et al., 2015) to specifically target exon1β.

Generation of the genome editing construct: lentiCRISPRv2-Cas9-sgRNA targeting the Arf gene.

In order to target exon 1β of p19ARF, the first step was the generation of a molecular construct containing two fundamental elements: a single guide RNA specifically targeting the sequence of interest and the coding sequence for the Cas9 protein.

I decided to use a validated sgRNA (Weber, et al., 2015) targeting a region located 70 bp downstream of the ATG of Arf, along with the lentiCRISPRv2 plasmid, which is a versatile tool for CRISPR-Cas technology (Addgene Plasmid 49535).

The lentiCRISPRv2 plasmid contains all the key elements necessary for the cloning strategy, as well as for subsequent transfection and selection in mammalian cells (Figure 12B) (see materials and methods).

The single guide RNA was specifically designed with the necessary 5' and 3' ends for cloning after vector digestion with BsmBI, according to the Zhang Lab protocol (Sanjana, et al., 2014; Shalem, et al., 2014) (Figure 12, A, C).

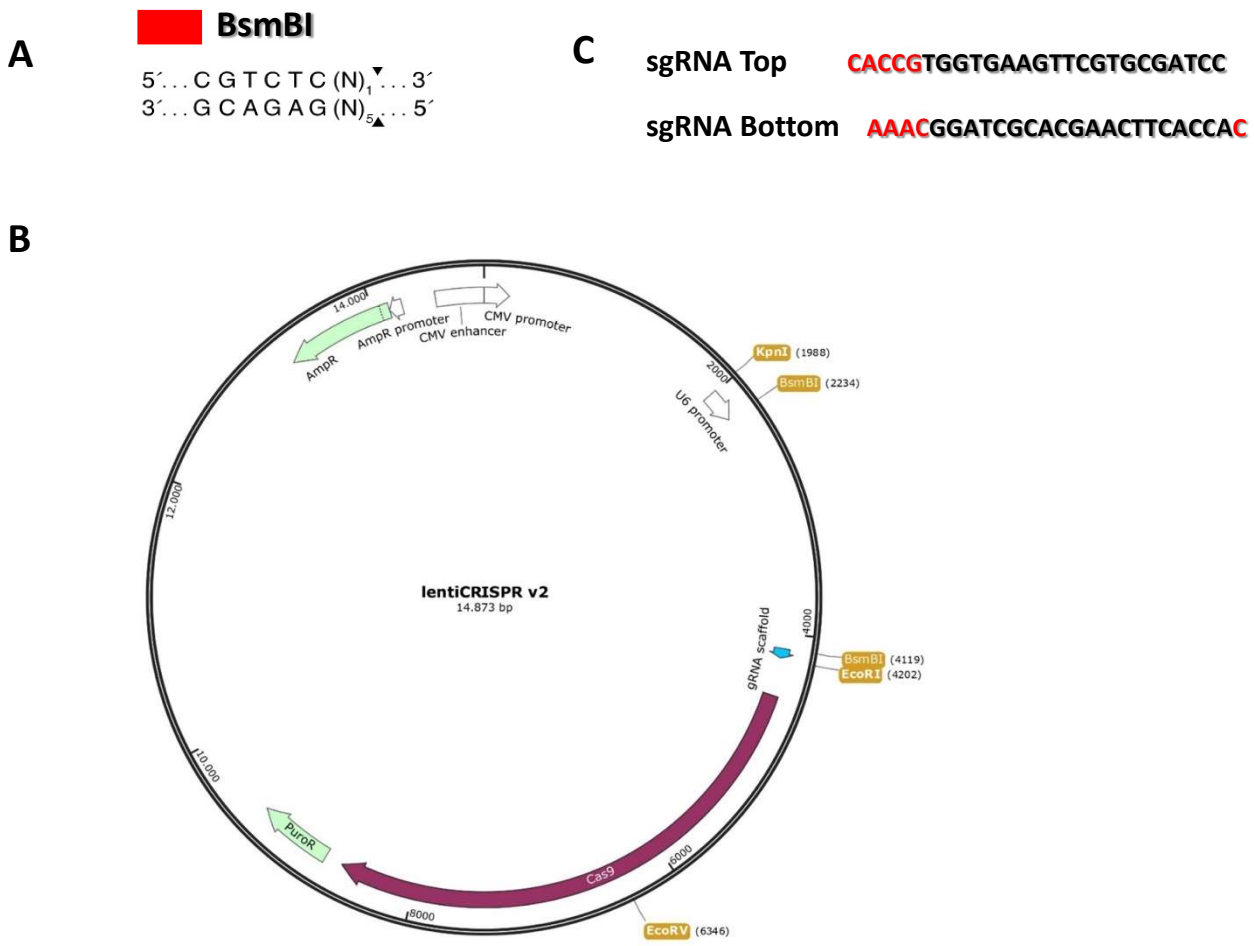

Figure 12. Preparation of the construct (Part 1)

A BsmBI non palindromic recognition sequence. Arrows indicate the cut occurring after 1 nucleotide (5'-3' strand) and 5 nucleotides (3'-5' strand) after the recognition site.

B LentiCRISPRv2 vector: the CMV enhancer and the U6 promoter controlling the transcription of the sgRNA and of the chimeric guide RNA; the BsmBI site to clone the sgRNA; the Cas9 coding sequence with a chicken promoter; the Puromycine and Ampicillin resistance.

C sequence of the single guide RNA to target exon 1β of p19Arf. In red are shown the 5' and 3' ends complementary to the 5' and 3' ends of the vector after BsmBI cut.

To clone sgArf into the lentiCRISPRv2, the plasmid was digested with the BsmBI enzyme and loaded on a preparative 0,8% agarose gel to isolate the linearized vector that, once purified, was ligated to the annealed sgArf (synthesized with 5' and 3' ends complementary to the BsmBI vector ends (Figure 13 and see Materials and Methods).

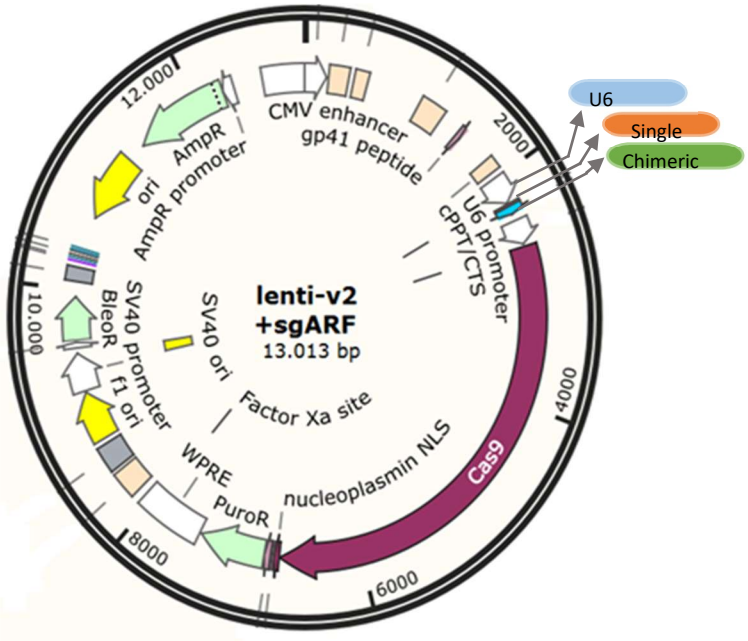

Figure 13. Preparation of the construct (Part 2)

The Figure shows the expected LentiCRISPRv2e vector after ligation with the single guide (sgArf) into the BsmBI restriction sites, downstream the U6 promoter and upstream the chimeric guide RNA.

The ligated product was then transformed in Stbl3 bacterial cells that were incubated over night at 37°C in the presence of 100µg/ml ampicillin. DNA was extracted from the two colonies obtained from the transformation of the ligation reaction and subjected to restriction map analysis (Figure 14), PCR amplification and Sanger sequencing (Figure 15).

For restriction map analysis, digestions with the following enzymes were performed: EcoRI, EcoRV and KpnI alone and together in different combinations. In particular, both the control vector (uncut lentiCRISPRv2) and the DNA obtained from the two colonies were digested as indicated in Figure 14:

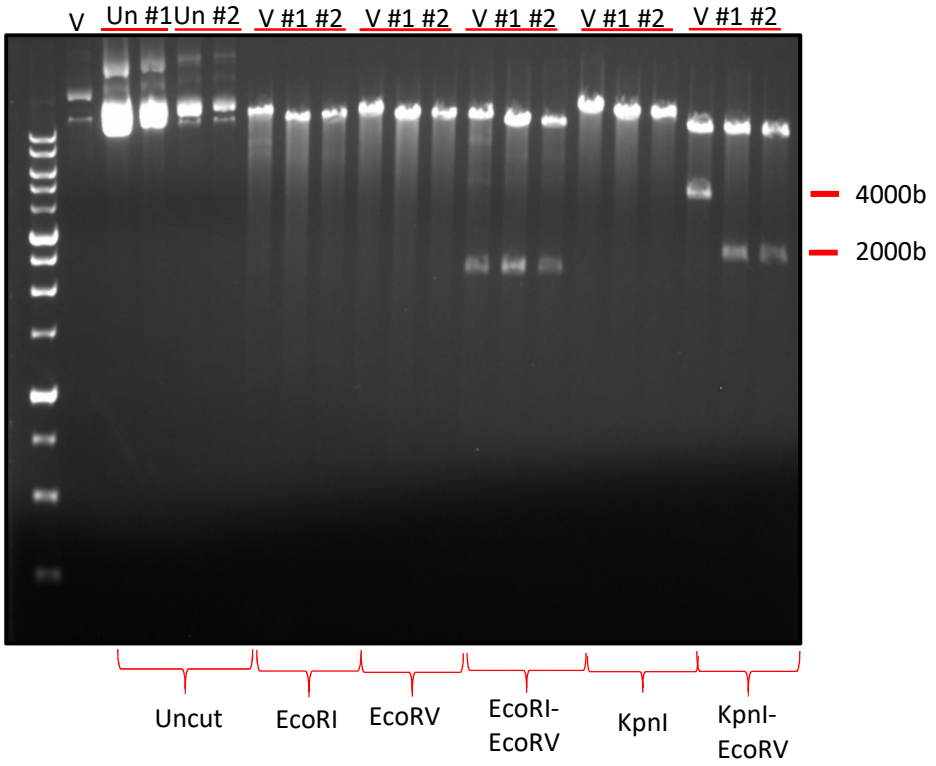

Figure 14. Restriction map of clones #1 and #2

Lane M: 1kb molecular weight Marker

Lane 1: V: Uncut *lentiCRISPRv2* vector

Lane 2 and 3: Uncut lentiCRISPRv2-sgArf Midiprep **#1** (two different concentrations)

Lane 4 and 5: Uncut Midiprep **#2** lentiCRISPRv2-sgArf (two different concentrations)

Lanes 6-20: lentiCRISPRv2 control vector **(V)**, Midiprep #1 (**#1**) Midiprep2 (**#2**) digested with the restriction enzymes indicated below.

As shown, both clone #1 and clone #2, following a double digestion with KpnI and EcoRV, release a fragment of 2000 bp, suggesting the success of the cloning strategy (see Figure 14, lanes 18, 19, 20)

Before proceeding with the sequencing of the clones, a PCR amplification was performed using a pair of primers that anneal to the U6 promoter and the sgArf.

The final check was performed by Sanger sequencing using the same primers that were used in the PCR.

Sequencing results confirmed that the sgp19Arf was correctly cloned into the lentiCRISPv2 vector without unexpected mutations (Figure 15).

Therefore, both molecular clones were good candidates for our purposes.

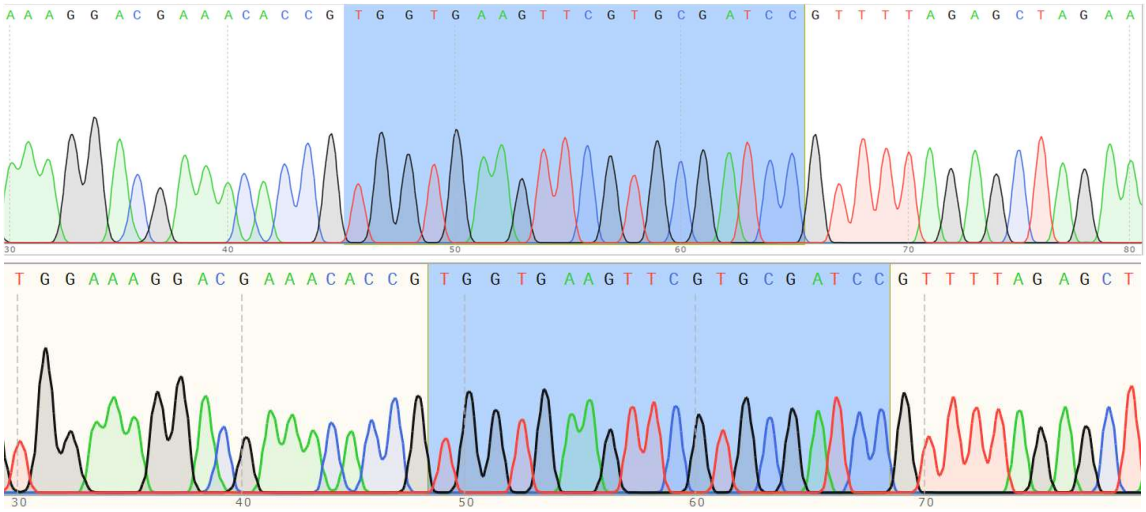

Figure 15. Electropherogram showing the Sanger sequencing results for the lentiCRISPRv2 sgArf on clones #1 and #2. The highlighted section shows the sequence of sgArf correctly cloned into the lentiCRISPRv2 vector.

Generation of p19Arf mutated mouse embryonic stem cells (mESCs)

Once the molecular constructs were validated, clone #1 (CRISPRv2Arf#1) was selected for transfection into mouse embryonic stem cells (mESCs) to obtain stably mutated p19Arf clones.

mESCs were transfected with either CRISPRv2Arf#1 or lentiCRISPRv2 (as negative control) vectors. Additionally, to quickly assess transfection efficiency, a plasmid containing a GFP cassette (pcDNA3-eGFP) was used in parallel.

For each experimental condition, 6 x 10^5 ESC (E14TG2a) cells were seeded in 60 mm dishes 24 hours prior to transfection (see Materials & Methods) and subsequently transfected using Lipofectamine® 2000.

Twenty-four hours after transfection, cells transfected with pcDNA3-eGFP were observed under phase contrast and fluorescence microscopy to evaluate the approximate rate of transfected cells that was estimated around 30% (Figure 16).

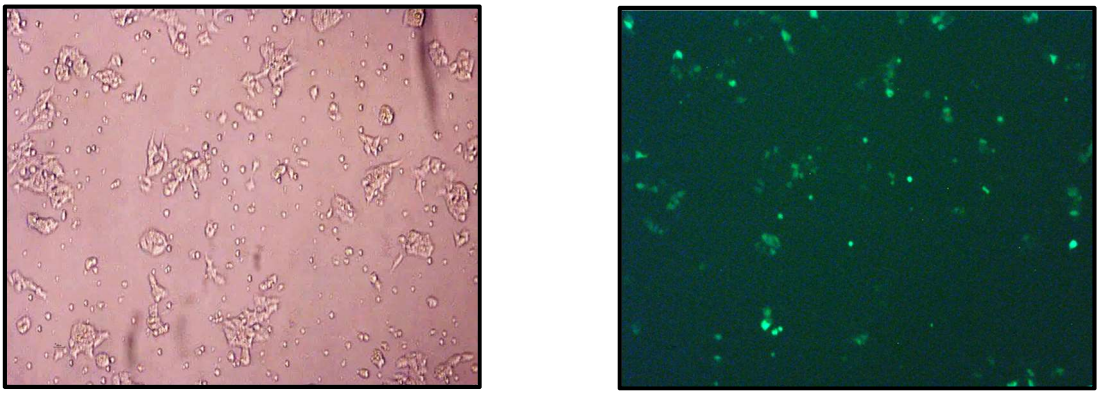

Figure 16. Evaluation of transfection efficiency

The left image shows transfected cells observed under phase contrast microscopy, while the right image displays only the transfected cells that express eGFP observed at fluorescence microscopy (Leica DMi8).

Forty-eight hours after transfection, cells were detached, and 1 x 10^6 cells for each experimental condition were replated in 100 mm dishes with 0.8 µg/mL puromycin added to the medium.

After 8 days cells were harvested from the 100 mm plates and plated in 0.32 cm^2 multiwell plates while maintaining high puromycin selection (0.8 µg/mL) (see the timeline in Figure 17) to obtain single clones.

42 clones were obtained from transfection with CRISPRv2Arf#1 and were plated in 96-well plates; of these, 14 clones were successfully transferred to a 24-well plates (1.9 cm^2) and subsequently to a 12-well plates (4 cm^2), while maintaining a puromycin concentration of 0.4 µg/mL. The clones were then expanded for validation. Similarly, E14TG2a cells were transfected with lentiCRISPRv2 ("empty" without sgRNA) to obtain a valid control for subsequent experiments (named CTRL).

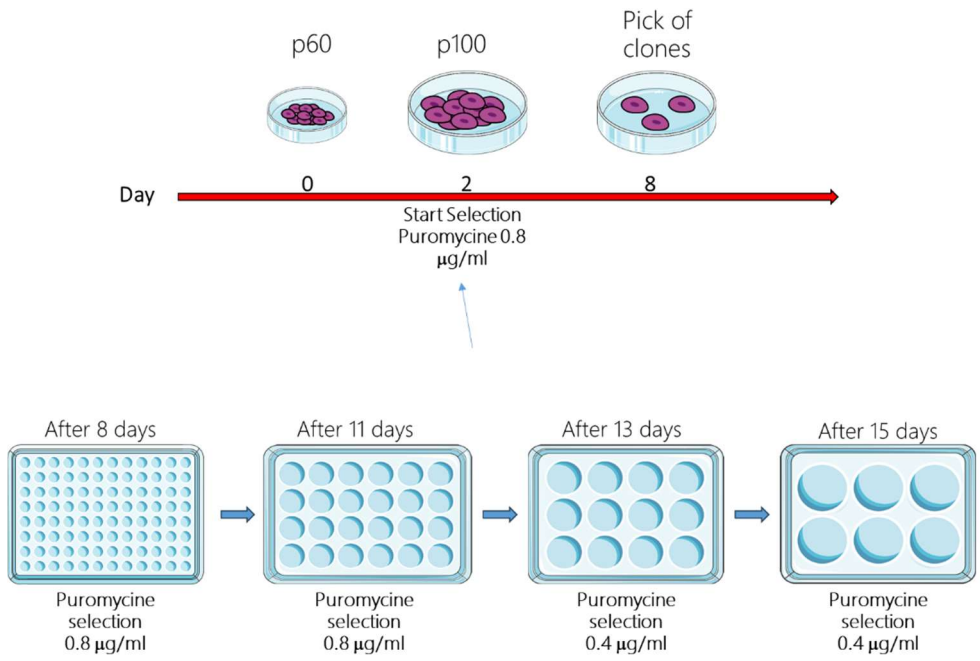

Figure 17. Workflow for the generation of E14-lentiv2-Cas9-sgp19Arf cell clones.

"E14 ES cells (E14TG2a) were transfected with lentiv2-Cas9-sgp19Arf (Day 0) in p60 dishes. Two days later, cells were plated in 100 mm dishes, and 0.8 µg/mL puromycin was added to start clone selection. Eight days after transfection clones were picked up and transferred to a 96-well plate while maintaining the same selection. The clones were then expanded by plating them in a 24-well plate, and then in a 12-well plate and a 6-well plate reducing puromycin concentration selection (0.4 µg/mL puromycin).

Validation of transgenic clones generated by transfection with CRISPRv2Arf#1

In order to introduce alterations in the targeted sequence using CRISPR-Cas9 technology, the first requirement is the expression of the Cas9 enzyme. So, at a first attempt, we decided to check its expression in transfected clones. To this attempt, total protein extracts from 14 clones derived by transfection with CRISPRv2Arf#1 (herein named mArf clones) were analyzed by Western Blot using a polyclonal antibody α-Cas9 (see Materials and Methods).

Western blot analysis revealed that three clones express the Cas9 protein at high or detectable levels (Figure 18).

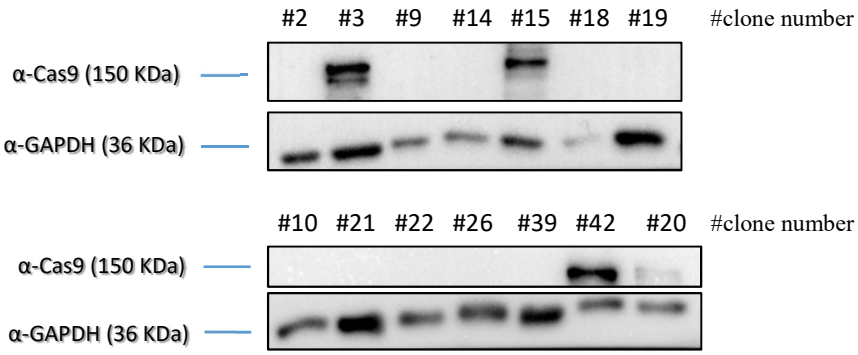

Figure 18. Evaluation of Cas9 protein expression levels in mArf clones.

Western Blot analysis on transgenic clones obtained by transfection with *CRISPRv2Arf#1*

As figure 18 shows, the Cas9 protein is expressed in mArf clones #3, #15 #42 and #20, Therefore, these clones were chosen for subsequent characterization.

Genomic DNA was extracted and subjected to PCR amplification of the region of interest to obtain sufficient template for sequencing analysis.

Due to the unique and repetitive nature of the p19 genome sequence, we tried different oligos in various combinations before succeeding. Figure 19 shows the sequence and the annealing regions of the selected oligos, which map at the 5'UTR and at an internal position of Exon 1β.

Figure 19. Sequence and position of Forward (Fw) and reverse oligos on the to p19Arf genomic sequence

The Fw oligo recognizes a sequence at the 5'UTR that is 126 bp upstream of the region targeted by Crispr-Cas9. The Rv oligo anneals to a sequence on exon 1β located 73 bp downstream of the sgArf target region. The image also shows the site of annealing of the guide (purple) and the potential cut site located upstream of the PAM sequence (red).

The 219 bp amplicon obtained from the PCR was then subjected to Sanger sequencing at the Eurofins Genomics facility.

The electropherogram results are shown in the Figure 20, 21, 22 and 23.

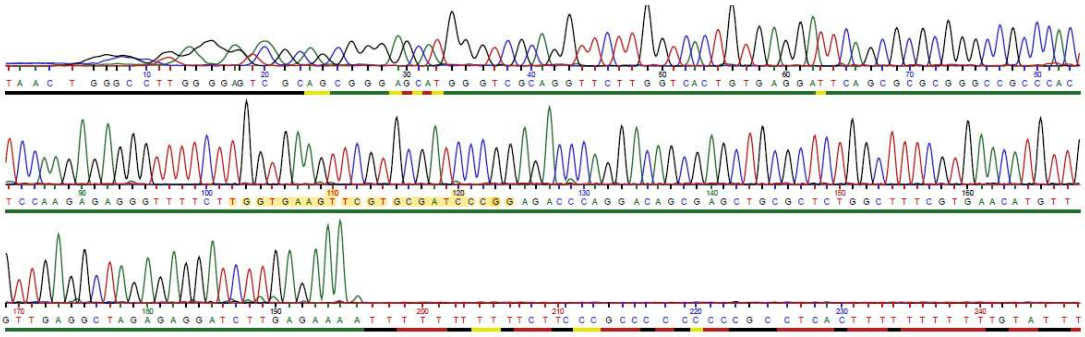

Figure 20. Electropherogram results of mArf clone #3

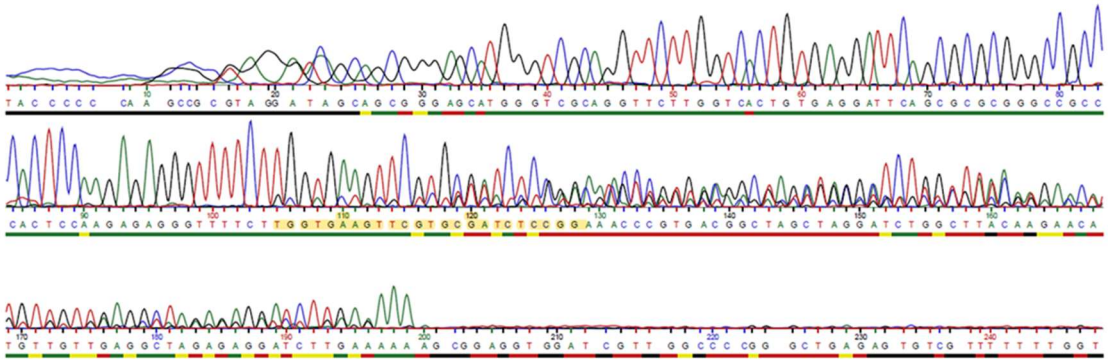

Figure 21. Electropherogram results of mArf clone #15

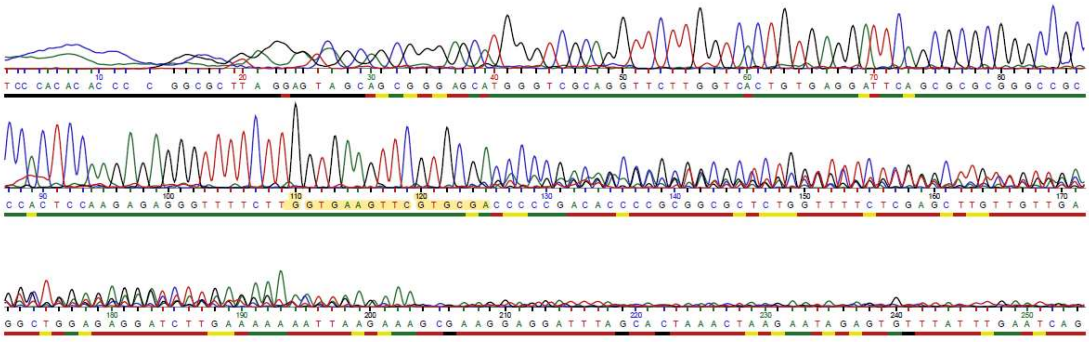

Figure 22. Electropherogram results of mArf clone #42

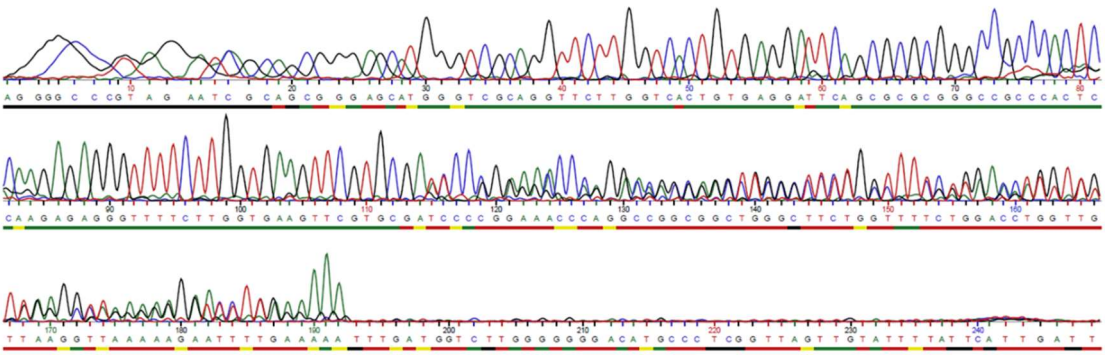

Figure 23. Electropherogram results of clone #20

The sequencing results were analyzed by identifying the wild-type sequence peaks through alignment with the p19Arf wild-type sequence. From this analysis it turned out that clone #3 is completely wild type while clones #15, #42 and #20 appear significantly altered in the region of interest. However, sequencing results are not optimal as indicated by the presence of more than two peaks, suggesting that the samples are not derived from single clones. Therefore, we decided to proceed with a subcloning strategy in order to obtain more homogeneous clones.

To this purpose, $1x10^6$ cells for each clone (#42, #15 and #20) were plated in a two 100mm dish in the presence of 0,4 μg/mL puromycine (Figure 24). After 4 days visible clones were picked up and plated again into a 0,32 cm^2 well. The cells were then plated in progressively larger dishes to facilitate the separation of individual clones (see Materials and Methods).

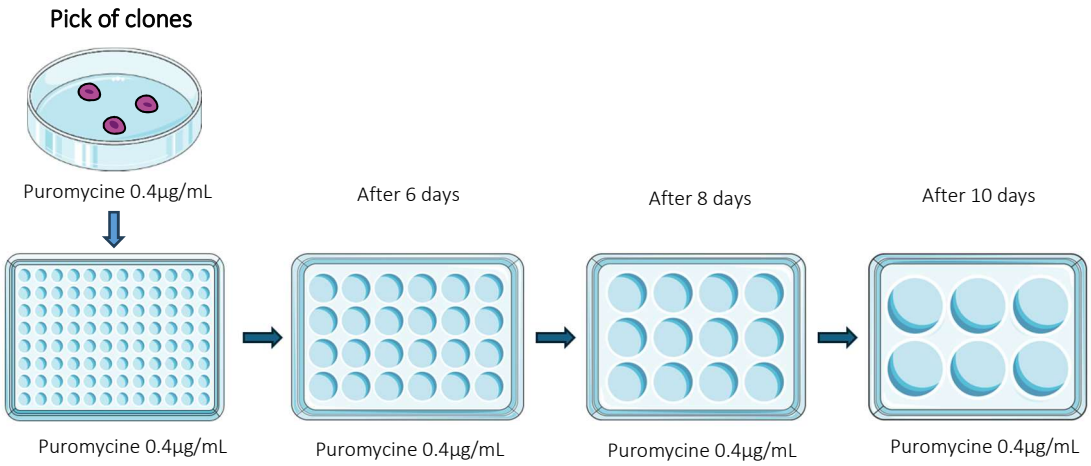

Figure 24. Workflow for subcloning.

After 10 days, we obtained well-separated clones from each of initial clones. Three clones in total were analyzed by sequencing as previously described: genomic DNA extraction and PCR amplification were used to amplify a 219 bp amplicon that was subsequently analyzed by Sanger sequencing thanks to Eurofins Genomics facility.

The sequencing results demonstrated a successful reduction in sequence variability among the subclones. The electropherogram results are shown in Figures 25, 26, and 27.

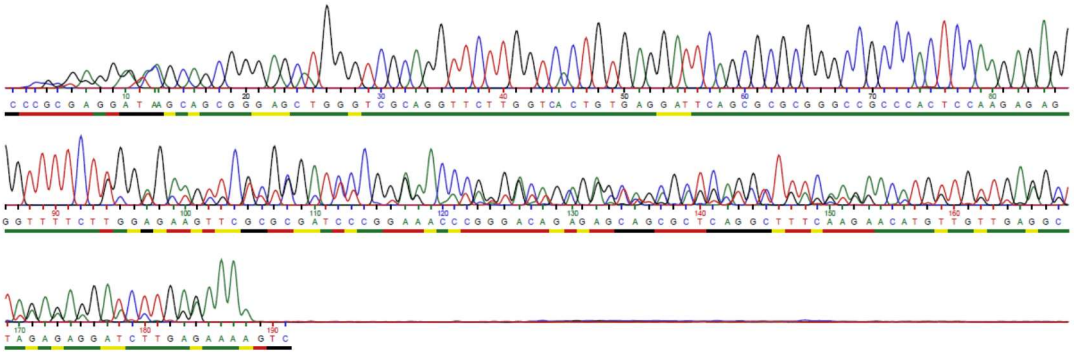

Figure 25. Electropherogram results of mArf subclone #15 .

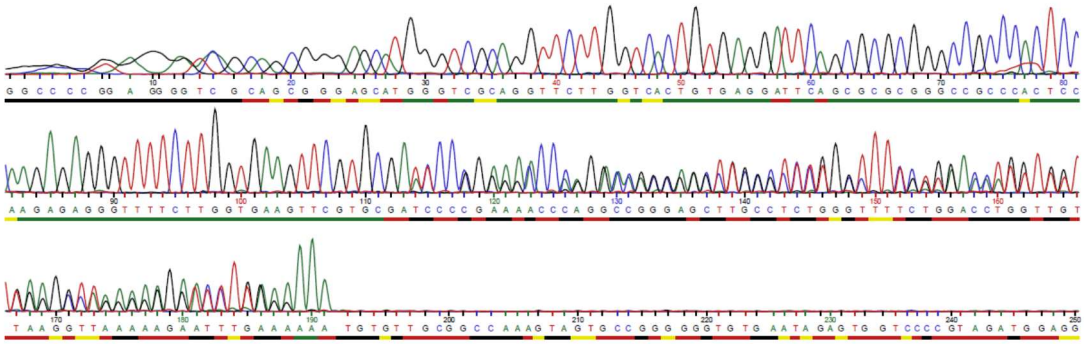

Figure 26. Electropherogram results of mArf subclone #20.

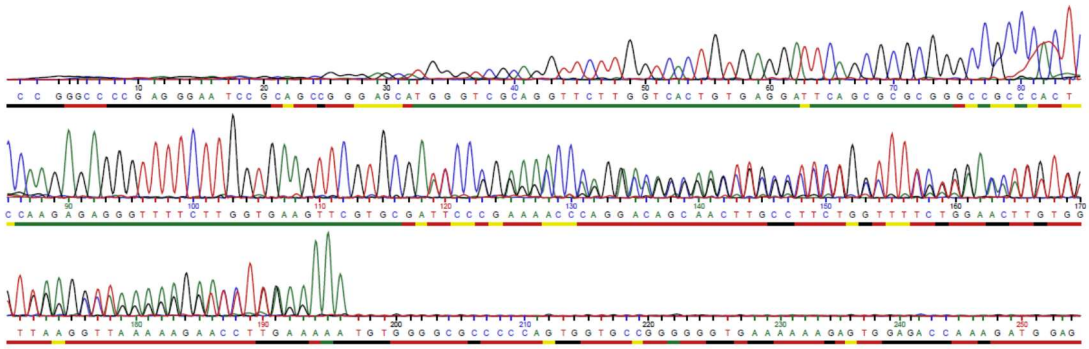

Figure 27. Electropherogram results of mArf subclone #42.

The obtained DNA sequences were compared to the wild-type sequence to identify the presence of mutations. Using the SnapGene Viewer software we identified the codons altered by the various mutations in the coding sequence (Figure 28). In all cases, there are profound alterations in the expected region. In particular, all mArf clones present a truncated allele and various changes in the remaining allele, except for clone 20.

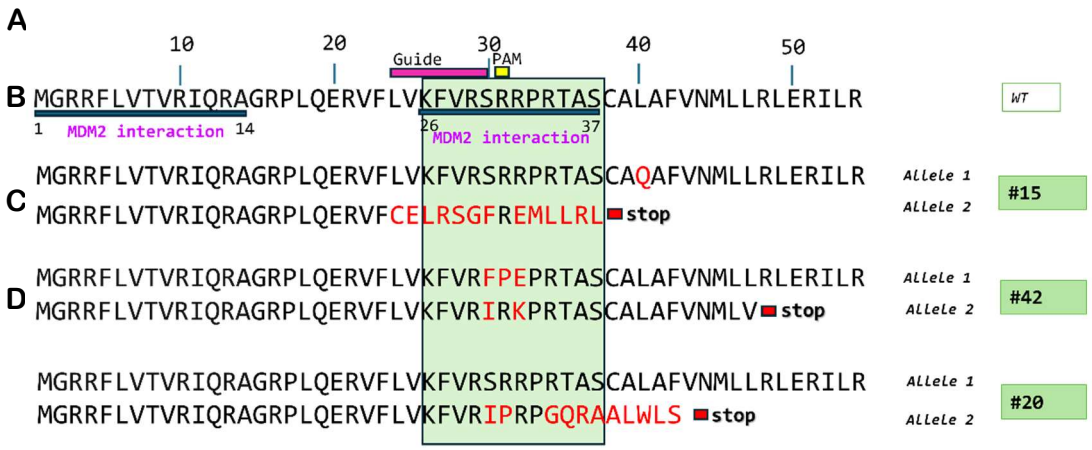

Figure 28. Deduced amino acidic sequence of mArf clones

The image shows the amino acidic sequence of p19Arf exon 1β in wild type (A), mArf #15 (B), mArf #42 (C) and mArf #20 (D). Evidenced are the MDM2 interaction sites (purple line), the sgArf (Guide) recognition site (pink) and the PAM sequence (yellow). All clones exhibit an allele containing a STOP codon between aa 37-47 depending on the clone, along with various alterations in the remaining allele (except for clone 20).

Set up of mESCs and control cells differentiation toward PPCs (pancreatic progenitor cells)

Once the presence of extensive mutations in the desired region of Arf's exon 1β in the three subclones was confirmed by sequencing analysis, we decided to analyze the effect of these mutations. However, since p19Arf is absent in ESCs and is expressed during a specific time window during pancreatic differentiation (see preliminary data in the Aim of the thesis), it is necessary to differentiate ESCs toward the pancreatic lineage in order to analyze the phenotype.

Using a validated differentiation protocol (De Angelis, et al., 2014), we first analyzed the phenotypes of wild-type ESC-E14TG2a vs control cells (CTRL) (derived by transfection of ESCs with the empty vector) that were induced to differentiate (Figure 29).

Briefly, definitive endoderm (DE) formation is induced during the priming step by Activin A on Day 4. Subsequently, the cells are further directed toward posterior foregut endoderm (PPCs) on Day 8 using RA and FGF10 (for details see Materials and Methods).

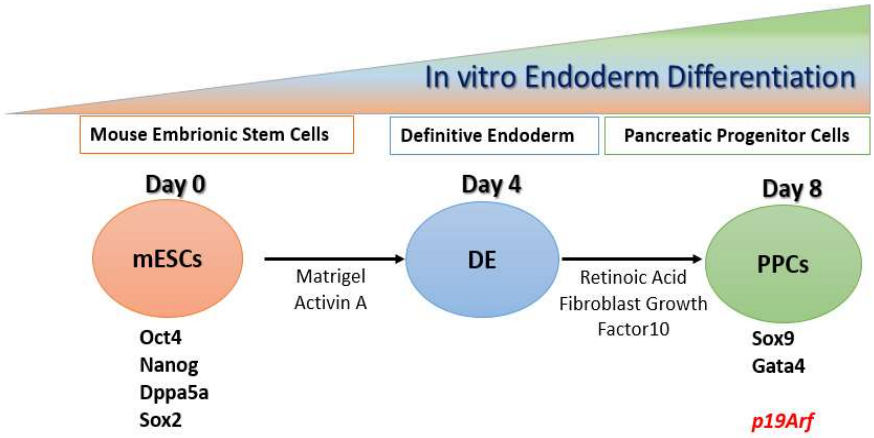

Figure 29. Protocol of mESCs differentiation toward pancreatic lineage.

The figure shows the timeline used to differentiate mESCs into pancreatic progenitor cells over 8 days. On day 0, the cells (expressing Oct4, Nanog, Sox2, and Dppa5a) were treated with Activin A in Matrigel for the first four days to generate definitive endoderm (DE). For the subsequent four days, the cells were treated with retinoic acid and fibroblast growth factor10 to differentiate the definitive endoderm into pancreatic progenitor cells. The evaluated markers for the pancreatic progenitor cells were Sox9, Gata4, and p19Arf.

Wild type mESCs and the control (CTRL) were plated in 6-well dishes (9 cm^2) and treated as described to induce pancreatic differentiation (Figure 29).

The first evaluation we conducted was a morphological analysis using a phase contrast microscope (Leica DMIL Led) to observe changes occurring during the differentiation process (Figure 30).

As expected, the morphology of the cells changed during treatment: at day 0, the cells exhibited a rounded morphology typical of mESCs in culture. They then formed a distinct structure by joining together, and by day 8, they acquired a 'spider web' or basket-like structure characteristic of pancreatic progenitor cells. Importantly, there were no significant differences between the wild-type and control cells, both of which exhibited the same morphology.

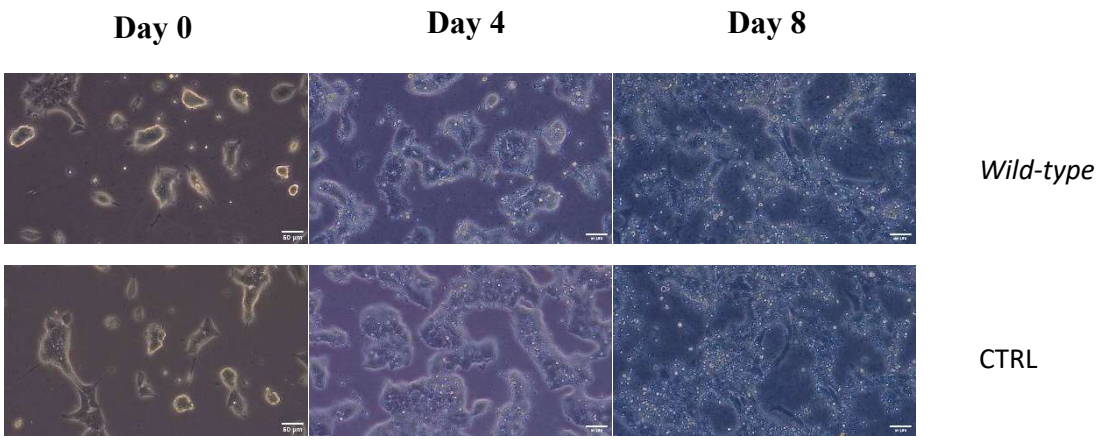

Figure 30. Phase contrast microscopy images (Leica DMIL LED) of clones during pancreatic differentiation.

Cells were observed at three experimental time points: day 0, day 4, and day 8, using a 20X objective. The morphological analysis indicates that there are no differences between wild-type cells and CTRL (control) cells during pancreatic differentiation. By day 8, both exhibited a basket-like morphology typical of pancreatic progenitor cells.

Subsequently, as differentiation toward PPCs is characterized by a change in the expression patterns of specific markers (see Figure 29), we decided to analyze the expression of p19Arf, as well as stemness and differentiation markers using Real-Time PCR at different time points (day 0, day 4, and day 8) during differentiation of wild type and control cells. To this end, cells were collected, RNA was extracted, retrotranscribed into cDNA, and subjected to Real-Time PCR (see Materials and Methods). We choose to analyze the expression of Oct4 as a stem cells marker and of Sox9 which marks PPCs. As expected, Oct4 expression decreased significantly as the cells differentiated from day 0 to day 8, while Sox9 expression gradually increased, confirming that the differentiation process was, indeed, correctly occurring (Figure 31). Importantly, Arf's levels increase, as expected, both in wild type cells and in CTRL cells mostly at the same extent.

Western Blot analysis are almost in agreement with Real Time PCR results (Figure 32). Since the CTRL exhibited a completely overlapping trend with that of the wild

type (particularly at the end of differentiation), both at cellular and molecular levels it was used in most of the subsequent experiments as it serves as a more suitable reference point.

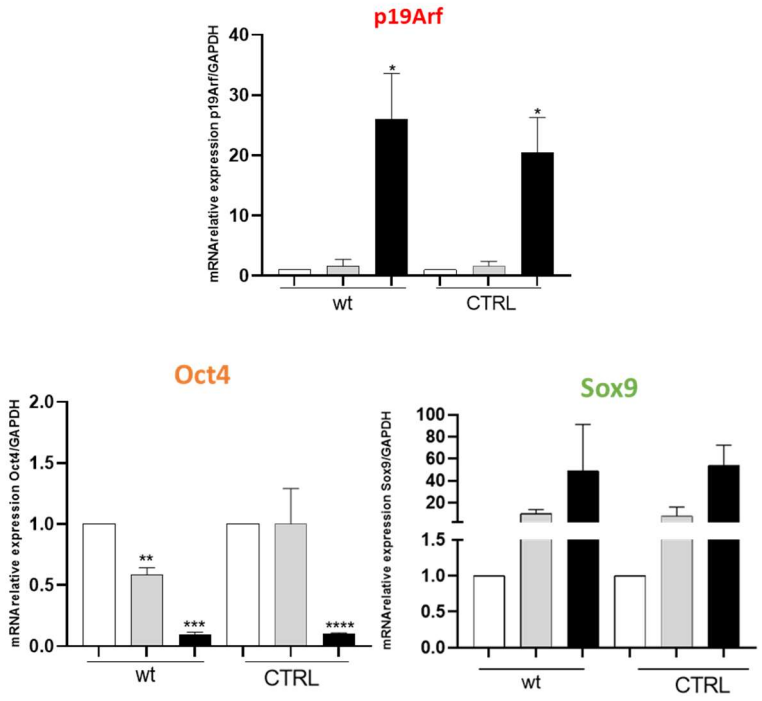

Figure 31. Analysis of the expression of Arf, Oct4 and Sox9 markers in wild type cells and control cells at day D0, day D4 and day D8 by qPCR. The graph shows data from a representative experiment performed in technical triplicate ± SD. Significance was determined using unpaired t-test followed by Dunnett's multiple comparison tests. ** ($p < 0.01$), ***($p < 0.001$) and ****($p < 0.0001$) represent the significance of the reduction compared to day 0 (D0).

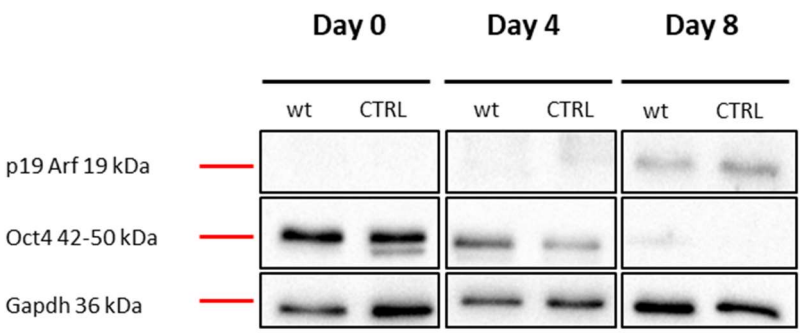

Figure 32. Representative western blot showing the expression of p19Arf and Oct4 markers in wild type cells and control cells at Day 0, Day 4 and Day 8 of differentiation.

The panel is a representative Western Blot showing p19Arf protein levels at Day 0 and Day 8. Cells were collected at the time points indicated and total protein extract was prepared and run on a 12%SDS gel, transferred to a nitrocellulose filter and hybridized to α-arf antibody and α-Gapdh antibody (see materials and Methods for details). Band intensities were quantified by ImageLab BioRad software and normalized respect to loading controls (Gapdh).

Analysis of the effects of mutations in p19Arf on pancreatic differentiation

After setting up the differentiation protocol, we proceeded with the treatment of the p19Arf mutated clones. Control cells and cells from mArf clones #15, #42, and #20 were induced to differentiate toward PPCs as previously described (see also the Materials and Methods section), and phenotyping was performed using several approaches.

Morphological analysis of p19Arf mutated clones during pancreatic differentiation.

Cells (both from control, CTRL, and mArf #15, #20, #42 clones) were plated in 6-well dishes (9 cm^2) and treated as described above to induce pancreatic differentiation. Morphological analysis by confocal microscopy at the three different time points (Day 0, Day 4 and Day 8) revealed significant differences in the behavior of p19Arf mutated clones compared to control (Figure 33). Specifically, at day 0, all cells displayed a rounded, stem-like morphology typical of cultured mESCs in both the control and p19Arf mutated clones. This is not unexpected, as Arf is silenced in stem cells (Li, et al., 2009 and 2012) and start to be expressed *in vitro* at day 4 (Montano, et al., 2021).

In contrast, several differences emerged during treatment. On day 4, when control cells began to lose their stem phenotype and tend to adopt a differentiative morphology, the subclones (#15, #42, and #20) maintained a rounded shape, indicating defects in the differentiative program. By day 8, the differences are more striking as control cells acquired a basket-like morphology typical of progenitor cells, indicating a correct execution of the differentiative program, while mutated clones maintain a stem-like phenotype (especially clones #20 and #42).

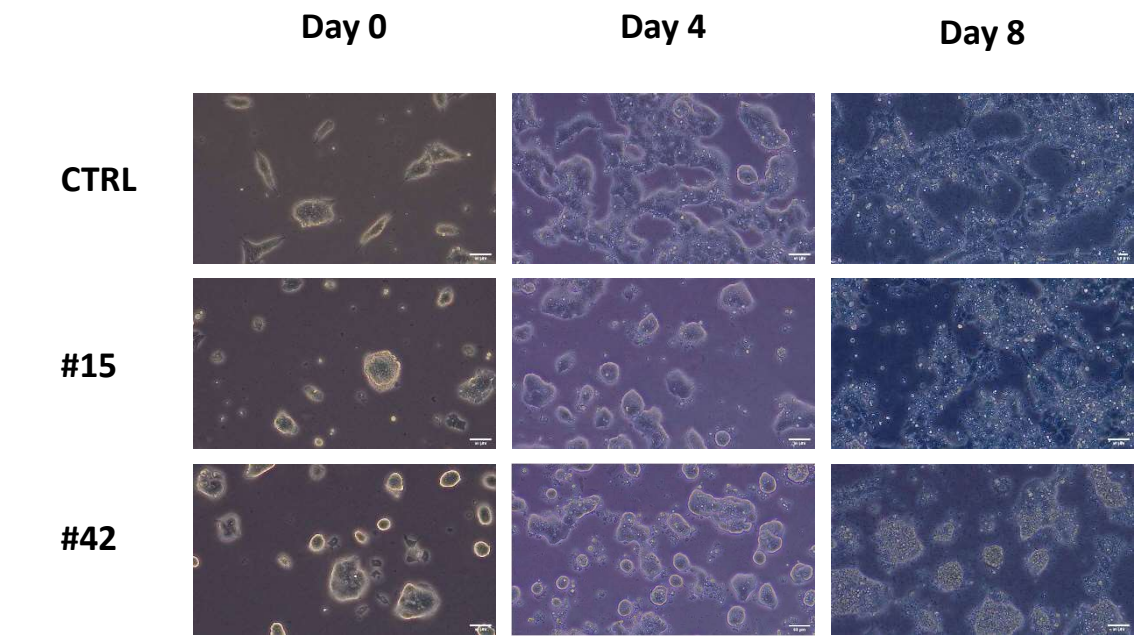
Day 0
Day 4
Day 8
CTRL
#15
#42

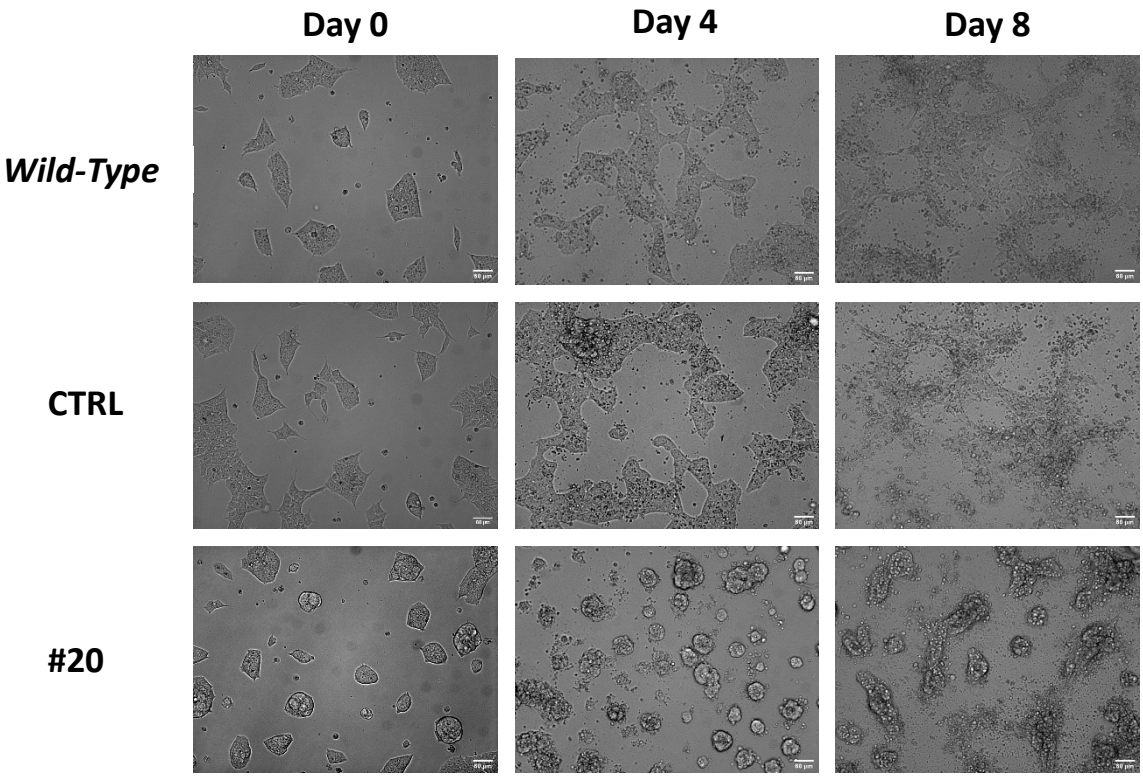
Day 0
Day 4
Day 8
Wild-Type
CTRL
#20

Figure 33. Phase contrast microscopy analysis of cell morphology during pancreatic differentiation toward the pancreatic lineage. The images are representative of the behavior of control and p19Arf mutated clones during pancreatic differentiation in two representative experiments. Upper panel was captured with a phase contrast Leica microscope DMIL LED using a 20X objective, and the lower panel with a phase contrast Leica microscope DMi8 using a 20X objective. Initially, all cells exhibit a clonal morphology; however, by day 4, differences emerged between control cells and mutated clones. In particular, clones #15 and #42 (upper panel) and #20 (lower panel) display rounded morphology, while control cells acquire the morphology of definitive endoderm cells. By day 8, control cells exhibit a "basket-like" morphology, while #15 shows a structure that appears to have some basket characteristics but differs from control cells. The most significant differences compared to controls were observed in #42 and #20, which seem to maintain rounded morphology even at day 8 of differentiation.

We then decided to explore the morphology of the clones by staining them with a fluorescent conjugate of phalloidin which stains F-actin filaments and allows us to reveal changes in cytoskeletal rearrangements during differentiation.

Cells from control, clone #20 and #42 were plated in LabTech plates (2.5 cm^2) and treated to differentiate toward PPCs as described before (Figure 29 and Materials and Methods). At different time points cells were fixed with paraformaldehyde and stained with rhodamine-phalloidin and DAPI to stain the nuclei (see Materials and Methods) (Figure 34).

Strikingly, p19Arf mutated clones clearly tend to maintain a more prolonged rounded morphology compared to the control, which acquired the correct basket-like structure at the end of the *in vitro* differentiation, further suggesting that p19Arf mutated clones tend to maintain a more prolonged stem like phenotype.

In particular, while CTRL cells acquire the correct structure by day 8, #42 and #20 cells tend to assume either an enlarged and cohesive structure resembling the typical definitive endoderm morphology or maintain the rounded morphology characteristic of day 0.

We also attempted to analyze p19Arf localization by immunofluorescence, as we expected that a mutated p19Arf might not localize correctly. Unfortunately, attempts to analyze p19Arf localization were unsuccessful probably because cells are poorly permeable to the antibody due to their tendency to grow in clusters. Therefore, experiments are ongoing to improve the protocol by optimizing cell permeabilization and preparing sections using a cryostat.

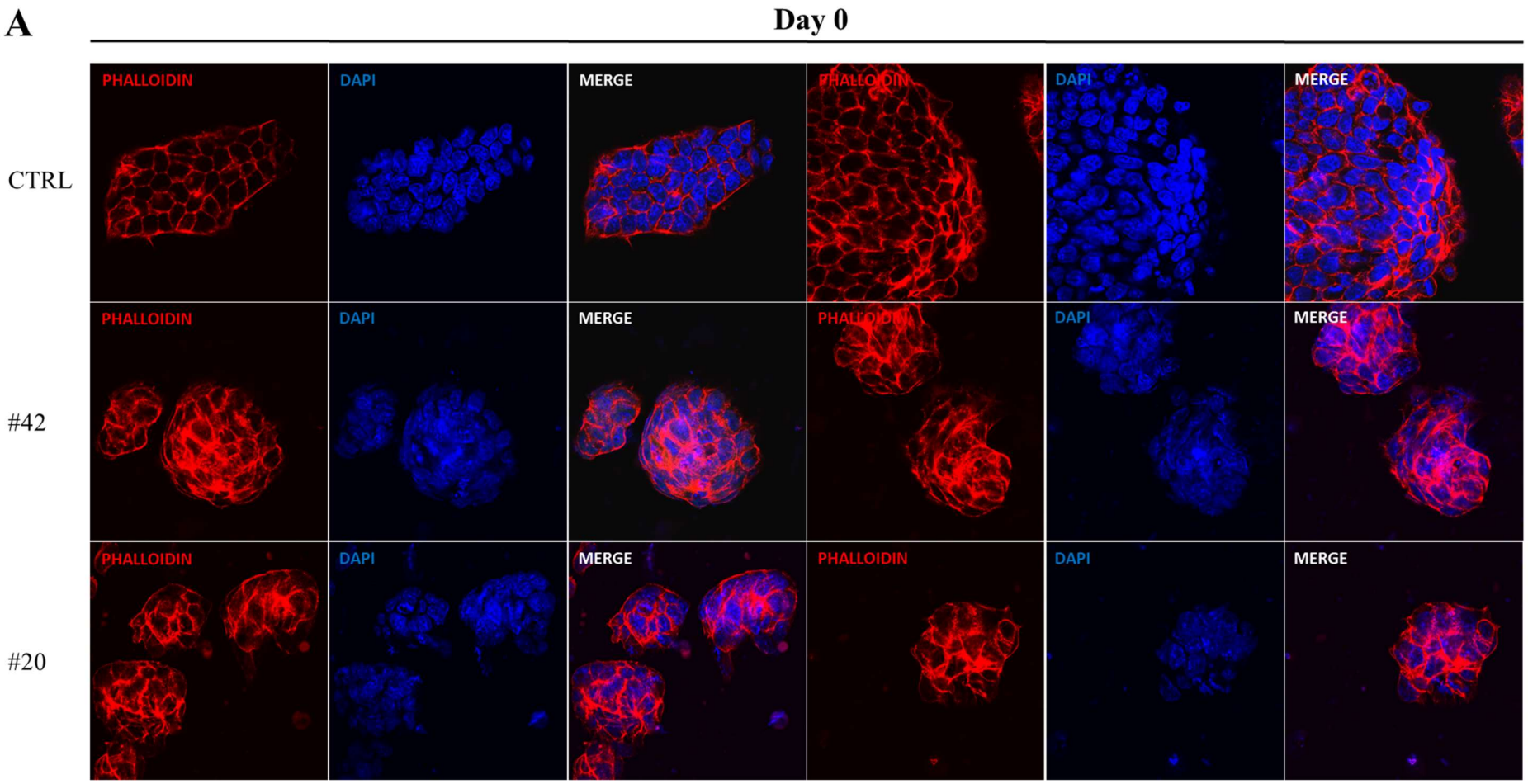
A
Day 0
CTRL
#42
#20
PHALLOIDIN
DAPI
MERGE

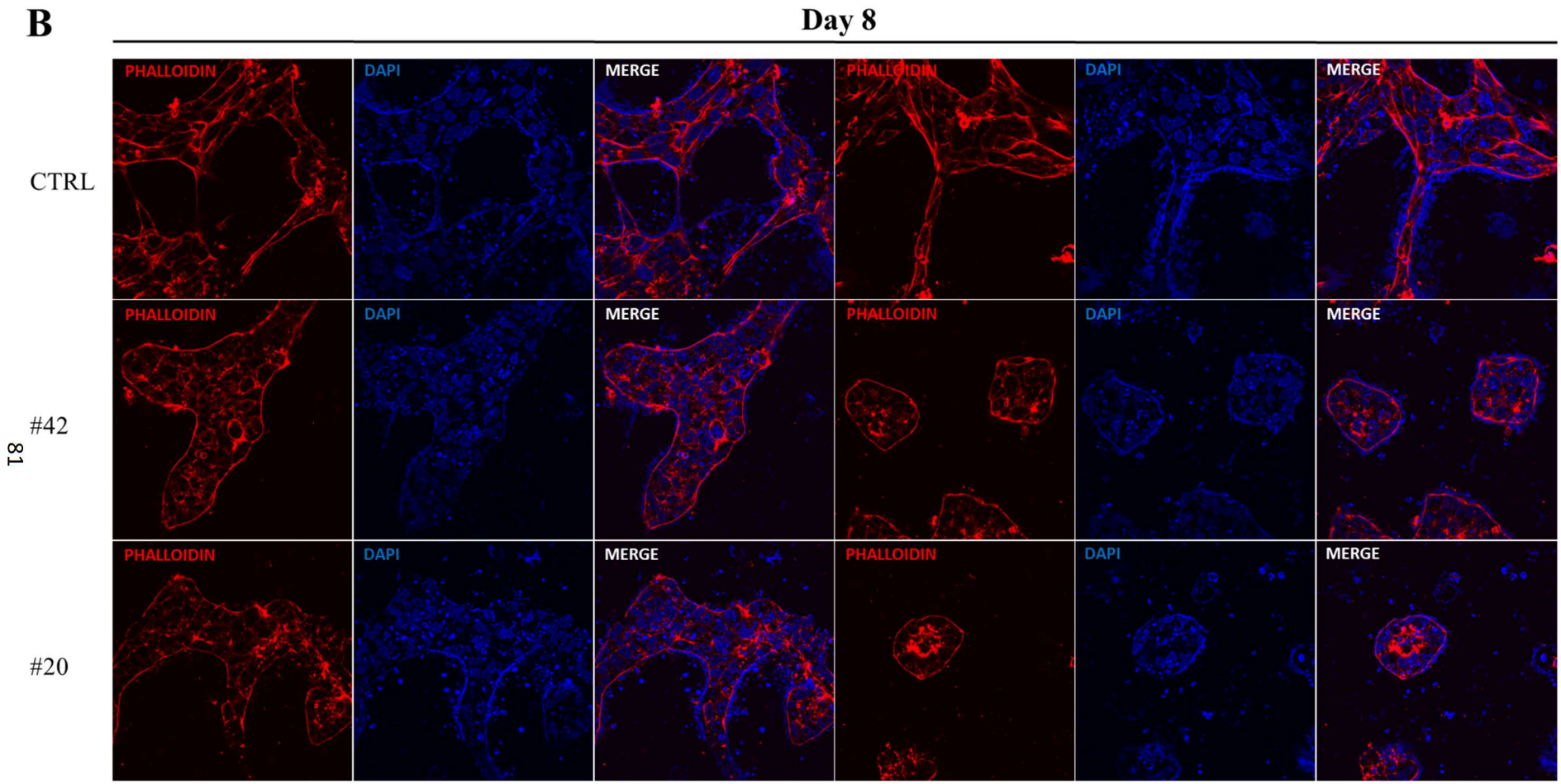
B
Day 8
CTRL
#42
#20
PHALLOIDIN
DAPI
MERGE

Figure 34. Evaluation of morphological changes at day 8 by rhodamine-phalloidin staining.

The panels show representative images acquired with 60X objectives of an Olympus confocal microscope FV3000. Phalloidin staining of F-actin is shown in red (by using rhodamine-phalloidin), while DAPI staining to highlight the nuclei is shown in blue. At day 0 (A) all cells exhibit the rounded morphology typical of stem cells in culture. By day 8 (B), the control cells form 'basket structures,' while the mutated clones #42 and #20 tend to maintain the rounded morphology or acquire broader and less structured structures resembling those observed on day 4.

Molecular analysis of p19Arf mutated clones during pancreatic differentiation.

To analyze whether the morphological differentiation defects observed are also accompanied by changes in the pattern of gene expression during differentiation, RNA was extracted from control cells and mArf mutated clones at Day 0 and Day 8, reverse-transcribed into cDNA and levels of expression of different stemness and differentiation markers was analyzed by RT-qPCR (see Materials and Methods). Day 4 was excluded from the analysis because the most striking phenotype is observed on Day 8, when Arf levels also reach their highest levels.

We chose to analyze the following markers: Oct4, Nanog, Sox2, and Dppa5a as stemness markers, and Gata-4, Sox9, Pdx1, and p21 as differentiation markers, for several reasons outlined below. Collectively, chosen differentiation markers are among the key factors involved, on one hand, in maintaining the multipotency of pancreatic progenitors by ensuring a continuous reserve necessary for organ's plasticity, and, on the other hand, because they serve as pioneering factors in the specification of the pancreatic lineage.

Oct4 plays a crucial role in regulating pluripotency in embryonic stem cells, being highly expressed in these cells but silenced during differentiation. The level of Oct4 expression significantly influences the fate of the stem cells. Together with Sox2, Nanog, and other key regulators, Oct4 activates essential protein-coding genes and noncoding RNAs for maintaining pluripotency. Additionally, Oct4 works with transcriptional repressive complexes to suppress genes associated with developmental processes (Shi, et al., 2010).

Nanog is a homeodomain protein essential for the propagation of undifferentiated embryonic stem (ES) cells, present in pluripotent mouse and human cell lines but absent in differentiated cells. In preimplantation embryos, Nanog is confined to founder cells that give rise to ES cells. It functions alongside cytokine stimulation

of Stat3 to promote ES cell self-renewal. Interestingly, increased Nanog expression from transgene constructs can lead to clonal expansion of ES cells, bypassing the need for Stat3 while maintaining Oct4 levels (Chambers, et al., 2003).

Maintaining pluripotency in stem cells requires precise regulation of *Sox2* expression; both high and low levels can lead to a loss of pluripotency by diminishing the activity of Sox2-Oct4 target genes. Sox2 expression must remain in dynamic equilibrium with other synergistic factors. This is further supported by the cooperation of Sox2 with other dose-dependent transcription factors, such as Oct4 and Nanog, in regulating pluripotency (Zhang, et al., 2014). Together, Oct4 and Sox2 control downstream genes essential for maintaining pluripotency and inhibiting differentiation (Loh, et., al 2006).

Dppa5a/Esg-1 transcripts are low in the unfertilized egg but significantly increase during zygotic genome activation at the two-cell stage, continuing through preimplantation to the blastocyst stage. This differs from Oct3/4, which is present in oocytes but activated only at the eight-cell stage. Esg-1 and Oct3/4 show similar gene expression patterns, and Esg-1 appears to be downstream of Oct3/4, as repressing Oct3/4 in mouse ES cells leads to a decrease in Esg-1 expression (Tanaka, et al., 2002).

Sox9 is a specific marker and maintenance factor for multipotential progenitors during pancreas organogenesis as well as of multiple organs, including testis, chondrocytes, heart, lung, pancreas, bile duct, hair follicles, kidney, inner ear, retina and the central nervous system (Stolt, et al., 2003; Chaboissier, et al., 2004; Akiyama, et al., 2005; Furuyama, et al., 2010; Seymour, et al., 2007). It is expressed in a mitotically active, Notch-responsive subset of $PDX1^{+}$ pluripotent progenitors, but not in committed endocrine precursors or differentiated cells. Sox9 helps maintain these pancreatic progenitors by promoting their proliferation, survival, and retention in an undifferentiated state (Seymour, et al., 2006).

Gata4 is a transcriptional regulatory factor that governs the development of endoderm-derived organs, such as the heart and the gut. It may functions as a putative tumor suppressor, as its re-expression increases p53 gene expression. The findings suggest that GATA4 may also influence cell proliferation and differentiation during pancreatic cancer progression (Gong, et al., 2018).

Pdx1 is a master regulator of early pancreatic development, initially expressed in all pancreatic progenitors but later restricted to β- and δ-cells during endocrine differentiation (Wang, et al., 2018). The three differentiated adult pancreatic cell types , acinar, ductal, and endocrine, arise from a common $Pdx1^+$ progenitor during embryonic development. Ablation of Pdx1 results in pancreatic agenesis, underscoring its critical role in the formation of both exocrine and endocrine cells (Edlund, et al., 2002; Offield, et al., 1996; Stoffers, et al., 1997).

The Nkx family of homeodomain factors includes several members, with *Nkx6-1* being crucial for foregut patterning, pancreas organogenesis, and the development of both the central and peripheral nervous systems (Burtscher, et al., 2021; Li et al., 2016; Prakash, et al., 2009). Specifically, during pancreas development, Nkx6-1 is vital for the patterning of the pancreatic epithelium (Schaffer, et al., 2010).

Furthermore, Pancreatic and Duodenal Homeobox 1 (PDX1) and NKX6.1 are two primary transcription factors expressed in multipotent pancreatic progenitor cells (MPCs) and functional β cells. NKX6.1 is expressed from early stages of pancreatic development and persists in adult β cells, playing several essential roles throughout this process (Aigha, et al., 2020). In mice, Nkx6.1 is first expressed in the pancreatic epithelium at embryonic day 9.5 (E9.5) and continues to be expressed until embryonic day 13 (E13).

Cell cycle arrest or exit from cell cycle is a crucial first step toward terminal differentiation, quiescence, or senescence, often associated with increased *p21* expression. Several evidences suggest that p21 can have either a positive or

negative impact on differentiation, depending on the cell type and stage of differentiation. Overexpression of p21 can induce differentiation in various normal and tumor cells by promoting cell cycle exit (Kreis, et al., 2019).

At a first attempt we checked the transcriptional and protein levels of p19Arf in control cells and mArf #15, #42 and #20 clones (Figure 35 A and B). As expected, Arf levels rise up at Day 8 in both control and mutated clones, confirming that experimental conditions are effective. Analysis by Western Blot reveal lower levels of p19Arf proteins in mArf clones.

Therefore, the expression levels of stemness markers (Oct4, Nanog, Sox2 and Dppa5a) and differentiation markers (Sox9, Gata4, Pdx1 and p21) were analyzed in both the control and p19Arf-mutated clones both at Day0 and Day8 of differentiation (Figure 36).

A

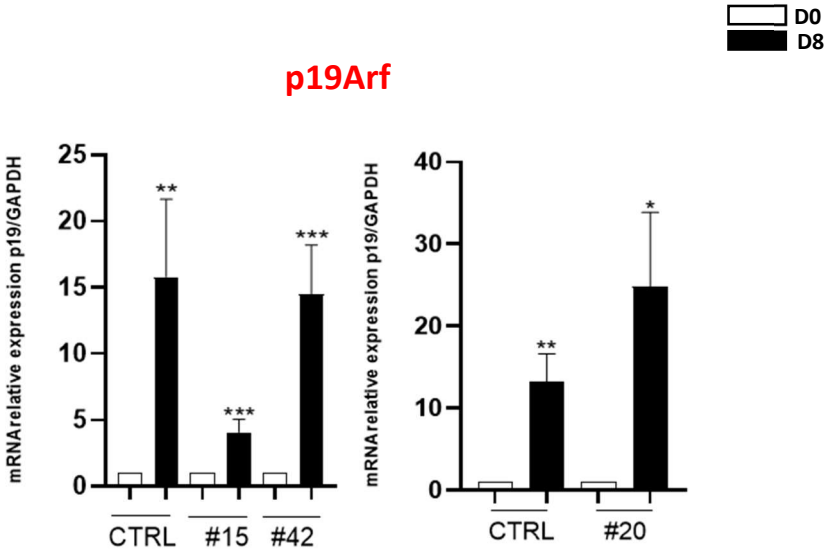
D0
D8
p19Arf
mRNArelative expression p19/GAPDH
25
20
15
10
5
0
**
***
***
CTRL
#15
#42
mRNArelative expression p19/GAPDH
40
30
20
10
0
**
*
CTRL
#20

B

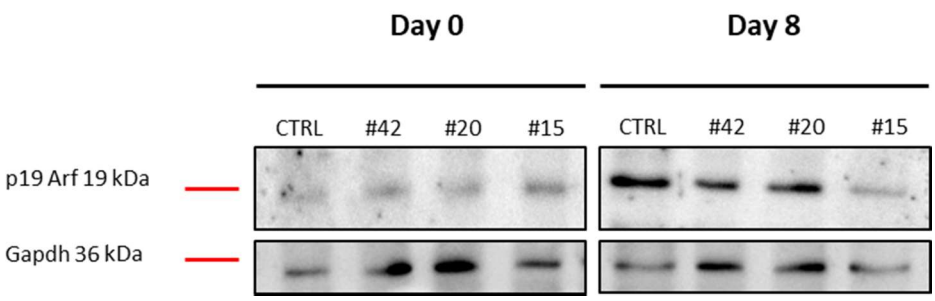
Day 0
Day 8
CTRL
#42
#20
#15
CTRL
#42
#20
#15
p19 Arf 19 kDa
Gapdh 36 kDa

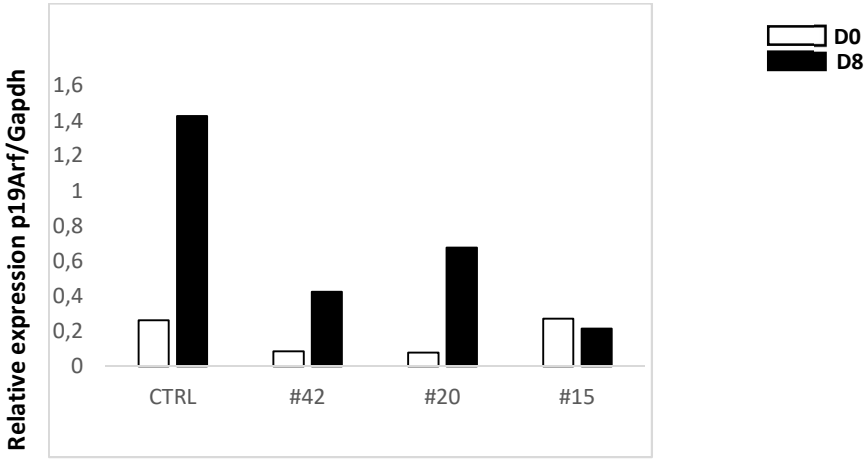
D0
D8
Relative expression p19Arf/Gapdh
1,6
1,4
1,2
1
0,8
0,6
0,4
0,2
0
CTRL
#42
#20
#15

Figure 35. RTqPCR and Western Blot to evaluate p19Arf levels. (A) Each graph is the result of five biological replicates for CTRL, #15, #42 and four biological replicates for CTRL and #20. Significance was determined by unpaired t-test followed by Dunnett's multiple comparison tests. * represent significance in reduction/increase respect to D0, *($p < 0.05$),**($p < 0.01$),***($p < 0.001$) and ****($p < 0.0001$); # represent significance at D8 between clones #($p < 0.05$), ##($p < 0.01$) and ###($p < 0.001$).

Panel **B** is a representative Western Blot showing p19Arf protein levels at Day 0 and Day 8. Cells were collected at the time points indicated and total protein extract was prepared and run on a 12%SDS gel, transferred to a nitrocellulose filter and hybridized to α-arf antibody and α-Gapdh antibody (see materials and Methods for details). Band intensities were quantified by ImageLab BioRad software and normalized respect to loading controls (Gapdh).

The behavior of stemness markers (Oct4, Nanog, Sox2, and Dppa5a) was particularly interesting as they appeared collectively much less reduced in p19Arf mutated clones by Day 8 compared to control cells (Figure 36A).

On the other hand, differentiation markers (Sox9, Gata4, Nkx6.1, Pdx1, and p21) show an increase in all clones during differentiation, which, although varying in extent, is notably lower in Arf-mutated clones (Figure 36 B).

A

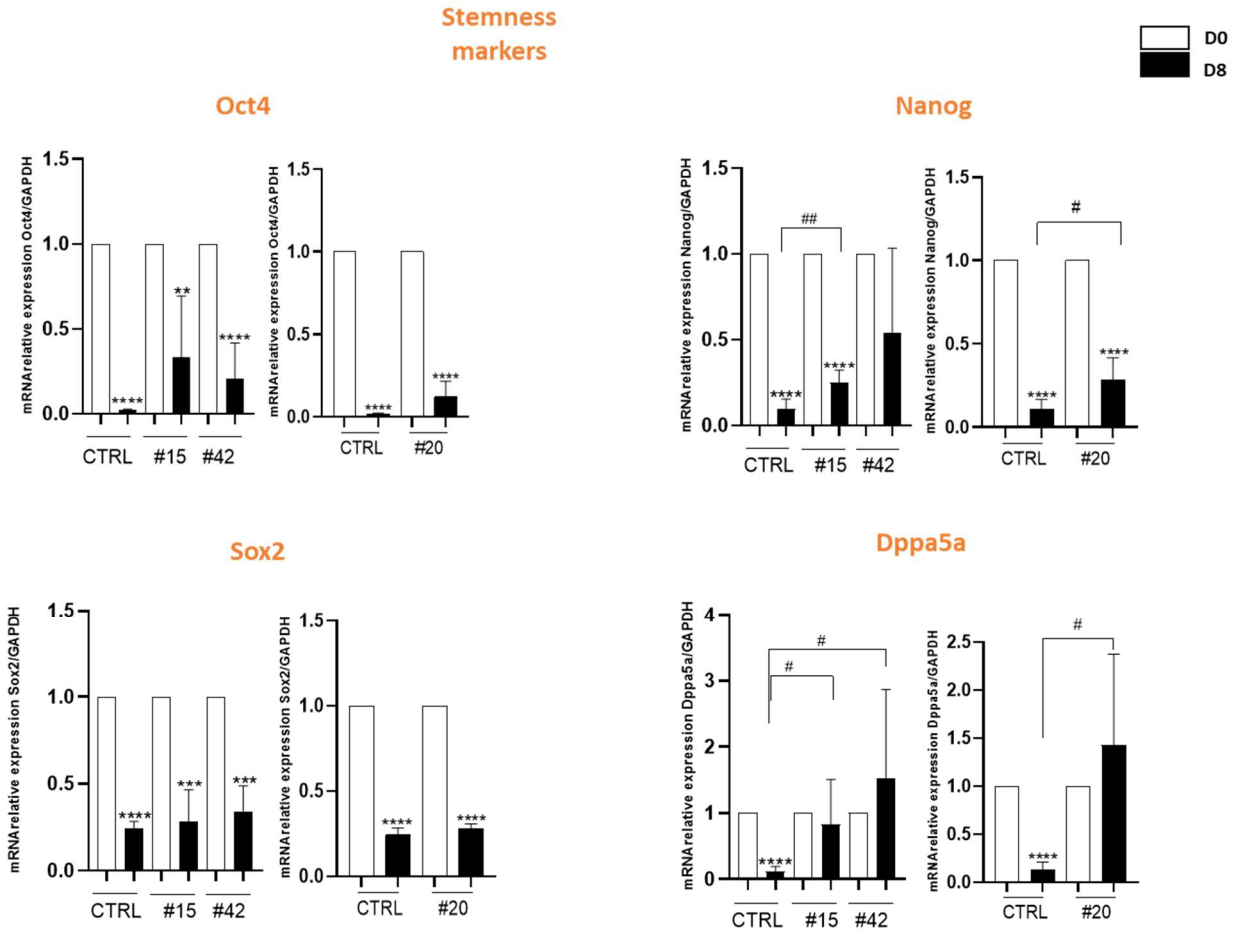
Stemness markers
D0
D8
Oct4
mRNArelative expression Oct4/GAPDH
CTRL
#15
#42
#20
Nanog
mRNArelative expression Nanog/GAPDH
Sox2
mRNArelative expression Sox2/GAPDH
Dppa5a
mRNArelative expression Dppa5a/GAPDH

B

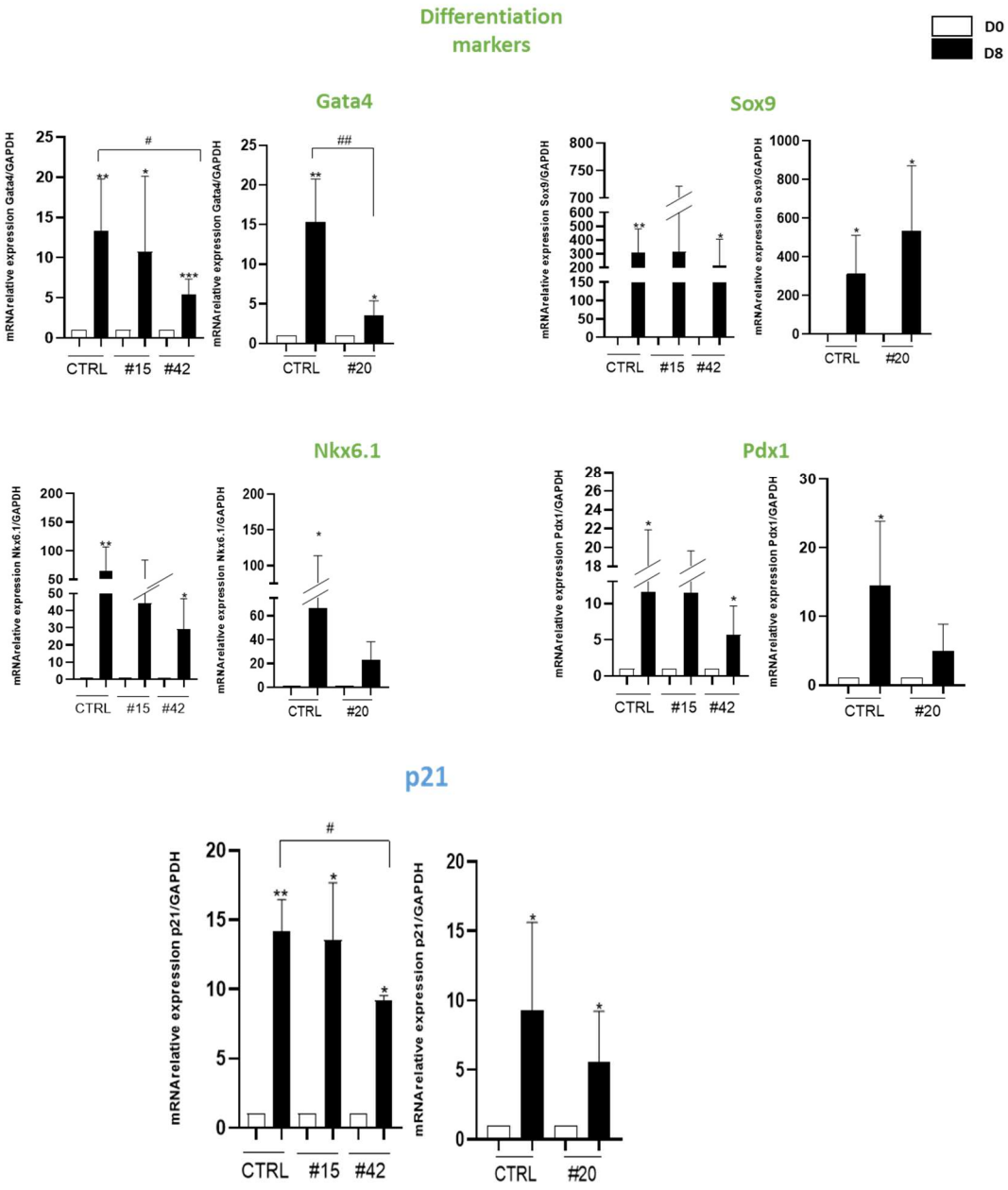
Differentiation markers
D0
D8
Gata4
Sox9
Nkx6.1
Pdx1
p21
mRNArelative expression Gata4/GAPDH
mRNArelative expression Sox9/GAPDH
mRNArelative expression Nkx6.1/GAPDH
mRNArelative expression Pdx1/GAPDH
mRNArelative expression p21/GAPDH
CTRL
#15
#42
#20

Figure 36. RTqPCR on control and p19Arf mutated clones at Day 0 and Day 8 of differentiation. Each graph is the result of five biological replicates for CTRL, #15, #42 and four biological replicates for CTRL and #20. In panel **A** Stemness markers Oct4, Nanog, Sox2 and Dppa5a are shown, in panel **B** the differentiation markers Gata4, Sox9, Nkx6.1 Pdx1 and p21. Significance was determined by unpaired t-test followed by Dunnett's multiple comparison tests. * represent significance in reduction/increase respect to D0, *($p < 0.05$),**($p < 0.01$),***($p < 0.001$) and ****($p < 0.0001$); # represent significance at D8 between clones #($p < 0.05$), ##($p < 0.01$) and ###($p < 0.001$).

Analysis by Western Blot of the stemness marker Oct4 are in line with was observed by Real Time (Figure 37).

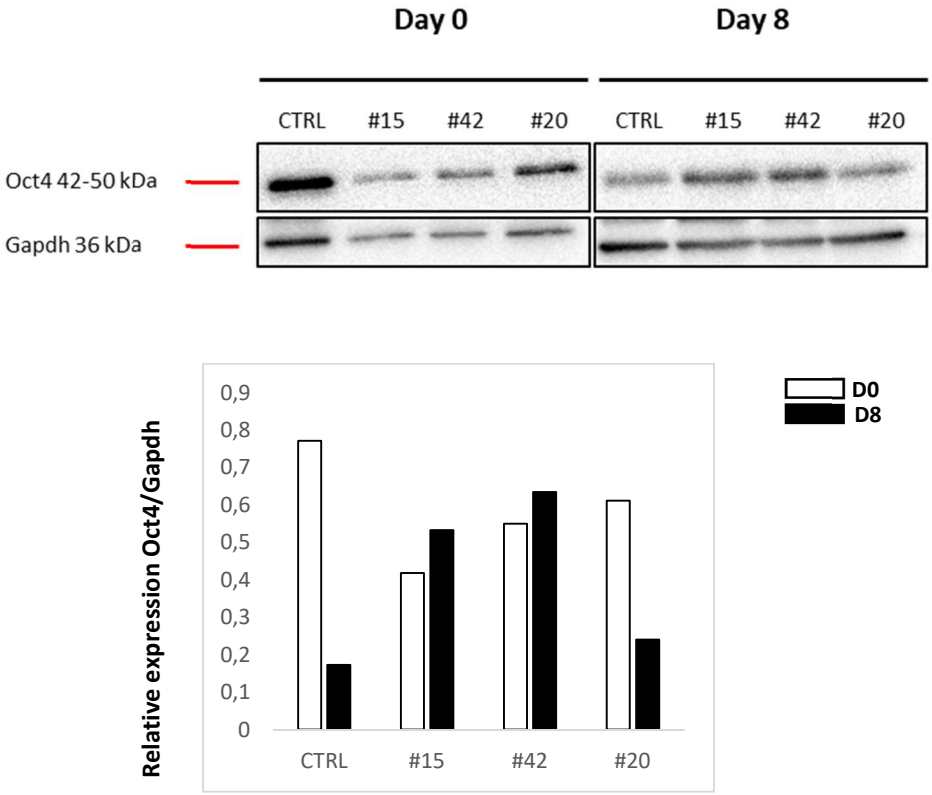

Figure 37. Representative Western Blot of Oct4 protein levels at day 0 and day 8 of differentiation. Cells were collected at the time points indicated and total protein extract was prepared and run on a 10 %SDS gel, transferred to a nitrocellulose filter and hybridized to α-Oct4 antibody and α-Gapdh antibody (see materials and Methods for details). Band intensities were quantified by ImageLab BioRad software and normalized respect to loading controls (Gapdh).

Collectively, morphological and molecular data indicate a defect in the differentiation program. The elevated expression of pluripotency markers (particularly Oct4, Nanog and Dppa5a) observed on Day 8 in mArf clones suggests that, in the absence of functional Arf, cells have a tendency to retain a pluripotent phenotype. Figures 38 A and B more clearly show that mArf clones at Day 8 present a sustained expression of pluripotency markers at the RNA levels respect to CTRL cells that more clearly express higher levels of differentiation markers.

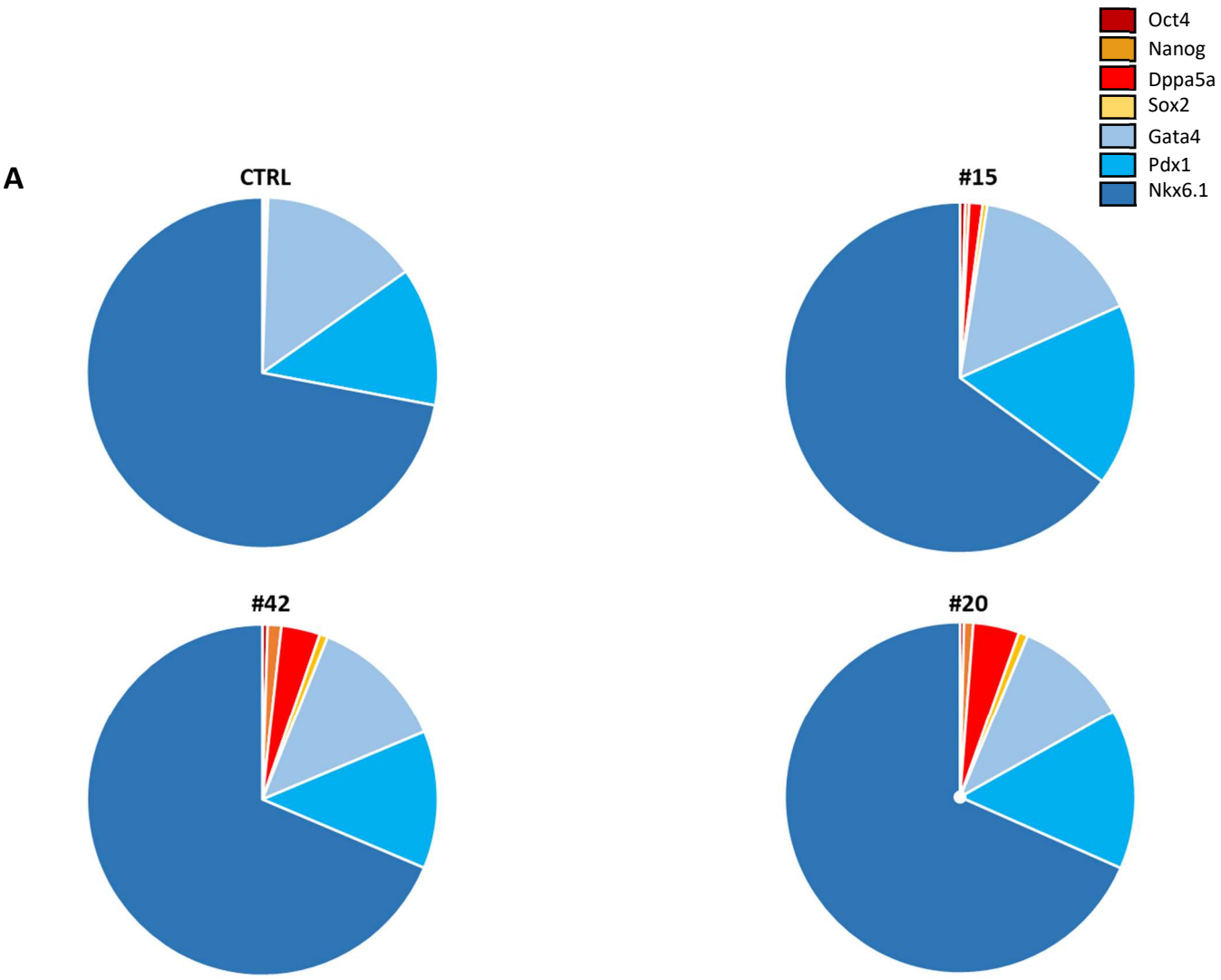
A
CTRL
#15
#42
#20
Oct4
Nanog
Dppa5a
Sox2
Gata4
Pdx1
Nkx6.1

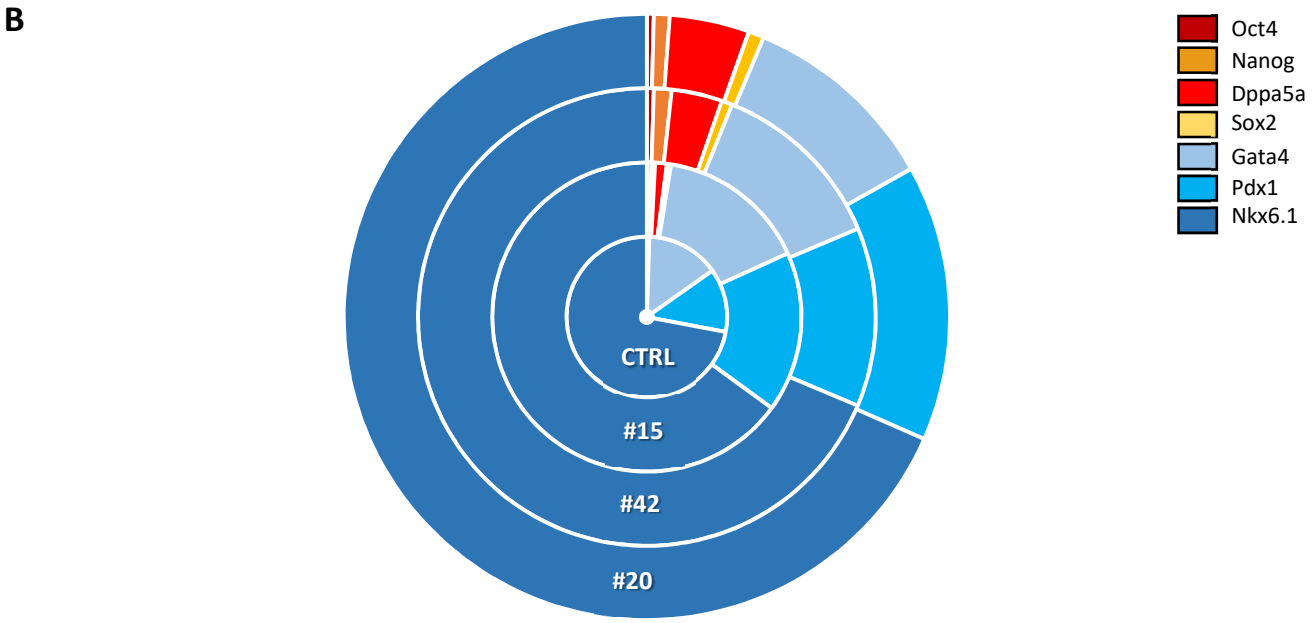
B
CTRL
#15
#42
#20
Oct4
Nanog
Dppa5a
Sox2
Gata4
Pdx1
Nkx6.1

Figure 38. Summary of Real Time PCR Data. This panel presents a graphical overview of the general behavior of mArf clones on **Day 8** of differentiation using pie charts to illustrate the distribution of specific markers in CTRL cells and the mArf clones analyzed. Each slice represents a distinct marker of either stemness or differentiation. Panel A displays the marker distribution in CTRL cells and in individually mArf clones #15, #42, and #20. On Day 8, CTRL cells exclusively express differentiation markers, as shown by the presence of only three slices corresponding to Gata4, Pdx1, and Nkx6.1. In contrast, mArf clones #15, #42, and #20 retain higher levels of stemness markers as indicated by the high proportion of the red slice (representing Dppa5a expression), followed by the orange and yellow slices, representing Nanog and Sox2 expression, respectively.

Panel B provides a summary of the data presented in Panel A, highlighting the overall trend in marker expression across CTRL and mArf clones.

DISCUSSION

While the p19Arf protein critically functions as a tumor suppressor, more recent evidences brought new insights into this intriguing protein positioning it at a critical intersection between oncogenesis and cellular differentiation. Among the various cellular process in which Arf has been shown to be involved, a major one appears to be its involvement in development and differentiation (see also Introduction). It is now well-documented that p19Arf expression can be induced in response to differentiation signals as observed in processes such as neurogenesis and hematopoiesis, where it acts to prevent unchecked cell proliferation and to ensure appropriate development and cellular maturation (Kamijo, et al., 1999; Sherr, et al., 1999). Initial evidence of p19Arf's involvement in developmental processes originates from Arf knock-out (KO) mice studies, which exhibit significant eye development anomalies. Moreover, p19Arf shows transient expression in spermatogonia during the first synchronized wave of spermatogenesis, ceasing in meiotic spermatocytes and their more mature derivatives (Gromley et al., 2009). In addition, while the p19Arf protein is generally absent in fetal and young adult mouse tissues, it appears expressed in the fetal yolk sac, underscoring its function in the late-stage differentiation of extraembryonic endoderm (ExEn) cells (Li, et al., 2013). Furthermore, particularly during pregnancy and lactation, p19Arf levels increase in response to progesterone stimulation and play a role in the mammary gland homeostasis (Yi, et al., 2004). Notably, the Ink4a-Arf locus is epigenetically silenced in stem cells, a mechanism essential for preserving their self-renewal capabilities, reflecting a complex regulatory interaction in cellular differentiation and developmental biology (Li, et al., 2012).

However, the mechanisms through which Arf acts in differentiation processes are still unclear and are just beginning to be partially elucidated. On the other hand, given Arf’s established role in cancer and the growing body of knowledge on the role of the homeostasis of Stem cells, Progenitor Cells and Cancer stem cells, it appears particularly urgent to elucidate the role(s) that Arf plays in this context.

The role of Progenitor Cells (PCs) appears particularly important as they are essential for the maintenance and repair of organs and tissues, especially those with high cell turnover such as pancreas. Their role in the homeostasis supports normal organ development while their unbalance could be responsible of the onset of pathological conditions. The importance of progenitor cells in adult mammalian pancreatic regeneration is increasingly growing, highlighting their importance in understanding pancreatic repair mechanisms (Tanase, et al., 2014). Of note, mutations in Arf are highly prevalent in pancreatic cancer, second only to mutations in p53, underscoring its crucial role in tumorigenesis within this tissue type (Aguirre, et al., 2003).

Therefore, interfere with Arf function to look for alterations in PPCs homeostasis could be important to better clarify its "dual" role in cancer and differentiation.

Our initial strategy predicted a CRISPR-Cas9 approach to knock out p19Arf in mouse ESCs. However, due to the intrinsic complexity of the INK4a/ARF locus (Quelle, et al., 1995; Duro, et al., 1995; Mao, et al., 1995; Stone, et al., 1995; Swafford, et al., 1997)-which contains intertwined coding sequences for both Arf and p16-and the highly repetitive nature of the Arf sequence, after several attempts, we had to select a single guide RNA (sgRNA) previously validated *in vivo* by Weber et al. (2015). This allowed us to specifically target exon 1β although, up to now, we didn't obtain any knockout Arf clone. Intriguingly, all three selected clones exhibit alteration in the differentiation process toward PPCs both at morphological and molecular levels, despite the partial impairment of Arf. All clones analyzed so far exhibit a truncated allele (due to the presence of a stop codon) that retains about 40 N-ter amminoacids with extensive mutations in the region between aa 26-37. These alterations are likely to impair most of Arf's functions especially in the p53/Mdm2 pathway (Kamijo, et al., 1998; Weber, et al., 2000). The remaining allele exhibit various mutations—except for one clone—that may potentially further affect the interactions with key protein partners.

Given the unfolded structure of the p19Arf protein, it is unlikely that mutations would lead to its degradation. However, mArf clones appear to express lower levels of the protein which could be attributed to the monoallelic truncation. Therefore, we are currently screening for additional clones in search of double null allele to fully investigate the impairment.

It should be noted that the initially selected clones were highly heterogeneous, prompting us to apply a subcloning strategy to enhance clone homogeneity and obtain clearer results. However, it is important to consider the intrinsic variability in these cells during the differentiative processes due to dynamic fluctuations among different differentiative states. This variability helps explain the challenges encountered in obtaining highly reproducible results (Canham, et al., 2010; Torres-Padilla, et al., 2014).

Despite the intrinsic variability and the fact that none of the clones analyzed were complete knockouts, our data quite robustly show that the p19Arf-mutant clones tend to maintain a prolonged pluripotency phenotype (both at morphological and molecular level) during *in vitro* differentiation respect to both wild type and control cells that, instead, acquire a more pronounced multipotent phenotype.

This is particularly evident when examining p19Arf-mutant clones at phase contrast and fluorescence microscopy: at day 0, all cells displayed a classical clonal morphology, as expected. However, by day 4, distinct morphological variations emerged; control cells began to acquire the definitive endoderm morphology, whereas mutant clones #15, #42, and #20 retained a rounded shape. By day 8, the control cells adopted a distinctive "basket-like" morphology typical of differentiated pancreatic progenitor cells while the clones continued to exhibit rounded morphology, suggesting impaired or delayed progression of differentiation. Staining with phalloidin (marking F-actin filaments) more markedly reveal the rounded phenotype of mArf clones at the end of the *in vitro* differentiation and/or the presence of enlarged aberrant basket-like structures. Since the mutations introduced in the Arf sequence in selected clones may have

altered the interaction with some of its binding partners and/or its subcellular localization, it would have been very interesting to analyze the potential resulting changes in Arf's intracellular localization. Several attempts were made to analyze these changes through immunostaining. However, we were unsuccessful in achieving our objective for different problems that we are trying to overcome. First, the presence of Matrigel coating in our samples results in basal autofluorescence, making permeabilization less efficient. Second, the growth patterns of the cells, which tend to form clusters, complicate both permeabilization and visualization. We are now trying several approaches to improve the results such as increasing the concentration of the permeabilizing agent, extending the reaction time, and freezing the samples to section them with a cryostat, all aimed at enhancing localization accuracy.

Evaluation of pluripotency (Oct4, Nanog, Dppa5a, and Sox2) and multipotency/differentiation markers (Gata4, Pdx1, and Nkx6.1) by RT-PCR analysis more precisely indicate alterations in the differentiative program toward PPCs of mArf clones that exhibited a marked retention of pluripotency at day 8, producing cells not fully multipotent. Our results align with findings that the Ink4a-Arf locus is fully silenced in both induced pluripotent stem (iPS) and embryonic stem (ES) cells (to preserve their self-renewal capacity) acquiring a bivalent chromatin state that enables reactivation during differentiation (Li, et al. (2009; Li, et al., 2012). Interestingly, in mouse cells, Arf is the primary barrier to reprogramming, whereas INK4a plays a more crucial role in human cells (Li, et al., 2009).

Although our data indicate a clear involvement of Arf in the differentiation of PPCs cells, we still do not have a precise understanding of the mechanisms of action of Arf in this context, nor direct evidence of its involvement in this process.

Regarding the last point, we would ideally need to rescue the mutant phenotype by re-introducing wild type p19Arf back into our clones, although this presents significant challenges that we are currently trying to overcome. First of all, it

should be noted that p19Arf is expressed only at late stages of differentiation (between Days 4 and 8), making the use of a constitutively expressing construct unsuitable. Furthermore, it is important to consider that the copy of exogenously introduced p19Arf must be engineered to evade targeting by Cas9. Actually, a modified p19Arf coding sequence was cloned in a vector containing a Tet-On promoter responsive to doxycycline. However, we ultimately did not proceed with transfection, due to the variability of the system, which posed several risks. First, re-transfecting the mArf selected clones could introduce further genetic alterations. Second, doxycycline treatment during differentiation could add further complexity to the process. The pancreatic differentiation protocol itself is delicate, requiring treatment with multiple factors over an 8-day period, during which cells experience considerable stress. The introduction of doxycycline could potentially interfere with the differentiation process, complicating the interpretation of results.

Regarding the potential mechanisms of action of Arf in PPCs differentiation, we cannot provide a precise mode of action, but we can offer some interesting speculations.

Notably, all our clones present mutations in the 26-37 amino acid region of exon 1β, resulting in a stop codon preceeded by many altered codons. This region has been extensively studied and turned out to be crucial for interaction with Mdm2 and nucleolar localization (Weber, et al., 2000). An impaired or less efficient interaction with Mdm2 in mArf clones may explain most of the phenotypes we observed. mArf clones should present an alteration of the classical p53-Mdm2 pathway leading to the observed differentiation defects. On the other hand, there are many evidences demonstrating the involvement of p53 in differentiation contexts:

- p53 can directly bind to the Nanog promoter lowering its level of expression (Pan, et al., 2007; Solozobova, et al., 2011 and Lin, et al., 2004). In embryonic stem (ES) cell differentiation, the swift downregulation of Nanog is associated

with the activation of p53's transcriptional activity and its phosphorylation at Ser315 (Pan, et al., 20017).

- p53 can directly upregulate miR-205 (Piovan, et al., 2012; Alla, et al., 2012). In the formation of extraembryonic endoderm (ExEn) starting from Pluripotent Stem Cells there is a rapid and timely increase in p19Arf that results in the activation of p53 and miR205. Arf null contexts present a significant temporal delay in ExEn formation that can be rescued by enforced expression of miRNA205. Further, miR205 is involved in the upregulation of the GATA-4 differentiation marker (Li, et al., 2012).

- p53 regulates p21, a cyclin-dependent kinase inhibitor, playing an essential role in promoting differentiation. Elevated p21 levels drive differentiation in murine embryonic stem cells (ESCs) by repressing SOX2, a key pluripotency factor, thereby accelerating the formation of cell types such as endothelial cells, hepatocytes, and neurons. p21 is also indispensable for maintaining the self-renewal of quiescent stem cell populations, including hematopoietic, keratinocyte, and neuronal stem cells, underlying its role in both differentiation and tissue homeostasis (Kreis, et al., 2019).

Consistent with the hypothesis of an alteration in the Arf/Mdm2/p53 pathway, mArf clones are expected to exhibit lower levels of active p53.This could explain the higher levels of the stemness markers Nanog and Sox-2 (that are negatively regulated by p53) and lower levels of the differentiation markers Gata-4 and p21 (positively regulated by p53) in mArf clones. Apart from these established observations, it would be noteworthy to investigate whether in mArf clones there are changes in the binding efficiency to Mdm2, alterations in subcellular distribution of Arf and variations in p53 protein levels. Many challenges in this type of analysis arise from the lack of antibodies efficiently working in mouse embryonic stem cells. Different settings for western blot and immunofluorescence analysis are being optimized to improve experimental conditions. Of course, other

explanations could be considered due to the intrinsic nature of Arf and the multitude of partners it can interact with.

Notably, all our clones potentially possess a single copy of the small ARF isoform, which is a short form of ARF translated from an internal methionine at amino acid 45. This isoform localizes to the mitochondria and plays a role in autophagy (Reef, et al., 2006). Interestingly, the observation that smARF can rescue the eye phenotype and fertility in Arf-null mice -although with a yet undefined mechanism-(van Oosterwijk, et al., 2017) led to the hypothesis that this form of Arf may also play a role in pancreatic differention. On the other hand, this isoform has been shown to be unable to regulate the cell cycle (van Oosterwijk, et al. 2017) and constitutes only a small fraction compared to full length Arf, making it difficult to hypothesize its function in our experimental conditions. However, we are planning experiments aimed at uncovering a potential role of smArf in PPCs differentiation. Immunofluorescence experiments will enable us to assess its colocalization with mitochondria and the changes in mArf clones compared to the control (CTRL).

All these hypotheses, even if indirect, could reveal important cellular connections that could explain the alterations in balancing stem cell self-renewal and differentiation, promoting genetic stability and appropriate cellular responses under physiological stress conditions.

Imminent transcriptomic and subsequent proteomic analyses in the near future will help clarify the effective molecular pathways involved.

This research may advance the understanding not only of the molecular mechanisms underlying differentiation toward pancreatic progenitor cells but also of the critical balance within progenitor cell populations. Progenitor cells serve as an essential reserve for organ regeneration and plasticity, making their equilibrium a key objective. Our results could provide insights into maintaining pancreatic progenitor cells for regenerative medicine applications, while also elucidating the

role of tumor suppressor genes in multipotent cells. This dual role supports both tissue regeneration and cancer prevention, addressing two sides of the same biological coin.

MATERIALS AND METHODS

CRISPR/Cas9 genome editing

Clustered Regularly Interspaced Short Palindromic Repeats (CRISPR) and the associated protein Cas-9 form a highly effective genome editing tool used across various fields. The system consists of two main components: guide RNA (gRNA) and Cas-9 protein. CRISPR/Cas-9 editing involves three steps: recognition, cleavage, and repair. The designed sgRNA identifies the target gene through complementary base pairing, while Cas-9 creates double-stranded breaks (DSBs) at a specific site upstream of the protospacer adjacent motif (PAM). This break is then repaired through either non-homologous end joining or homology-directed repair (Asmamaw, et al., 2021).

Cas-9, derived from *Streptococcus pyogenes*, is a large multi-domain DNA endonuclease that functions as a genetic scissor, cleaving DNA to generate DSBs. The system's effectiveness relies on the sgRNA directing Cas-9 to the target sequence, as Cas-9 is inactive without it. The PAM sequence, typically a conserved 2–5 base pair sequence, is crucial for Cas-9's recognition and varies among bacterial species, with the common PAM being 5'-NGG-3' (Mei, et al., 2016; Jiang, et al., 2017).

This prokaryotic system has been adapted for molecular biology, becoming one of the most powerful and versatile platforms for precise genome mutagenesis. After transfecting or transforming target cells with a construct expressing guide RNA and Cas9 protein, a double-strand break in the DNA is induced. The cell can then repair this break using either homologous recombination (HR) or non-homologous end joining (NHEJ). HR relies on the presence of an externally provided DNA template similar to or different from the deleted DNA sequence. In contrast, NHEJ has a high probability of introducing errors, resulting in small insertions and deletions (indels) at targeted sites.

Cloning of sgRNA into lentiCRISPRv2 vector

In order to apply the CRISPR/Cas9 system in our context we decided to use LentiCRISPRv2 vector (Addgene #52961).

The lentiCRISPRv2 plasmid contains all the key elements necessary for the cloning strategy, as well as for subsequent transfection and selection in mammalian cells:

- the coding sequence for the Cas9 protein;
- the ampicillin resistance to select bacterial cells after transformation;
- the puromycine resistance necessary to select stable clones after the transfection;
- Two BsmBI restriction sites, fundamental for the directional cloning of the selected single guide into the vector (with the elimination of a fragment of 1885 bp). This enzyme recognizes an asymmetric DNA sequences and cleave outside the recognition sequence itself (N1-N5); (see Figure 12 A).
- The Chimeric guide RNA (gRNA scaffold) that will fall downstream the U6 promoter after the digestion with BsmBI enzyme.
- The CMV enhancer and the U6 promoter to efficiently transcribe the sgRNA and the chimeric guide RNA;

The single guide RNA was specifically designed with the necessary 5' and 3' ends for cloning after vector digestion with BsmBI, according to the Zhang Lab protocol (Sanjana, et al., 2014; Shalem, et al., 2014).

sgArf TOP	5’- CACCGTGGTGAAGTTCGTGCGATCC-3’
sgArf BOTTOM	5’- AAACGGATCGCACGAACTTCACCAC-3’

Before starting the sgRNA top and bottom provided us by Eurofins Genomics S.R.L were annealed. The sgArf top and bottom were resuspendend in milliQ water at a final concentration of 100 µM and were annealed as follow:

Components	Amount
sgArf TOP (100 µM)	4,44 µL
sgArf BOTTOM (100 µM)	5,71 µL
Annealing Buffer (10X)	1X
bdH_2O	To 20 µL
Total volume	20 µL

For the annealing reaction, the sgRNAs were placed in boiling H2O at 100°C to completely denature, and then left in water to cool for proper annealing of the top and bottom guides. Finally, the resulting double-stranded DNA molecules were diluted 1:200 (2 µL ligase mix + 398 µL H2O). Subsequently, the paired oligonucleotides were subjected to a ligation reaction with the vector.

LentiCRISPRv2 digestion with BsmBI enzyme

The first step to obtain the ligated construct was the LentiCRISPRv2 digestion with BsmBI enzyme (*New England Biolabs* #R0580 *GmbH* Brüningstr). The digestion was performed as follow and according to manufacture's protocol:

Components	Amount
LentiCRISPRv2 vector (1γ/μL)	5γ
BsmBI enzyme (10.000 U/mL)	50 U
NEB Buffer 10X	1X
bdH_2O	To 60 μL
Total volume	60 μL

The reaction was incubated for 1 hour and 30 minutes at 55°C. Subsequently, to extract the linearized vector, 60 μL of the digestion reaction was loaded into four wells on a 0.8% agarose gel in 1X TAE.

After the electrophoresis run the band corresponding to the digested vector was extracted using the QIAquick Gel Extraction Kit (Qiagen, Hilden Germany) according to manufactures protocol.

DNA was eluted in 30 µL of elution buffer and the concentration and purity of the sample were assessed using a NanoDrop® 1000 analysis.

Sample	ng/µL
BsmBI digested LentiCRISPRv2	7,4

After the purification, the digested vector was ligated using T4 DNA ligase (NEB #M0202S) according to manufacture's protocol:

Components	Amount
Digested vector (8 ng/µL)	48 ng
Annealed sgArf (0,5 ng/ µL)	0,5 ng
T4 ligase Buffer 10X	1X
T4 DNA ligase (1U/ µL)	1 U
bdH_2O	To 20 µL
Total volume	20 µL

The ligation mix, was incubated overnight at 16°C and then incubated for 10 minutes at 65°C. After the ligation mix and a negative control, using the same reaction mix but without the guide were transformed in Stbl3 bacterial cells and incubated O.N. at 37°C. After bacterial transformation, the construct was extracted using midi-preparations of plasmid DNA.

Transformation in bacterial cells and DNA MIDI preparation

Competent *E. coli* Stbl3 cells, were made competent to acquire foreign DNA with a chemical reaction using calcium chloride and after with thermal shock incubating cells 42°C for 30 second and after in ice for 1 minute. 50 µL of competent cells were incubated with 10 µL of the ligation reaction. The cells were

incubated on ice for 30 minutes, then subjected to a 30-second heat shock at 42°C, followed by 1 minute on ice.

Next, were added 950 µL of LB medium without antibiotic, and the mixture incubated for 1 hour at 37°C with shaking to express antibiotic resistance. The samples were centrifuged at 1100 g for 5 minutes, and the pellet was resuspended in 100 µL of LB, then plated on agar containing 100 µg/mL. The plates were incubated overnight at 37°C, yielding two colonies, which were inoculated into 5 mL of LB with ampicillin and grown for 6 hours at 37°C. This pre-culture was then used to grow 100 mL of LB overnight at 37°C for DNA midi-preparations.

For plasmid DNA extraction ZymoPURE II Plasmid Midiprep kit was used according to manufacture's protocol. At the end of protocol 200 µL of ZymoPURE™ Elution Buffer was added to the column, incubated at room temperature for 2 minutes, and centrifuged at ≥ 10,000 g for 1 minute. The eluted plasmid DNA was stored at ≤ -20°C, and its purity and concentration were assessed using a NanoDrop 1000.

Sample	ng/ µL
MIDIprep 1	2774,1
MIDIprep 1	1019,6

Resctriction analysis of DNA preparation

The two ligated Midipreps products and the control vector were digested with various restriction enzymes. 300 ng of the vectors were digested both with single (EcoRI R601A, EcoRV R635A, KpnI R634A; Promega, Madison, Winsconsin

USA) and double (EcoRI-EcoRV, KpnI-EcoRV) digestions. All digestions were performed following the manufacture's protocol and using MULTI-CORE™10X Buffer (R999A Promega).

The obtained fragments were analyzed using 0.8% agarose gel electrophoresis in 1X TAE buffer with the addition of SybrSafe ® DNA gel stain 1X (Thermo Fisher Scientific Waltham, Massachusetts, Stati Uniti).

Transfection of E14Tg2a.4 cells with LentiCRISPRv2-sgArf and LentiCRISPRv2#1

The lentiCRISPRv2#1 vector and the control vector were transfected into mESCs E14Tg2a.4 usign Lipofectamine ® 2000 (Invitrogen Waltham, Massachusetts, Stati Uniti). Our aim was to obtain stable clones expressing Cas9 protein. The transfection control was performed using *pcDNA3-eGFP*. The day before transfection $6x10^5$ were plated into 60mm dish and the day after the cells were transfected using Lipofectamine 2000 with a 1:3 ration. The transfection mix were prepared using manufacture's protocol. After 24h from transfection the cells transfected with the pcDNA3eGFP vector were observed under phase contrast and fluorescence microscopy to evaluate the approximate rate of transfected cells. Forty-eight hours after transfection, cells were detached, and 1 x 10^6 cells for each experimental condition were replated in 100 mm dishes with 0.8 μg/mL puromycin added to the medium. After 8 day, colonies were growing in the culture plate. Using 100 μL pipette tips, the colonies were picked up and placed individually in the 96 well culture plate filled with trypsin that was inactivated by adding complete medium. The day after the medium was changed with fresh medium. After 11 days the cells were detached and plated into 24-well (1.9 cm^2) and by maintaining high the concentration puromycine subsequently to a 12-well plates (4 cm while maintaining a puromycin concentration of 0.4 μg/mL. The clones were then expanded for validation. Furthermore, the genotyping by PCR and chromatogram sequencing were used to analyze the mutations and select

the positive clones for our analysis. 42 clones were obtained from transfection with CRISPRv2Arf#1. Similarly, E14TG2a cells were transfected with lentiCRISPRv2 (“empty” without sgRNA) to obtain a valid control for subsequent experiments (named CTRL); cells were then collected and used without any subcloning for successive experiments.

Cell cultures and differentiation protocol

Murine E14Tg2a.4 ES cells derived from mouse inner cell mass of the blastocyst (*CRL-1821*™ ATCC® Manassas, VA, USA). Cells were cultured on gelatin-coated in complete ES medium: GMEM (Glasgow Minimal Essential Medium, Sigma-Aldrich, St. Louis, MO), 15% FBS (HyClone), 1,000 U/ml-1 leukaemia inhibitory factor (LIF) (Millipore, USA), 1.0 mM sodium pyruvate (Invitrogen, Carlsbad, CA, USA), 0.1 mM non-essential amino acids (Invitrogen, Carlsbad, CA, USA), 2.0 mM L-glutamine (Invitrogen, Carlsbad, CA, USA), 0.1 mM β-mercaptoethanol (Sigma-Aldrich, St. Louis, MO), 500 U ml-1 penicillin/streptomycin (Invitrogen, Carlsbad, CA, USA) were used. ESCs were incubated at 37°C in 5% CO_2. Cell culture medium was changed daily, and cells were split every 2–3 days routinely. For the endoderm differentiation, $5x10^5$/plate cells were seeded in 35 mm dishes, and $1x10^6$/plate cells were seeded in 60mm dishes as a feeder free monolayer. The differentiation medium consists of DMEM Low Glucose non-essential amino acids (Gibco, Dublin, Ireland), 100 U-µg/mL Penicillin/Streptomycin (Gibco),0.1 mM β-Mercaptoethanol (Sigma Aldrich,, depleted of LIF, with 200 µg/mL Corning ® Matrigel Matrix (Corning, New York, USA) and treated sequentially with several molecules at different time point for 8 days. These factors included activin A (20 ng/mL, R&D Systems, Minneapolis, MN, USA), all trans retinoic acid (RA, 5 µM, Sigma Aldrich), fibroblast growth factor 10 (Fgf10, 10 ng/mL, R&D Systems). Medium was changed every 2 days. These cells were incubates t 37°C in 5% CO_2.

Subcloning

1 × 10^6 cells for each clone (#42, #15, and #20) were plated in two 100 mm dishes in the presence of 0.4 µg/mL puromycin. After 4 days, visible clones were picked and replated into 0.32 cm² wells. After 6 days, the clones were harvested and transferred to a 24-well plate (1.9 cm²). Subsequently, the cells were plated in 12-well plates (4 cm²) while maintaining a puromycin concentration of 0.4 µg/mL. The clones were then expanded in 35 mm dishes and after reaching 60 mm plates, they were frozen and genomic DNA was extracted for validation.

PCR-genotyping of mESCs stable clones

The genomic DNA was extracted from our clones using HiPurA® Mammalian Genomic DNA Purification Kit according to manufacture's protocol (HiMedia Modautal, Germany). Il DNA estratto è stato poi quantizzato utilizzando il NanoDrop (ThermoFisher Waltham, Massachusetts, Stati Uniti). After the extraction the DNA integrity was evaluated with electrophoresis. So the samples was loaded into a 0,8% agarose gel with TAE 1X using SybrSafe ® DNA gel stain 1X (Thermo Fisher Scientific Waltham, Massachusetts, Stati Uniti).
To evaluate the mutation we performed a PCR analysis using *ROCHE Faststart Taq* (Roche, Basel, Switzerland). The PCR was performed according to manufacture's protocol using the following primers:

Name	Primer sequence (5'-3')
Primer Fw (5' UTR)	TTCTCACCTCGCTTGTCAC
Primer Rv (CDS Arf)	TTCTCAAGATCCTCTCTAGCC

The 219 bp amplicon obtained from the PCR was then subjected to Sanger sequencing at the Eurofins Genomics facility. The sequencing results were

analyzed by identifying the wild-type sequence peaks through manually alignment with the p19Arf wild-type sequence. After the coding sequence of mutated clones were analyzed thanks to SnapGene Viewer software (Sand Diego, California, USA).

RNA extraction and qPCR analysis

Total RNAs were extracted from cells using TRIzol (Invitrogen) method according to the manufacturer's protocol. One microgram of total RNA was reverse-transcribed by iScript ™ cDNA synthesis kit (Biorad, Hercules California USA) according to the manufacturer's protocol. qPCR analyses were performed using

20 ng or 100 ng cDNA per well with the iTaq Universal SYBR Green Supermix (Biorad, Hercules California USA). Each sample was repeated three times and normalized with the expression of housekeeping glyceraldehyde 3-phosphate dehydrogenase (GAPDH) gene. Reactions were run on the Aria Mx Real-Time PCR system (Agilent, Santa Clara, California, USA). Fold induction was calculated using ddCt method. All Primers are listed in the following table.

Gene	**Primer Fw (5'-3')**	**Primer Rv (5'-3')**
Gapdh	AATGGTGAAGGTCGGTGTG	GAAGATGGTGATGGGCTTCC
Oct4	CCGTGTGAGGTGGAGTCTGGAGAC	CGCCGGTTACAGAACCATACTCG
Nanog	AACCAGTGGTTGAAGACTAGCAATGGTC	TTCCAGATGCGTTCACCAGATAGC
Sox2	AACGGCAGCTACAGCATGATGC	CGAGCTGGTCATGGAGTTGTAC
Dppa5a	CGAGGTCTTCATTTACGGCTCTC	GGTCTTCATGGATTCCTCCAGC
Gata4	TCAAACCAGAAAACGGAAGC	CTGCTGTGCCCATAGTGAGA
Sox9	GGTCTGCCTGGACTGTATGTGGATG	CTGTCCGATGTCTCTCTGCAGGAG
Nkx6.1	GACAGCAAATCTTCGCCCTGG	TTCTCCGAAGTCCCCTTGAGCC
Pdx1	GCTCACCTCCACCGGACCTTC	GGGTCCTCTTGTTTTCCTCGGG
p19	TGAGGCTAGAGAGGATCTT	CGTGAACGTTGCCCATCAT
p21	GAACATCTCAGGGCCGAAAA	CAATCTGCGCTTGGAGTGAT

Rhodamine-Phalloidin staining

For Rhodamine-phalloidin staining, 4 x 10^4 cells D0 (2.5 cm^2) and 1.4 x 10^5D8 (2.5 cm^2) were plated and then were fixed with 3.7% PFA (Sigma-Aldrich St. Louis, Missouri, USA) permeabilized with 0.5% Triton X-100 (Sigma-Aldrich St. Louis, Missouri, USA), and blocked with 3% BSA (Sigma-Aldrich St. Louis, Missouri, USA) in PBS-Tween 0.05%. Then, they were incubated with primary antibody for 1 h at RT, and after for 1 h in the dark in Alexa-Fluor™ 488 secondary antibodies (Thermo Fisher Scientific Waltham, Massachusetts, Stati Uniti). Lastly, cells were incubated with rhodamine-phalloidin 1:1000 to localize filamentous actin and then counterstained with DAPI (4′,6-diamidin-2-phenilindol) 1:10,000 for nucleus visualization (Thermo Fisher Scientific Waltham, Massachusetts, Stati Uniti).

Western Blot analysis

Total protein were extracted using RIPA cell lysis buffer and 1X Protease Inhibitor Cocktail (Sigma-Aldrich St. Louis, Missouri, USA). Protein concentration was determined using the Bio-rad protein assay (Bradford) (Biorad Hercules, California, USA) and after denaturation at 90 °C for 10 min, 15γ or 30γ (depending on protein we want to detect) of total protein were electrophoretically separated through 12% or 10% SDS polyacrylamide gels transferred on Amersham™ Protran® Nitrocellulose membranes (Sigma-Aldrich St. Louis, Missouri, USA) . The membranes were blocked with 5% non-fat milk and probed with primary antibodies overnight at 4 °C with a gentle shaker, followed by incubation with HRP-conjugated secondary antibodies for 2 h at room temperature (RT) (Cell Signaling Technologies Danvers, Massachusetts, Stati Uniti). Proteins were detected by the ECL system (BioRad Biorad Hercules, California, USA), and images were taken with ChemiDoc XRS System (Bio-Rad Laboratories) and quantified with densitometric analysis by Image J Software. Total protein extracts

were normalized to Gapdh. The antibodies rabbit anti-Cas9 antibody (1:1000; Diagenode, Belgium), rabbit anti-p19Arf (1:500; Cayman Chemical, Ann Arbor, MI, USA), mouse anti-Gapdh (1:10.000; Santa Cruz Biotech, Dallas, TX, USA), rabbit anti-Oct4 (1:500; Santa Cruz Biotech, Dallas, TX, USA).

Statistics

Graphpad Prism 8.0.1 software was used to perform statistical analysis. Values are presented as mean ± SD. p-values were determined using a two-tail unpaired t-test. $p < 0.05$ was used as a threshold for statistical discernibility.

REFERENCES

- Abbas T, Dutta A. p21 in cancer: intricate networks and multiple activities. Nat Rev Cancer. 2009 Jun;9(6):400-14. doi: 10.1038/nrc2657.
- Abida WM, Gu W. p53-Dependent and p53-independent activation of autophagy by ARF. Cancer Res. 2008 Jan 15;68(2):352-7. doi: 10.1158/0008-5472.CAN-07-2069.
- Adinolfi S, Bagni C, Castiglione Morelli MA, Fraternali F, Musco G, Pastore A. Novel RNA-binding motif: the KH module. Biopolymers. 1999;51(2):153-64. doi: 10.1002/(SICI)1097-0282(1999)51:2<153::AID-BIP5>3.0.CO;2-6.
- Aguirre AJ, Bardeesy N, Sinha M, Lopez L, Tuveson DA, Horner J, Redston MS, DePinho RA. Activated Kras and Ink4a/Arf deficiency cooperate to produce metastatic pancreatic ductal adenocarcinoma. Genes Dev. 2003 Dec 15;17(24):3112-26. doi: 10.1101/gad.1158703. Epub 2003 Dec 17.
- Ahlgren U, Jonsson J, Edlund H. The morphogenesis of the pancreatic mesenchyme is uncoupled from that of the pancreatic epithelium in IPF1/PDX1-deficient mice. Development. 1996 May;122(5):1409-16. doi: 10.1242/dev.122.5.1409.
- Ahlgren U, Jonsson J, Jonsson L, Simu K, Edlund H. beta-cell-specific inactivation of the mouse Ipf1/Pdx1 gene results in loss of the beta-cell phenotype and maturity onset diabetes. Genes Dev. 1998 Jun 15;12(12):1763-8. doi: 10.1101/gad.12.12.1763.
- Aigha II, Abdelalim EM. NKX6.1 transcription factor: a crucial regulator of pancreatic β cell development, identity, and proliferation. Stem Cell Res Ther. 2020 Oct 29;11(1):459. doi: 10.1186/s13287-020-01977-0.
- Akala OO, Park IK, Qian D, Pihalja M, Becker MW, Clarke MF. Long-term haematopoietic reconstitution by Trp53-/-p16Ink4a-/-p19Arf-/- multipotent progenitors. Nature. 2008 May 8;453(7192):228-32. doi: 10.1038/nature06869. Epub 2008 Apr 16.
- Akiyama H, Kim JE, Nakashima K, Balmes G, Iwai N, Deng JM, Zhang Z, Martin JF, Behringer RR, Nakamura T, de Crombrugghe B. Osteo-chondroprogenitor cells are derived from Sox9 expressing precursors. Proc Natl Acad Sci U S A. 2005 Oct 11;102(41):14665-70. doi: 10.1073/pnas.0504750102. Epub 2005 Oct 3.
- Akiyama H, Kim JE, Nakashima K, Balmes G, Iwai N, Deng JM, Zhang Z, Martin JF, Behringer RR, Nakamura T, de Crombrugghe B. Osteo-chondroprogenitor cells are derived from Sox9 expressing precursors. Proc Natl Acad Sci U S A. 2005 Oct 11;102(41):14665-70. doi: 10.1073/pnas.0504750102. Epub 2005 Oct 3.
- Al-Khawaga S, Memon B, Butler AE, Taheri S, Abou-Samra AB, Abdelalim EM. Pathways governing development of stem cell-derived

pancreatic β cells: lessons from embryogenesis. Biol Rev Camb Philos Soc. 2018 Feb;93(1):364-389. doi: 10.1111/brv.12349. Epub 2017 Jun 22.

- Alla V, Kowtharapu BS, Engelmann D, Emmrich S, Schmitz U, Steder M, Pützer BM. E2F1 confers anticancer drug resistance by targeting ABC transporter family members and Bcl-2 via the p73/DNp73-miR-205 circuitry. Cell Cycle. 2012 Aug 15;11(16):3067-78. doi: 10.4161/cc.21476. Epub 2012 Aug 8.
- Alvarez Fallas ME, Pedraza-Arevalo S, Cujba AM, Manea T, Lambert C, Morrugares R, Sancho R. Stem/progenitor cells in normal physiology and disease of the pancreas. Mol Cell Endocrinol. 2021 Dec 1;538:111459. doi: 10.1016/j.mce.2021.111459. Epub 2021 Sep 20.
- Andrews PW. From teratocarcinomas to embryonic stem cells. Philos Trans R Soc Lond B Biol Sci. 2002 Apr 29;357(1420):405-17. doi: 10.1098/rstb.2002.1058.
- Asada M, Yamada T, Ichijo H, Delia D, Miyazono K, Fukumuro K, Mizutani S. Apoptosis inhibitory activity of cytoplasmic p21(Cip1/WAF1) in monocytic differentiation. EMBO J. 1999 Mar 1;18(5):1223-34. doi: 10.1093/emboj/18.5.1223.
- Aslanian A, Iaquinta PJ, Verona R, Lees JA. Repression of the Arf tumor suppressor by E2F3 is required for normal cell cycle kinetics. Genes Dev. 2004 Jun 15;18(12):1413-22. doi: 10.1101/gad.1196704. Epub 2004 Jun 2.
- Asmamaw M, Zawdie B. Mechanism and Applications of CRISPR/Cas-9-Mediated Genome Editing. Biologics. 2021 Aug 21;15:353-361. doi: 10.2147/BTT.S326422.
- Avilion AA, Nicolis SK, Pevny LH, Perez L, Vivian N, Lovell-Badge R. Multipotent cell lineages in early mouse development depend on SOX2 function. Genes Dev. 2003 Jan 1;17(1):126-40. doi: 10.1101/gad.224503.
- Baccini V, Roy L, Vitrat N, Chagraoui H, Sabri S, Le Couedic JP, Debili N, Wendling F, Vainchenker W. Role of p21(Cip1/Waf1) in cell-cycle exit of endomitotic megakaryocytes. Blood. 2001 Dec 1;98(12):3274-82. doi: 10.1182/blood.v98.12.3274.
- Bani-Yaghoub M, Tremblay RG, Lei JX, Zhang D, Zurakowski B, Sandhu JK, Smith B, Ribecco-Lutkiewicz M, Kennedy J, Walker PR, Sikorska M. Role of Sox2 in the development of the mouse neocortex. Dev Biol. 2006 Jul 1;295(1):52-66. doi: 10.1016/j.ydbio.2006.03.007. Epub 2006 Apr 24.
- Bao XY, Xie C, Yang MS. Association between type 2 diabetes and CDKN2A/B: a meta-analysis study. Mol Biol Rep. 2012 Feb;39(2):1609-16. doi: 10.1007/s11033-011-0900-5. Epub 2011 May 31.
- Barrionuevo F, Taketo MM, Scherer G, Kispert A. Sox9 is required for notochord maintenance in mice. Dev Biol. 2006 Jul 1;295(1):128-40. doi: 10.1016/j.ydbio.2006.03.014. Epub 2006 May 6.
- Bartsch DK, Sina-Frey M, Lang S, Wild A, Gerdes B, Barth P, Kress R, Grützmann R, Colombo-Benkmann M, Ziegler A, Hahn SA, Rothmund M,

Rieder H. CDKN2A germline mutations in familial pancreatic cancer. Ann Surg. 2002 Dec;236(6):730-7. doi: 10.1097/00000658-200212000-00005.

- Bastidas-Ponce A, Scheibner K, Lickert H, Bakhti M. Cellular and molecular mechanisms coordinating pancreas development. Development. 2017 Aug 15;144(16):2873-2888. doi: 10.1242/dev.140756.
- Bergsland M, Ramsköld D, Zaouter C, Klum S, Sandberg R, Muhr J. Sequentially acting Sox transcription factors in neural lineage development. Genes Dev. 2011 Dec 1;25(23):2453-64. doi: 10.1101/gad.176008.111. Epub 2011 Nov 15.
- Bertwistle D, Sugimoto M, Sherr CJ. Physical and functional interactions of the Arf tumor suppressor protein with nucleophosmin/B23. Mol Cell Biol. 2004 Feb;24(3):985-96. doi: 10.1128/MCB.24.3.985-996.2004.
- Blache P, van de Wetering M, Duluc I, Domon C, Berta P, Freund JN, Clevers H, Jay P. SOX9 is an intestine crypt transcription factor, is regulated by the Wnt pathway, and represses the CDX2 and MUC2 genes. J Cell Biol. 2004 Jul 5;166(1):37-47. doi: 10.1083/jcb.200311021.
- Boroviak T, Nichols J. Primate embryogenesis predicts the hallmarks of human naïve pluripotency. Development. 2017 Jan 15;144(2):175-186. doi: 10.1242/dev.145177.
- Bouchard C, Lee S, Paulus-Hock V, Loddenkemper C, Eilers M, Schmitt CA. FoxO transcription factors suppress Myc-driven lymphomagenesis via direct activation of Arf. Genes Dev. 2007 Nov 1;21(21):2775-87. doi: 10.1101/gad.453107.
- Boyer LA, Lee TI, Cole MF, Johnstone SE, Levine SS, Zucker JP, Guenther MG, Kumar RM, Murray HL, Jenner RG, Gifford DK, Melton DA, Jaenisch R, Young RA. Core transcriptional regulatory circuitry in human embryonic stem cells. Cell. 2005 Sep 23;122(6):947-56. doi: 10.1016/j.cell.2005.08.020.
- Bracken AP, Kleine-Kohlbrecher D, Dietrich N, Pasini D, Gargiulo G, Beekman C, Theilgaard-Mönch K, Minucci S, Porse BT, Marine JC, Hansen KH, Helin K. The Polycomb group proteins bind throughout the INK4A-ARF locus and are disassociated in senescent cells. Genes Dev. 2007 Mar 1;21(5):525-30. doi: 10.1101/gad.415507. Erratum in: Genes Dev. 2023 Sep 1;37(17-18):861. doi: 10.1101/gad.351178.123.
- Brissova M, Shiota M, Nicholson WE, Gannon M, Knobel SM, Piston DW, Wright CV, Powers AC. Reduction in pancreatic transcription factor PDX-1 impairs glucose-stimulated insulin secretion. J Biol Chem. 2002 Mar 29;277(13):11225-32. doi: 10.1074/jbc.M111272200. Epub 2002 Jan 7.
- Budina-Kolomets A, Hontz RD, Pimkina J, Murphy ME. A conserved domain in exon 2 coding for the human and murine ARF tumor suppressor protein is required for autophagy induction. Autophagy. 2013 Oct;9(10):1553-65. doi: 10.4161/auto.25831. Epub 2013 Aug 7.

- Buetow L, Huang DT. Structural insights into the catalysis and regulation of E3 ubiquitin ligases. Nat Rev Mol Cell Biol. 2016 Oct;17(10):626-42. doi: 10.1038/nrm.2016.91. Epub 2016 Aug 3.
- Burtscher I, Tarquis-Medina M, Salinno C, Schirge S, Beckenbauer J, Bakhti M, Lickert H. Generation of a Novel Nkx6-1 Venus Fusion Reporter Mouse Line. Int J Mol Sci. 2021 Mar 26;22(7):3434. doi: 10.3390/ijms22073434.
- Bylund M, Andersson E, Novitch BG, Muhr J. Vertebrate neurogenesis is counteracted by Sox1-3 activity. Nat Neurosci. 2003 Nov;6(11):1162-8. doi: 10.1038/nn1131. Epub 2003 Sep 28.
- Cai JB, Shi GM, Dong ZR, Ke AW, Ma HH, Gao Q, Shen ZZ, Huang XY, Chen H, Yu DD, Liu LX, Zhang PF, Zhang C, Hu MY, Yang LX, Shi YH, Wang XY, Ding ZB, Qiu SJ, Sun HC, Zhou J, Shi YG, Fan J. Ubiquitin-specific protease 7 accelerates p14(ARF) degradation by deubiquitinating thyroid hormone receptor-interacting protein 12 and promotes hepatocellular carcinoma progression. Hepatology. 2015 May;61(5):1603-14. doi: 10.1002/hep.27682.
- Canham MA, Sharov AA, Ko MS, Brickman JM. Functional heterogeneity of embryonic stem cells revealed through translational amplification of an early endodermal transcript. PLoS Biol. 2010 May 25;8(5):e1000379. doi: 10.1371/journal.pbio.1000379.
- Carnero A, Hudson JD, Price CM, Beach DH. p16INK4A and p19ARF act in overlapping pathways in cellular immortalization. Nat Cell Biol. 2000 Mar;2(3):148-55. doi: 10.1038/35004020.
- Carnero A, Hudson JD, Price CM, Beach DH. p16INK4A and p19ARF act in overlapping pathways in cellular immortalization. Nat Cell Biol. 2000 Mar;2(3):148-55. doi: 10.1038/35004020.
- Carrasco M, Delgado I, Soria B, Martín F, Rojas A. GATA4 and GATA6 control mouse pancreas organogenesis. J Clin Invest. 2012 Oct;122(10):3504-15. doi: 10.1172/JCI63240. Epub 2012 Sep 24.
- Carvalho J. Cell Reversal From a Differentiated to a Stem-Like State at Cancer Initiation. Front Oncol. 2020 Apr 15;10:541. doi: 10.3389/fonc.2020.00541.
- Cerulo L, Tagliaferri D, Marotta P, Zoppoli P, Russo F, Mazio C, DeFelice M, Ceccarelli M, Falco G. Identification of a novel gene signature of ES cells self-renewal fluctuation through system-wide analysis. PLoS One. 2014 Jan 2;9(1):e83235. doi: 10.1371/journal.pone.0083235.
- Chaboissier MC, Kobayashi A, Vidal VI, Lützkendorf S, van de Kant HJ, Wegner M, de Rooij DG, Behringer RR, Schedl A. Functional analysis of Sox8 and Sox9 during sex determination in the mouse. Development. 2004 May;131(9):1891-901. doi: 10.1242/dev.01087. Epub 2004 Mar 31.
- Chambers I, Colby D, Robertson M, Nichols J, Lee S, Tweedie S, Smith A. Functional expression cloning of Nanog, a pluripotency sustaining factor in

embryonic stem cells. Cell. 2003 May 30;113(5):643-55. doi: 10.1016/s0092-8674(03)00392-1.

- Chambers I, Colby D, Robertson M, Nichols J, Lee S, Tweedie S, Smith A. Functional expression cloning of Nanog, a pluripotency sustaining factor in embryonic stem cells. Cell. 2003 May 30;113(5):643-55. doi: 10.1016/s0092-8674(03)00392-1.
- Chen D, Kon N, Li M, Zhang W, Qin J, Gu W. ARF-BP1/Mule is a critical mediator of the ARF tumor suppressor. Cell. 2005 Jul 1;121(7):1071-83. doi: 10.1016/j.cell.2005.03.037.
- Chen D, Kon N, Zhong J, Zhang P, Yu L, Gu W. Differential effects on ARF stability by normal versus oncogenic levels of c-Myc expression. Mol Cell. 2013 Jul 11;51(1):46-56. doi: 10.1016/j.molcel.2013.05.006. Epub 2013 Jun 6.
- Chen D, Shan J, Zhu WG, Qin J, Gu W. Transcription-independent ARF regulation in oncogenic stress-mediated p53 responses. Nature. 2010 Mar 25;464(7288):624-7. doi: 10.1038/nature08820. Epub 2010 Mar 7.
- Chen G, Ghosh P, O'Farrell T, Munk R, Rezanka LJ, Sasaki CY, Longo DL. Transforming growth factor β1 (TGF-β1) suppresses growth of B-cell lymphoma cells by p14(ARF)-dependent regulation of mutant p53. J Biol Chem. 2012 Jun 29;287(27):23184-95. doi: 10.1074/jbc.M112.351411. Epub 2012 May 23.
- Chen IH, Sciabica KS, Sandri-Goldin RM. ICP27 interacts with the RNA export factor Aly/REF to direct herpes simplex virus type 1 intronless mRNAs to the TAP export pathway. J Virol. 2002 Dec;76(24):12877-89. doi: 10.1128/jvi.76.24.12877-12889.2002.
- Chen J, Zhang Z, Li L, Chen BC, Revyakin A, Hajj B, Legant W, Dahan M, Lionnet T, Betzig E, Tjian R, Liu Z. Single-molecule dynamics of enhanceosome assembly in embryonic stem cells. Cell. 2014 Mar 13;156(6):1274-1285. doi: 10.1016/j.cell.2014.01.062.
- Chen X, Xu H, Yuan P, Fang F, Huss M, Vega VB, Wong E, Orlov YL, Zhang W, Jiang J, Loh YH, Yeo HC, Yeo ZX, Narang V, Govindarajan KR, Leong B, Shahab A, Ruan Y, Bourque G, Sung WK, Clarke ND, Wei CL, Ng HH. Integration of external signaling pathways with the core transcriptional network in embryonic stem cells. Cell. 2008 Jun 13;133(6):1106-17. doi: 10.1016/j.cell.2008.04.043.
- Cheung M, Chaboissier MC, Mynett A, Hirst E, Schedl A, Briscoe J. The transcriptional control of trunk neural crest induction, survival, and delamination. Dev Cell. 2005 Feb;8(2):179-92. doi: 10.1016/j.devcel.2004.12.010.
- Cheung M, Chaboissier MC, Mynett A, Hirst E, Schedl A, Briscoe J. The transcriptional control of trunk neural crest induction, survival, and delamination. Dev Cell. 2005 Feb;8(2):179-92. doi: 10.1016/j.devcel.2004.12.010.

- Chinzei N, Hayashi S, Ueha T, Fujishiro T, Kanzaki N, Hashimoto S, Sakata S, Kihara S, Haneda M, Sakai Y, Kuroda R, Kurosaka M. P21 deficiency delays regeneration of skeletal muscular tissue. PLoS One. 2015 May 5;10(5):e0125765. doi: 10.1371/journal.pone.0125765.
- Conacci-Sorrell M, McFerrin L, Eisenman RN. An overview of MYC and its interactome. Cold Spring Harb Perspect Med. 2014 Jan 1;4(1):a014357. doi: 10.1101/cshperspect.a014357. Erratum in: Cold Spring Harb Perspect Med. 2014 Apr;4(4). doi:10.1101/cshperspect.a023325.
- D'Angelo W, Chen B, Gurung C, Guo YL. Characterization of embryonic stem cell-differentiated fibroblasts as mesenchymal stem cells with robust expansion capacity and attenuated innate immunity. Stem Cell Res Ther. 2018 Oct 25;9(1):278. doi: 10.1186/s13287-018-1033-8.
- De Angelis MT, Russo F, D'Angelo F, Federico A, Gemei M, Del Vecchio L, Ceccarelli M, De Felice M, Falco G. Novel pancreas organogenesis markers refine the pancreatic differentiation roadmap of embryonic stem cells. Stem Cell Rev Rep. 2014 Apr;10(2):269-79. doi: 10.1007/s12015-013-9489-5.
- de Rooij DG. Proliferation and differentiation of spermatogonial stem cells. Reproduction. 2001 Mar;121(3):347-54. doi: 10.1530/rep.0.1210347.
- de Stanchina E, McCurrach ME, Zindy F, Shieh SY, Ferbeyre G, Samuelson AV, Prives C, Roussel MF, Sherr CJ, Lowe SW. E1A signaling to p53 involves the p19(ARF) tumor suppressor. Genes Dev. 1998 Aug 1;12(15):2434-42. doi: 10.1101/gad.12.15.2434.
- Decker K, Goldman DC, Grasch CL, Sussel L. Gata6 is an important regulator of mouse pancreas development. Dev Biol. 2006 Oct 15;298(2):415-29. doi: 10.1016/j.ydbio.2006.06.046. Epub 2006 Jul 4.
- DeGregori J, Leone G, Miron A, Jakoi L, Nevins JR. Distinct roles for E2F proteins in cell growth control and apoptosis. Proc Natl Acad Sci U S A. 1997 Jul 8;94(14):7245-50. doi: 10.1073/pnas.94.14.7245.
- del Arroyo AG, Peters G. The Ink4a/Arf network--cell cycle checkpoint or emergency brake? Adv Exp Med Biol. 2005;570:227-47. doi: 10.1007/1-4020-3764-3_8.
- di Tommaso A, Hagen J, Tompkins V, Muniz V, Dudakovic A, Kitzis A, Ladeveze V, Quelle DE. Residues in the alternative reading frame tumor suppressor that influence its stability and p53-independent activities. Exp Cell Res. 2009 Apr 15;315(7):1326-35. doi: 10.1016/j.yexcr.2009.01.010. Epub 2009 Jan 27.
- Ding L, Paszkowski-Rogacz M, Nitzsche A, Slabicki MM, Heninger AK, de Vries I, Kittler R, Junqueira M, Shevchenko A, Schulz H, Hubner N, Doss MX, Sachinidis A, Hescheler J, Iacone R, Anastassiadis K, Stewart AF, Pisabarro MT, Caldarelli A, Poser I, Theis M, Buchholz F. A genome-scale RNAi screen for Oct4 modulators defines a role of the Paf1 complex for embryonic stem cell identity. Cell Stem Cell. 2009 May 8;4(5):403-15. doi: 10.1016/j.stem.2009.03.009. Epub 2009 Apr 2.

- Ding X, Wang X, Sontag S, Qin J, Wanek P, Lin Q, Zenke M. The polycomb protein Ezh2 impacts on induced pluripotent stem cell generation. Stem Cells Dev. 2014 May 1;23(9):931-40. doi: 10.1089/scd.2013.0267. Epub 2014 Jan 21.
- Dominguez G, Silva J, Garcia JM, Silva JM, Rodriguez R, Muñoz C, Chacón I, Sanchez R, Carballido J, Colás A, España P, Bonilla F. Prevalence of aberrant methylation of p14ARF over p16INK4a in some human primary tumors. Mutat Res. 2003 Sep 29;530(1-2):9-17. doi: 10.1016/s0027-5107(03)00133-7.
- Duro D, Bernard O, Della Valle V, Berger R, Larsen CJ. A new type of p16INK4/MTS1 gene transcript expressed in B-cell malignancies. Oncogene. 1995 Jul 6;11(1):21-9.
- Dutto I, Tillhon M, Cazzalini O, Stivala LA, Prosperi E. Biology of the cell cycle inhibitor p21(CDKN1A): molecular mechanisms and relevance in chemical toxicology. Arch Toxicol. 2015 Feb;89(2):155-78. doi: 10.1007/s00204-014-1430-4. Epub 2014 Dec 17.
- Edlund H. Pancreatic organogenesis--developmental mechanisms and implications for therapy. Nat Rev Genet. 2002 Jul;3(7):524-32. doi: 10.1038/nrg841.
- el-Deiry WS, Tokino T, Velculescu VE, Levy DB, Parsons R, Trent JM, Lin D, Mercer WE, Kinzler KW, Vogelstein B. WAF1, a potential mediator of p53 tumor suppression. Cell. 1993 Nov 19;75(4):817-25. doi: 10.1016/0092-8674(93)90500-p.
- Engeland K. Cell cycle arrest through indirect transcriptional repression by p53: I have a DREAM. Cell Death Differ. 2018 Jan;25(1):114-132. doi: 10.1038/cdd.2017.172. Epub 2017 Nov 10.
- Esch D, Vahokoski J, Groves MR, Pogenberg V, Cojocaru V, Vom Bruch H, Han D, Drexler HC, Araúzo-Bravo MJ, Ng CK, Jauch R, Wilmanns M, Schöler HR. A unique Oct4 interface is crucial for reprogramming to pluripotency. Nat Cell Biol. 2013 Mar;15(3):295-301. doi: 10.1038/ncb2680. Epub 2013 Feb 3.
- Esteller M, Tortola S, Toyota M, Capella G, Peinado MA, Baylin SB, Herman JG. Hypermethylation-associated inactivation of p14(ARF) is independent of p16(INK4a) methylation and p53 mutational status. Cancer Res. 2000 Jan 1;60(1):129-33.
- Eymin B, Claverie P, Salon C, Leduc C, Col E, Brambilla E, Khochbin S, Gazzeri S. p14ARF activates a Tip60-dependent and p53-independent ATM/ATR/CHK pathway in response to genotoxic stress. Mol Cell Biol. 2006 Jun;26(11):4339-50. doi: 10.1128/MCB.02240-05.

- Eymin B, Claverie P, Salon C, Leduc C, Col E, Brambilla E, Khochbin S, Gazzeri S. p14ARF activates a Tip60-dependent and p53-independent ATM/ATR/CHK pathway in response to genotoxic stress. Mol Cell Biol. 2006 Jun;26(11):4339-50. doi: 10.1128/MCB.02240-05.

- Eymin B, Karayan L, Séité P, Brambilla C, Brambilla E, Larsen CJ, Gazzéri S. Human ARF binds E2F1 and inhibits its transcriptional activity. Oncogene. 2001 Mar 1;20(9):1033-41. doi: 10.1038/sj.onc.1204220.
- Fidalgo M, Faiola F, Pereira CF, Ding J, Saunders A, Gingold J, Schaniel C, Lemischka IR, Silva JC, Wang J. Zfp281 mediates Nanog autorepression through recruitment of the NuRD complex and inhibits somatic cell reprogramming. Proc Natl Acad Sci U S A. 2012 Oct 2;109(40):16202-7. doi: 10.1073/pnas.1208533109. Epub 2012 Sep 17.
- Fontana R, Guidone D, Sangermano F, Calabrò V, Pollice A, La Mantia G, Vivo M. PKC Dependent p14ARF Phosphorylation on Threonine 8 Drives Cell Proliferation. Sci Rep. 2018 May 4;8(1):7056. doi: 10.1038/s41598-018-25496-4.
- Fontana R, Ranieri M, La Mantia G, Vivo M. Dual Role of the Alternative Reading Frame ARF Protein in Cancer. Biomolecules. 2019 Mar 4;9(3):87. doi: 10.3390/biom9030087.
- Freyer L, Schröter C, Saiz N, Schrode N, Nowotschin S, Martinez-Arias A, Hadjantonakis AK. A loss-of-function and H2B-Venus transcriptional reporter allele for Gata6 in mice. BMC Dev Biol. 2015 Oct 24;15:38. doi: 10.1186/s12861-015-0086-5.
- Furuyama K, Kawaguchi Y, Akiyama H, Horiguchi M, Kodama S, Kuhara T, Hosokawa S, Elbahrawy A, Soeda T, Koizumi M, Masui T, Kawaguchi M, Takaori K, Doi R, Nishi E, Kakinoki R, Deng JM, Behringer RR, Nakamura T, Uemoto S. Continuous cell supply from a Sox9-expressing progenitor zone in adult liver, exocrine pancreas and intestine. Nat Genet. 2011 Jan;43(1):34-41. doi: 10.1038/ng.722. Epub 2010 Nov 28.
- Gabbert H, Wagner R, Moll R, Gerharz CD. Tumor dedifferentiation: an important step in tumor invasion. Clin Exp Metastasis. 1985 Oct-Dec;3(4):257-79. doi: 10.1007/BF01585081.
- Gardie B, Cayuela JM, Martini S, Sigaux F. Genomic alterations of the p19Arf encoding exons in T-cell acute lymphoblastic leukemia. Blood. 1998 Feb 1;91(3):1016-20.
- Gartel AL, Tyner AL. Transcriptional regulation of the p21((WAF1/CIP1)) gene. Exp Cell Res. 1999 Feb 1;246(2):280-9. doi: 10.1006/excr.1998.4319.
- Gerdes B, Bartsch DK, Ramaswamy A, Kersting M, Wild A, Schuermann M, Frey M, Rothmund M. Multiple primary tumors as an indicator for p16INK4a germline mutations in pancreatic cancer patients? Pancreas. 2000 Nov;21(4):369-75. doi: 10.1097/00006676-200011000-00007.
- Gong Y, Zhang L, Zhang A, Chen X, Gao P, Zeng Q. GATA4 inhibits cell differentiation and proliferation in pancreatic cancer. PLoS One. 2018 Aug 24;13(8):e0202449. doi: 10.1371/journal.pone.0202449.

- Gong Y, Zhang L, Zhang A, Chen X, Gao P, Zeng Q. GATA4 inhibits cell differentiation and proliferation in pancreatic cancer. PLoS One. 2018 Aug 24;13(8):e0202449. doi: 10.1371/journal.pone.0202449.

- Graham V, Khudyakov J, Ellis P, Pevny L. SOX2 functions to maintain neural progenitor identity. Neuron. 2003 Aug 28;39(5):749-65. doi: 10.1016/s0896-6273(03)00497-5.
- Graham V, Khudyakov J, Ellis P, Pevny L. SOX2 functions to maintain neural progenitor identity. Neuron. 2003 Aug 28;39(5):749-65. doi: 10.1016/s0896-6273(03)00497-5.
- Gromley A, Churchman ML, Zindy F, Sherr CJ. Transient expression of the Arf tumor suppressor during male germ cell and eye development in Arf-Cre reporter mice. Proc Natl Acad Sci U S A. 2009 Apr 14;106(15):6285-90. doi: 10.1073/pnas.0902310106. Epub 2009 Apr 1. Erratum in: Proc Natl Acad Sci U S A. 2009 Jun 2;106(22):9120.
- Gromley A, Churchman ML, Zindy F, Sherr CJ. Transient expression of the Arf tumor suppressor during male germ cell and eye development in Arf-Cre reporter mice. Proc Natl Acad Sci U S A. 2009 Apr 14;106(15):6285-90. doi: 10.1073/pnas.0902310106. Epub 2009 Apr 1. Erratum in: Proc Natl Acad Sci U S A. 2009 Jun 2;106(22):9120.
- Guo K, Wang J, Andrés V, Smith RC, Walsh K. MyoD-induced expression of p21 inhibits cyclin-dependent kinase activity upon myocyte terminal differentiation. Mol Cell Biol. 1995 Jul;15(7):3823-9. doi: 10.1128/MCB.15.7.3823.
- Guz Y, Montminy MR, Stein R, Leonard J, Gamer LW, Wright CV, Teitelman G. Expression of murine STF-1, a putative insulin gene transcription factor, in beta cells of pancreas, duodenal epithelium and pancreatic exocrine and endocrine progenitors during ontogeny. Development. 1995 Jan;121(1):11-8. doi: 10.1242/dev.121.1.11.
- Hagey DW, Bergsland M, Muhr J. SOX2 transcription factor binding and function. Development. 2022 Jul 15;149(14):dev200547. doi: 10.1242/dev.200547. Epub 2022 Jul 21.
- Hagey DW, Muhr J. Sox2 acts in a dose-dependent fashion to regulate proliferation of cortical progenitors. Cell Rep. 2014 Dec 11;9(5):1908-1920. doi: 10.1016/j.celrep.2014.11.013. Epub 2014 Dec 4.
- Hemmati PG, Gillissen B, von Haefen C, Wendt J, Stärck L, Güner D, Dörken B, Daniel PT. Adenovirus-mediated overexpression of p14(ARF) induces p53 and Bax-independent apoptosis. Oncogene. 2002 May 9;21(20):3149-61. doi: 10.1038/sj.onc.1205458.
- Herberg M, Roeder I. Computational modelling of embryonic stem-cell fate control. Development. 2015 Jul 1;142(13):2250-60. doi: 10.1242/dev.116343.
- Hewitt C, Lee Wu C, Evans G, Howell A, Elles RG, Jordan R, Sloan P, Read AP, Thakker N. Germline mutation of ARF in a melanoma kindred. Hum Mol Genet. 2002 May 15;11(11):1273-9. doi: 10.1093/hmg/11.11.1273.
- Hisada K, Sánchez C, Endo TA, Endoh M, Román-Trufero M, Sharif J, Koseki H, Vidal M. RYBP represses endogenous retroviruses and

preimplantation- and germ line-specific genes in mouse embryonic stem cells. Mol Cell Biol. 2012 Mar;32(6):1139-49. doi: 10.1128/MCB.06441-11. Epub 2012 Jan 23.

- Holland AM, Góñez LJ, Naselli G, Macdonald RJ, Harrison LC. Conditional expression demonstrates the role of the homeodomain transcription factor Pdx1 in maintenance and regeneration of beta-cells in the adult pancreas. Diabetes. 2005 Sep;54(9):2586-95. doi: 10.2337/diabetes.54.9.2586.
- Hou DR, Jin Y, Nie XW, Zhang ML, Ta N, Zhao LH, Yang N, Chen Y, Wu ZQ, Jiang HB, Li YR, Sun QY, Dai YF, Li RF. Derivation of Porcine Embryonic Stem-Like Cells from In Vitro-Produced Blastocyst-Stage Embryos. Sci Rep. 2016 May 13;6:25838. doi: 10.1038/srep25838.
- Humbert PO, Verona R, Trimarchi JM, Rogers C, Dandapani S, Lees JA. E2f3 is critical for normal cellular proliferation. Genes Dev. 2000 Mar 15;14(6):690-703.
- Inoue K, Roussel MF, Sherr CJ. Induction of ARF tumor suppressor gene expression and cell cycle arrest by transcription factor DMP1. Proc Natl Acad Sci U S A. 1999 Mar 30;96(7):3993-8. doi: 10.1073/pnas.96.7.3993.
- Inoue R, Shiraishi T. PKCalpha is involved in phorbol ester TPA-mediated stabilization of p14ARF. Biochem Biophys Res Commun. 2005 May 20;330(4):1314-8. doi: 10.1016/j.bbrc.2005.03.117.
- Itahana K, Bhat KP, Jin A, Itahana Y, Hawke D, Kobayashi R, Zhang Y. Tumor suppressor ARF degrades B23, a nucleolar protein involved in ribosome biogenesis and cell proliferation. Mol Cell. 2003 Nov;12(5):1151-64. doi: 10.1016/s1097-2765(03)00431-3.
- Itahana K, Zhang Y. Mitochondrial p32 is a critical mediator of ARF-induced apoptosis. Cancer Cell. 2008 Jun;13(6):542-53. doi: 10.1016/j.ccr.2008.04.002.
- Ito T, Nishida N, Fukuda Y, Nishimura T, Komeda T, Nakao K. Alteration of the p14(ARF) gene and p53 status in human hepatocellular carcinomas. J Gastroenterol. 2004;39(4):355-61. doi: 10.1007/s00535-003-1302-9.
- Jauch R, Choo SH, Ng CK, Kolatkar PR. Crystal structure of the dimeric Oct6 (POU3f1) POU domain bound to palindromic MORE DNA. Proteins. 2011 Feb;79(2):674-7. doi: 10.1002/prot.22916.
- Jennings RE, Berry AA, Strutt JP, Gerrard DT, Hanley NA. Human pancreas development. Development. 2015 Sep 15;142(18):3126-37. doi: 10.1242/dev.120063.
- Jensen J, Pedersen EE, Galante P, Hald J, Heller RS, Ishibashi M, Kageyama R, Guillemot F, Serup P, Madsen OD. Control of endodermal endocrine development by Hes-1. Nat Genet. 2000 Jan;24(1):36-44. doi: 10.1038/71657.
- Jiang F, Doudna JA. CRISPR-Cas9 Structures and Mechanisms. Annu Rev Biophys. 2017 May 22;46:505-529. doi: 10.1146/annurev-biophys-062215-010822. Epub 2017 Mar 30.

- Jiang H, Lin J, Su ZZ, Herlyn M, Kerbel RS, Weissman BE, Welch DR, Fisher PB. The melanoma differentiation-associated gene mda-6, which encodes the cyclin-dependent kinase inhibitor p21, is differentially expressed during growth, differentiation and progression in human melanoma cells. Oncogene. 1995 May 4;10(9):1855-64.
- Jiang J, Chan YS, Loh YH, Cai J, Tong GQ, Lim CA, Robson P, Zhong S, Ng HH. A core Klf circuitry regulates self-renewal of embryonic stem cells. Nat Cell Biol. 2008 Mar;10(3):353-60. doi: 10.1038/ncb1698. Epub 2008 Feb 10.
- Jiang J, Lv W, Ye X, Wang L, Zhang M, Yang H, Okuka M, Zhou C, Zhang X, Liu L, Li J. Zscan4 promotes genomic stability during reprogramming and dramatically improves the quality of iPS cells as demonstrated by tetraploid complementation. Cell Res. 2013 Jan;23(1):92-106. doi: 10.1038/cr.2012.157. Epub 2012 Nov 13.
- Johnson JD, Ahmed NT, Luciani DS, Han Z, Tran H, Fujita J, Misler S, Edlund H, Polonsky KS. Increased islet apoptosis in Pdx1+/- mice. J Clin Invest. 2003 Apr;111(8):1147-60. doi: 10.1172/JCI16537.
- Jonsson J, Carlsson L, Edlund T, Edlund H. Insulin-promoter-factor 1 is required for pancreas development in mice. Nature. 1994 Oct 13;371(6498):606-9. doi: 10.1038/371606a0.
- Kallas A, Pook M, Trei A, Maimets T. SOX2 Is Regulated Differently from NANOG and OCT4 in Human Embryonic Stem Cells during Early Differentiation Initiated with Sodium Butyrate. Stem Cells Int. 2014;2014:298163. doi: 10.1155/2014/298163. Epub 2014 Feb 19.
- Kamijo T, Bodner S, van de Kamp E, Randle DH, Sherr CJ. Tumor spectrum in ARF-deficient mice. Cancer Res. 1999 May 1;59(9):2217-22.
- Kamijo T, van de Kamp E, Chong MJ, Zindy F, Diehl JA, Sherr CJ, McKinnon PJ. Loss of the ARF tumor suppressor reverses premature replicative arrest but not radiation hypersensitivity arising from disabled atm function. Cancer Res. 1999 May 15;59(10):2464-9.
- Kamijo T, Weber JD, Zambetti G, Zindy F, Roussel MF, Sherr CJ. Functional and physical interactions of the ARF tumor suppressor with p53 and Mdm2. Proc Natl Acad Sci U S A. 1998 Jul 7;95(14):8292-7. doi: 10.1073/pnas.95.14.8292.
- Ketola I, Otonkoski T, Pulkkinen MA, Niemi H, Palgi J, Jacobsen CM, Wilson DB, Heikinheimo M. Transcription factor GATA-6 is expressed in the endocrine and GATA-4 in the exocrine pancreas. Mol Cell Endocrinol. 2004 Oct 29;226(1-2):51-7. doi: 10.1016/j.mce.2004.06.007.
- Khan SH, Moritsugu J, Wahl GM. Differential requirement for p19Arfin the p53-dependent arrest induced by DNA damage, microtubule disruption, and ribonucleotide depletion. Proc Natl Acad Sci U S A. 2000 Mar 28;97(7):3266-71. doi: 10.1073/pnas.97.7.3266.
- Kim WY, Sharpless NE. The regulation of INK4/ARF in cancer and aging. Cell. 2006 Oct 20;127(2):265-75. doi: 10.1016/j.cell.2006.10.003.

- Klemm JD, Rould MA, Aurora R, Herr W, Pabo CO. Crystal structure of the Oct-1 POU domain bound to an octamer site: DNA recognition with tethered DNA-binding modules. Cell. 1994 Apr 8;77(1):21-32. doi: 10.1016/0092-8674(94)90231-3.
- Klockenbusch C, Kast J. Optimization of formaldehyde cross-linking for protein interaction analysis of non-tagged integrin beta1. J Biomed Biotechnol. 2010;2010:927585. doi: 10.1155/2010/927585. Epub 2010 Jun 28.
- Ko A, Han SY, Choi CH, Cho H, Lee MS, Kim SY, Song JS, Hong KM, Lee HW, Hewitt SM, Chung JY, Song J. Oncogene-induced senescence mediated by c-Myc requires USP10 dependent deubiquitination and stabilization of p14ARF. Cell Death Differ. 2018 Jun;25(6):1050-1062. doi: 10.1038/s41418-018-0072-0. Epub 2018 Feb 22.
- Ko A, Han SY, Song J. Dynamics of ARF regulation that control senescence and cancer. BMB Rep. 2016 Nov;49(11):598-606. doi: 10.5483/bmbrep.2016.49.11.120.
- Ko A, Han SY, Song J. Regulatory Network of ARF in Cancer Development. Mol Cells. 2018 May 31;41(5):381-389. doi: 10.14348/molcells.2018.0100. Epub 2018 Apr 18.
- Ko A, Shin JY, Seo J, Lee KD, Lee EW, Lee MS, Lee HW, Choi IJ, Jeong JS, Chun KH, Song J. Acceleration of gastric tumorigenesis through MKRN1-mediated posttranslational regulation of p14ARF. J Natl Cancer Inst. 2012 Nov 7;104(21):1660-72. doi: 10.1093/jnci/djs424. Epub 2012 Oct 25.
- Komori H, Enomoto M, Nakamura M, Iwanaga R, Ohtani K. Distinct E2F-mediated transcriptional program regulates p14ARF gene expression. EMBO J. 2005 Nov 2;24(21):3724-36. doi: 10.1038/sj.emboj.7600836. Epub 2005 Oct 6.
- Konishi N, Nakamura M, Kishi M, Nishimine M, Ishida E, Shimada K. Heterogeneous methylation and deletion patterns of the INK4a/ARF locus within prostate carcinomas. Am J Pathol. 2002 Apr;160(4):1207-14. doi: 10.1016/S0002-9440(10)62547-3.
- Korgaonkar C, Zhao L, Modestou M, Quelle DE. ARF function does not require p53 stabilization or Mdm2 relocalization. Mol Cell Biol. 2002 Jan;22(1):196-206. doi: 10.1128/MCB.22.1.196-206.2002.
- Kreis NN, Louwen F, Yuan J. Less understood issues: p21(Cip1) in mitosis and its therapeutic potential. Oncogene. 2015 Apr 2;34(14):1758-67. doi: 10.1038/onc.2014.133. Epub 2014 May 26.
- Kreis NN, Louwen F, Yuan J. The Multifaceted p21 (Cip1/Waf1/*CDKN1A*) in Cell Differentiation, Migration and Cancer Therapy. Cancers (Basel). 2019 Aug 21;11(9):1220. doi: 10.3390/cancers11091220.
- Kwong RA, Kalish LH, Nguyen TV, Kench JG, Bova RJ, Cole IE, Musgrove EA, Sutherland RL. p14ARF protein expression is a predictor of both relapse and survival in squamous cell carcinoma of the anterior tongue.

Clin Cancer Res. 2005 Jun 1;11(11):4107-16. doi: 10.1158/1078-0432.CCR-04-2036.

- Lal G, Liu L, Hogg D, Lassam NJ, Redston MS, Gallinger S. Patients with both pancreatic adenocarcinoma and melanoma may harbor germline CDKN2A mutations. Genes Chromosomes Cancer. 2000 Apr;27(4):358-61.
- Lee C, Smith BA, Bandyopadhyay K, Gjerset RA. DNA damage disrupts the p14ARF-B23(nucleophosmin) interaction and triggers a transient subnuclear redistribution of p14ARF. Cancer Res. 2005 Nov 1;65(21):9834-42. doi: 10.1158/0008-5472.CAN-05-1759.
- Lee M, Sup Han W, Kyoung Kim O, Hee Sung S, Sun Cho M, Lee SN, Koo H. Prognostic value of p16INK4a and p14ARF gene hypermethylation in human colon cancer. Pathol Res Pract. 2006;202(6):415-24. doi: 10.1016/j.prp.2005.11.011. Epub 2006 May 3.
- Lee S, Cho YE, Kim SH, Kim YJ, Park JH. GLTSCR2 promotes the nucleoplasmic translocation and subsequent degradation of nucleolar ARF. Oncotarget. 2017 Mar 7;8(10):16293-16302. doi: 10.18632/oncotarget.9957.
- Levi BP, Morrison SJ. Stem cells use distinct self-renewal programs at different ages. Cold Spring Harb Symp Quant Biol. 2008;73:539-53. doi: 10.1101/sqb.2008.73.049. Epub 2009 Jan 15.
- Li C, Finkelstein D, Sherr CJ. Arf tumor suppressor and miR-205 regulate cell adhesion and formation of extraembryonic endoderm from pluripotent stem cells. Proc Natl Acad Sci U S A. 2013 Mar 19;110(12):E1112-21. doi: 10.1073/pnas.1302184110. Epub 2013 Mar 4.
- Li C, Finkelstein D, Sherr CJ. Arf tumor suppressor and miR-205 regulate cell adhesion and formation of extraembryonic endoderm from pluripotent stem cells. Proc Natl Acad Sci U S A. 2013 Mar 19;110(12):E1112-21. doi: 10.1073/pnas.1302184110. Epub 2013 Mar 4.
- Li H, Collado M, Villasante A, Strati K, Ortega S, Cañamero M, Blasco MA, Serrano M. The Ink4/Arf locus is a barrier for iPS cell reprogramming. Nature. 2009 Aug 27;460(7259):1136-9. doi: 10.1038/nature08290. Epub 2009 Aug 9.
- Li H, Collado M, Villasante A, Strati K, Ortega S, Cañamero M, Blasco MA, Serrano M. The Ink4/Arf locus is a barrier for iPS cell reprogramming. Nature. 2009 Aug 27;460(7259):1136-9. doi: 10.1038/nature08290. Epub 2009 Aug 9.
- Li M, Belmonte JC. Ground rules of the pluripotency gene regulatory network. Nat Rev Genet. 2017 Mar;18(3):180-191. doi: 10.1038/nrg.2016.156. Epub 2017 Jan 3.
- Li Y, Tzatzalos E, Kwan KY, Grumet M, Cai L. Transcriptional Regulation of Notch1 Expression by Nkx6.1 in Neural Stem/Progenitor Cells during Ventral Spinal Cord Development. Sci Rep. 2016 Dec 7;6:38665. doi: 10.1038/srep38665. PMID: 27924849; PMCID: PMC5141430.

- Lin T, Chao C, Saito S, Mazur SJ, Murphy ME, Appella E, Xu Y. p53 induces differentiation of mouse embryonic stem cells by suppressing Nanog expression. Nat Cell Biol. 2005 Feb;7(2):165-71. doi: 10.1038/ncb1211. Epub 2004 Dec 26.
- Lioubinski O, Müller M, Wegner M, Sander M. Expression of Sox transcription factors in the developing mouse pancreas. Dev Dyn. 2003 Jul;227(3):402-8. doi: 10.1002/dvdy.10311.
- Liu A, Yu X, Liu S. Pluripotency transcription factors and cancer stem cells: small genes make a big difference. Chin J Cancer. 2013 Sep;32(9):483-7. doi: 10.5732/cjc.012.10282. Epub 2013 Feb 19.
- Llanos S, Clark PA, Rowe J, Peters G. Stabilization of p53 by p14ARF without relocation of MDM2 to the nucleolus. Nat Cell Biol. 2001 May;3(5):445-52. doi: 10.1038/35074506.
- Lo D, Zhang Y, Dai MS, Sun XX, Zeng SX, Lu H. Nucleostemin stabilizes ARF by inhibiting the ubiquitin ligase ULF. Oncogene. 2015 Mar 26;34(13):1688-97. doi: 10.1038/onc.2014.103. Epub 2014 Apr 28.
- Loh YH, Wu Q, Chew JL, Vega VB, Zhang W, Chen X, Bourque G, George J, Leong B, Liu J, Wong KY, Sung KW, Lee CW, Zhao XD, Chiu KP, Lipovich L, Kuznetsov VA, Robson P, Stanton LW, Wei CL, Ruan Y, Lim B, Ng HH. The Oct4 and Nanog transcription network regulates pluripotency in mouse embryonic stem cells. Nat Genet. 2006 Apr;38(4):431-40. doi: 10.1038/ng1760. Epub 2006 Mar 5.
- Maggi LB Jr, Winkeler CL, Miceli AP, Apicelli AJ, Brady SN, Kuchenreuther MJ, Weber JD. ARF tumor suppression in the nucleolus. Biochim Biophys Acta. 2014 Jun;1842(6):831-9. doi: 10.1016/j.bbadis.2014.01.016. Epub 2014 Feb 10.
- Maglic D, Stovall DB, Cline JM, Fry EA, Mallakin A, Taneja P, Caudell DL, Willingham MC, Sui G, Inoue K. DMP1β, a splice isoform of the tumour suppressor DMP1 locus, induces proliferation and progression of breast cancer. J Pathol. 2015 May;236(1):90-102. doi: 10.1002/path.4504. Epub 2015 Feb 9.
- Mao L, Merlo A, Bedi G, Shapiro GI, Edwards CD, Rollins BJ, Sidransky D. A novel p16INK4A transcript. Cancer Res. 1995 Jul 15;55(14):2995-7.
- Martello G, Sugimoto T, Diamanti E, Joshi A, Hannah R, Ohtsuka S, Göttgens B, Niwa H, Smith A. Esrrb is a pivotal target of the Gsk3/Tcf3 axis regulating embryonic stem cell self-renewal. Cell Stem Cell. 2012 Oct 5;11(4):491-504. doi: 10.1016/j.stem.2012.06.008. Erratum in: Cell Stem Cell. 2013 May 2;12(5):630.
- Matsuda T, Nakamura T, Nakao K, Arai T, Katsuki M, Heike T, Yokota T. STAT3 activation is sufficient to maintain an undifferentiated state of mouse embryonic stem cells. EMBO J. 1999 Aug 2;18(15):4261-9. doi: 10.1093/emboj/18.15.4261.
- Mattout A, Aaronson Y, Sailaja BS, Raghu Ram EV, Harikumar A, Mallm JP, Sim KH, Nissim-Rafinia M, Supper E, Singh PB, Sze SK, Gasser SM,

Rippe K, Meshorer E. Heterochromatin Protein 1β (HP1β) has distinct functions and distinct nuclear distribution in pluripotent versus differentiated cells. Genome Biol. 2015 Sep 28;16:213. doi: 10.1186/s13059-015-0760-8.

- Meek DW. Tumour suppression by p53: a role for the DNA damage response? Nat Rev Cancer. 2009 Oct;9(10):714-23. doi: 10.1038/nrc2716. Epub 2009 Sep 4.
- Mei Y, Wang Y, Chen H, Sun ZS, Ju XD. Recent Progress in CRISPR/Cas9 Technology. J Genet Genomics. 2016 Feb 20;43(2):63-75. doi: 10.1016/j.jgg.2016.01.001. Epub 2016 Jan 18.
- Mercer SE, Ewton DZ, Deng X, Lim S, Mazur TR, Friedman E. Mirk/Dyrk1B mediates survival during the differentiation of C2C12 myoblasts. J Biol Chem. 2005 Jul 8;280(27):25788-801. doi: 10.1074/jbc.M413594200. Epub 2005 Apr 25.
- Mikawa R, Sato T, Suzuki Y, Baskoro H, Kawaguchi K, Sugimoto M. p19Arf Exacerbates Cigarette Smoke-Induced Pulmonary Dysfunction. Biomolecules. 2020 Mar 17;10(3):462. doi: 10.3390/biom10030462.
- Mitsui K, Tokuzawa Y, Itoh H, Segawa K, Murakami M, Takahashi K, Maruyama M, Maeda M, Yamanaka S. The homeoprotein Nanog is required for maintenance of pluripotency in mouse epiblast and ES cells. Cell. 2003 May 30;113(5):631-42. doi: 10.1016/s0092-8674(03)00393-3.
- Montano E, Pollice A, Lucci V, Falco G, Affinito O, La Mantia G, Vivo M, Angrisano T. Pancreatic Progenitor Commitment Is Marked by an Increase in Ink4a/Arf Expression. Biomolecules. 2021 Jul 30;11(8):1124. doi: 10.3390/biom11081124.
- Muniz VP, Barnes JM, Paliwal S, Zhang X, Tang X, Chen S, Zamba KD, Cullen JJ, Meyerholz DK, Meyers S, Davis JN, Grossman SR, Henry MD, Quelle DE. The ARF tumor suppressor inhibits tumor cell colonization independent of p53 in a novel mouse model of pancreatic ductal adenocarcinoma metastasis. Mol Cancer Res. 2011 Jul;9(7):867-77. doi: 10.1158/1541-7786.MCR-10-0475. Epub 2011 Jun 2.
- Nakagawa T, Araki T, Nakagawa M, Hirao A, Unno M, Nakayama K. S6 Kinase- and β-TrCP2-Dependent Degradation of p19Arf Is Required for Cell Proliferation. Mol Cell Biol. 2015 Oct;35(20):3517-27. doi: 10.1128/MCB.00343-15. Epub 2015 Aug 3.
- Nakai-Futatsugi Y, Niwa H. Transcription factor network in embryonic stem cells: heterogeneity under the stringency. Biol Pharm Bull. 2013;36(2):166-70. doi: 10.1248/bpb.b12-00958.
- Nakamura M, Sakaki T, Hashimoto H, Nakase H, Ishida E, Shimada K, Konishi N. Frequent alterations of the p14(ARF) and p16(INK4a) genes in primary central nervous system lymphomas. Cancer Res. 2001 Sep 1;61(17):6335-9.
- Nelson SB, Schaffer AE, Sander M. The transcription factors Nkx6.1 and Nkx6.2 possess equivalent activities in promoting beta-cell fate

specification in Pdx1+ pancreatic progenitor cells. Development. 2007 Jul;134(13):2491-500. doi: 10.1242/dev.002691. Epub 2007 May 30.

- Nemer G, Nemer M. Transcriptional activation of BMP-4 and regulation of mammalian organogenesis by GATA-4 and -6. Dev Biol. 2003 Feb 1;254(1):131-48. doi: 10.1016/s0012-1606(02)00026-x.
- Nichols J, Zevnik B, Anastassiadis K, Niwa H, Klewe-Nebenius D, Chambers I, Schöler H, Smith A. Formation of pluripotent stem cells in the mammalian embryo depends on the POU transcription factor Oct4. Cell. 1998 Oct 30;95(3):379-91. doi: 10.1016/s0092-8674(00)81769-9.
- Niwa H, Miyazaki J, Smith AG. Quantitative expression of Oct-3/4 defines differentiation, dedifferentiation or self-renewal of ES cells. Nat Genet. 2000 Apr;24(4):372-6. doi: 10.1038/74199.
- Offield MF, Jetton TL, Labosky PA, Ray M, Stein RW, Magnuson MA, Hogan BL, Wright CV. PDX-1 is required for pancreatic outgrowth and differentiation of the rostral duodenum. Development. 1996 Mar;122(3):983-95. doi: 10.1242/dev.122.3.983.
- Offield MF, Jetton TL, Labosky PA, Ray M, Stein RW, Magnuson MA, Hogan BL, Wright CV. PDX-1 is required for pancreatic outgrowth and differentiation of the rostral duodenum. Development. 1996 Mar;122(3):983-95. doi: 10.1242/dev.122.3.983.
- Offield MF, Jetton TL, Labosky PA, Ray M, Stein RW, Magnuson MA, Hogan BL, Wright CV. PDX-1 is required for pancreatic outgrowth and differentiation of the rostral duodenum. Development. 1996 Mar;122(3):983-95. doi: 10.1242/dev.122.3.983.
- Ohtsuka S, Nakai-Futatsugi Y, Niwa H. LIF signal in mouse embryonic stem cells. JAKSTAT. 2015 Sep 11;4(2):e1086520. doi: 10.1080/21623996.2015.1086520.
- Oosterveen T, Kurdija S, Ensterö M, Uhde CW, Bergsland M, Sandberg M, Sandberg R, Muhr J, Ericson J. SoxB1-driven transcriptional network underlies neural-specific interpretation of morphogen signals. Proc Natl Acad Sci U S A. 2013 Apr 30;110(18):7330-5. doi: 10.1073/pnas.1220010110. Epub 2013 Apr 15.
- Ozenne P, Eymin B, Brambilla E, Gazzeri S. The ARF tumor suppressor: structure, functions and status in cancer. Int J Cancer. 2010 Nov 15;127(10):2239-47. doi: 10.1002/ijc.25511.
- Pan G, Thomson JA. Nanog and transcriptional networks in embryonic stem cell pluripotency. Cell Res. 2007 Jan;17(1):42-9. doi: 10.1038/sj.cr.7310125.
- Papatsenko D, Darr H, Kulakovskiy IV, Waghray A, Makeev VJ, MacArthur BD, Lemischka IR. Single-Cell Analyses of ESCs Reveal Alternative Pluripotent Cell States and Molecular Mechanisms that Control Self-Renewal. Stem Cell Reports. 2015 Aug 11;5(2):207-20. doi: 10.1016/j.stemcr.2015.07.004.

- Papatsenko D, Waghray A, Lemischka IR. Feedback control of pluripotency in embryonic stem cells: Signaling, transcription and epigenetics. Stem Cell Res. 2018 May;29:180-188. doi: 10.1016/j.scr.2018.02.012. Epub 2018 Feb 20.
- Papatsenko, D., Xu, H., Ma'ayan, A., Lemischka, I. (2013). Quantitative Approaches to Model Pluripotency and Differentiation in Stem Cells. In: Sell, S. (eds) Stem Cells Handbook. Humana Press, New York, NY. pp. 59-74 https://doi.org/10.1007/978-1-4614-7696-2_4.
- Papetti M, Wontakal SN, Stopka T, Skoultchi AI. GATA-1 directly regulates p21 gene expression during erythroid differentiation. Cell Cycle. 2010 May 15;9(10):1972-80. doi: 10.4161/cc.9.10.11602. Epub 2010 May 15.
- Parisi S, Passaro F, Aloia L, Manabe I, Nagai R, Pastore L, Russo T. Klf5 is involved in self-renewal of mouse embryonic stem cells. J Cell Sci. 2008 Aug 15;121(Pt 16):2629-34. doi: 10.1242/jcs.027599. Epub 2008 Jul 24.
- Parisi T, Pollice A, Di Cristofano A, Calabrò V, La Mantia G. Transcriptional regulation of the human tumor suppressor p14(ARF) by E2F1, E2F2, E2F3, and Sp1-like factors. Biochem Biophys Res Commun. 2002 Mar 15;291(5):1138-45. doi: 10.1006/bbrc.2002.6591.
- Parker SB, Eichele G, Zhang P, Rawls A, Sands AT, Bradley A, Olson EN, Harper JW, Elledge SJ. p53-independent expression of p21Cip1 in muscle and other terminally differentiating cells. Science. 1995 Feb 17;267(5200):1024-7. doi: 10.1126/science.7863329.
- Peterson KA, Nishi Y, Ma W, Vedenko A, Shokri L, Zhang X, McFarlane M, Baizabal JM, Junker JP, van Oudenaarden A, Mikkelsen T, Bernstein BE, Bailey TL, Bulyk ML, Wong WH, McMahon AP. Neural-specific Sox2 input and differential Gli-binding affinity provide context and positional information in Shh-directed neural patterning. Genes Dev. 2012 Dec 15;26(24):2802-16. doi: 10.1101/gad.207142.112.
- Piovan C, Palmieri D, Di Leva G, Braccioli L, Casalini P, Nuovo G, Tortoreto M, Sasso M, Plantamura I, Triulzi T, Taccioli C, Tagliabue E, Iorio MV, Croce CM. Oncosuppressive role of p53-induced miR-205 in triple negative breast cancer. Mol Oncol. 2012 Aug;6(4):458-72. doi: 10.1016/j.molonc.2012.03.003. Epub 2012 Apr 19.
- Pollice A, Nasti V, Ronca R, Vivo M, Lo Iacono M, Calogero R, Calabrò V, La Mantia G. Functional and physical interaction of the human ARF tumor suppressor with Tat-binding protein-1. J Biol Chem. 2004 Feb 20;279(8):6345-53. doi: 10.1074/jbc.M310957200. Epub 2003 Dec 9.
- Pollice A, Sepe M, Villella VR, Tolino F, Vivo M, Calabrò V, La Mantia G. TBP-1 protects the human oncosuppressor p14ARF from proteasomal degradation. Oncogene. 2007 Aug 2;26(35):5154-62. doi: 10.1038/sj.onc.1210313. Epub 2007 Mar 5.
- Pomerantz J, Schreiber-Agus N, Liégeois NJ, Silverman A, Alland L, Chin L, Potes J, Chen K, Orlow I, Lee HW, Cordon-Cardo C, DePinho RA. The

Ink4a tumor suppressor gene product, p19Arf, interacts with MDM2 and neutralizes MDM2's inhibition of p53. Cell. 1998 Mar 20;92(6):713-23. doi: 10.1016/s0092-8674(00)81400-2.

- Prakash N, Puelles E, Freude K, Trümbach D, Omodei D, Di Salvio M, Sussel L, Ericson J, Sander M, Simeone A, Wurst W. Nkx6-1 controls the identity and fate of red nucleus and oculomotor neurons in the mouse midbrain. Development. 2009 Aug;136(15):2545-55. doi: 10.1242/dev.031781.
- Quelle DE, Cheng M, Ashmun RA, Sherr CJ. Cancer-associated mutations at the INK4a locus cancel cell cycle arrest by p16INK4a but not by the alternative reading frame protein p19Arf. Proc Natl Acad Sci U S A. 1997 Jan 21;94(2):669-73. doi: 10.1073/pnas.94.2.669.
- Quelle DE, Zindy F, Ashmun RA, Sherr CJ. Alternative reading frames of the INK4a tumor suppressor gene encode two unrelated proteins capable of inducing cell cycle arrest. Cell. 1995 Dec 15;83(6):993-1000. doi: 10.1016/0092-8674(95)90214-7.
- Randerson-Moor JA, Harland M, Williams S, Cuthbert-Heavens D, Sheridan E, Aveyard J, Sibley K, Whitaker L, Knowles M, Bishop JN, Bishop DT. A germline deletion of p14(ARF) but not CDKN2A in a melanoma-neural system tumour syndrome family. Hum Mol Genet. 2001 Jan 1;10(1):55-62. doi: 10.1093/hmg/10.1.55.
- Reef S, Zalckvar E, Shifman O, Bialik S, Sabanay H, Oren M, Kimchi A. A short mitochondrial form of p19Arf induces autophagy and caspase-independent cell death. Mol Cell. 2006 May 19;22(4):463-75. doi: 10.1016/j.molcel.2006.04.014.
- Ritz-Laser B, Mamin A, Brun T, Avril I, Schwitzgebel VM, Philippe J. The zinc finger-containing transcription factor Gata-4 is expressed in the developing endocrine pancreas and activates glucagon gene expression. Mol Endocrinol. 2005 Mar;19(3):759-70. doi: 10.1210/me.2004-0051. Epub 2004 Nov 11.
- Rizos H, Darmanian AP, Holland EA, Mann GJ, Kefford RF. Mutations in the INK4a/ARF melanoma susceptibility locus functionally impair p14ARF. J Biol Chem. 2001 Nov 2;276(44):41424-34. doi: 10.1074/jbc.M105299200. Epub 2001 Aug 22.
- Rizos H, Puig S, Badenas C, Malvehy J, Darmanian AP, Jiménez L, Milà M, Kefford RF. A melanoma-associated germline mutation in exon 1beta inactivates p14ARF. Oncogene. 2001 Sep 6;20(39):5543-7. doi: 10.1038/sj.onc.1204728.
- Rizzino A. Concise review: The Sox2-Oct4 connection: critical players in a much larger interdependent network integrated at multiple levels. Stem Cells. 2013 Jun;31(6):1033-9. doi: 10.1002/stem.1352.
- RochaS, Garrett MD, Campbell KJ, Schumm K, Perkins ND. Regulation of NF-kappaB and p53 through activation of ATR and Chk1 by the ARF

tumour suppressor. EMBO J. 2005 Mar 23;24(6):1157-69. doi: 10.1038/sj.emboj.7600608. Epub 2005 Mar 10.

- Rodriguez-Terrones D, Gaume X, Ishiuchi T, Weiss A, Kopp A, Kruse K, Penning A, Vaquerizas JM, Brino L, Torres-Padilla ME. A molecular roadmap for the emergence of early-embryonic-like cells in culture. Nat Genet. 2018 Jan;50(1):106-119. doi: 10.1038/s41588-017-0016-5. Epub 2017 Dec 18.
- Rojas A, Schachterle W, Xu SM, Black BL. An endoderm-specific transcriptional enhancer from the mouse Gata4 gene requires GATA and homeodomain protein-binding sites for function in vivo. Dev Dyn. 2009 Oct;238(10):2588-98. doi: 10.1002/dvdy.22091.
- Roninson IB. Oncogenic functions of tumour suppressor p21(Waf1/Cip1/Sdi1): association with cell senescence and tumour-promoting activities of stromal fibroblasts. Cancer Lett. 2002 May 8;179(1):1-14. doi: 10.1016/s0304-3835(01)00847-3.
- Rosner MH, Vigano MA, Ozato K, Timmons PM, Poirier F, Rigby PW, Staudt LM. A POU-domain transcription factor in early stem cells and germ cells of the mammalian embryo. Nature. 1990 Jun 21;345(6277):686-92. doi: 10.1038/345686a0.
- Ruijtenberg S, van den Heuvel S. Coordinating cell proliferation and differentiation: Antagonism between cell cycle regulators and cell type-specific gene expression. Cell Cycle. 2016;15(2):196-212. doi: 10.1080/15384101.2015.1120925. PMID: 26825227;
- Rutter JL, Goldstein AM, Dávila MR, Tucker MA, Struewing JP. CDKN2A point mutations D153spl(c.457G>T) and IVS2+1G>T result in aberrant splice products affecting both p16INK4a and p14ARF. Oncogene. 2003 Jul 10;22(28):4444-8. doi: 10.1038/sj.onc.1206564.
- Sailasree R, Abhilash A, Sathyan KM, Nalinakumari KR, Thomas S, Kannan S. Differential roles of p16INK4A and p14ARF genes in prognosis of oral carcinoma. Cancer Epidemiol Biomarkers Prev. 2008 Feb;17(2):414-20. doi: 10.1158/1055-9965.EPI-07-0284.
- Sanjana NE, Shalem O, Zhang F. Improved vectors and genome-wide libraries for CRISPR screening. Nat Methods. 2014 Aug;11(8):783-784. doi: 10.1038/nmeth.3047.
- Sartori DJ, Wilbur CJ, Long SY, Rankin MM, Li C, Bradfield JP, Hakonarson H, Grant SF, Pu WT, Kushner JA. GATA factors promote ER integrity and β-cell survival and contribute to type 1 diabetes risk. Mol Endocrinol. 2014 Jan;28(1):28-39. doi: 10.1210/me.2013-1265. Epub 2013 Jan 1.
- Schaffer AE, Freude KK, Nelson SB, Sander M. Nkx6 transcription factors and Ptf1a function as antagonistic lineage determinants in multipotent pancreatic progenitors. Dev Cell. 2010 Jun 15;18(6):1022-9. doi: 10.1016/j.devcel.2010.05.015.

- Schmidt EE, Taylor DS, Prigge JR, Barnett S, Capecchi MR. Illegitimate Cre-dependent chromosome rearrangements in transgenic mouse spermatids. Proc Natl Acad Sci U S A. 2000 Dec 5;97(25):13702-7. doi: 10.1073/pnas.240471297.
- Schöler HR, Hatzopoulos AK, Balling R, Suzuki N, Gruss P. A family of octamer-specific proteins present during mouse embryogenesis: evidence for germline-specific expression of an Oct factor. EMBO J. 1989 Sep;8(9):2543-50. doi: 10.1002/j.1460-2075.1989.tb08392.x.
- Seo J, Kim MW, Bae KH, Lee SC, Song J, Lee EW. The roles of ubiquitination in extrinsic cell death pathways and its implications for therapeutics. Biochem Pharmacol. 2019 Apr;162:21-40. doi: 10.1016/j.bcp.2018.11.012. Epub 2018 Nov 16.
- Seo J, Seong D, Lee SR, Oh DB, Song J. Post-Translational Regulation of ARF: Perspective in Cancer. Biomolecules. 2020 Aug 4;10(8):1143. doi: 10.3390/biom10081143.
- Seymour PA, Freude KK, Tran MN, Mayes EE, Jensen J, Kist R, Scherer G, Sander M. SOX9 is required for maintenance of the pancreatic progenitor cell pool. Proc Natl Acad Sci U S A. 2007 Feb 6;104(6):1865-70. doi: 10.1073/pnas.0609217104. Epub 2007 Jan 31.
- Shalem O, Sanjana NE, Hartenian E, Shi X, Scott DA, Mikkelson T, Heckl D, Ebert BL, Root DE, Doench JG, Zhang F. Genome-scale CRISPR-Cas9 knockout screening in human cells. Science. 2014 Jan 3;343(6166):84-87. doi: 10.1126/science.1247005. Epub 2013 Dec 12.
- Sharpless NE, DePinho RA. The INK4A/ARF locus and its two gene products. Curr Opin Genet Dev. 1999 Feb;9(1):22-30. doi: 10.1016/s0959-437x(99)80004-5.
- Sharpless NE. INK4a/ARF: a multifunctional tumor suppressor locus. Mutat Res. 2005 Aug 25;576(1-2):22-38. doi: 10.1016/j.mrfmmm.2004.08.021.
- Sherr CJ, Weber JD. The ARF/p53 pathway. Curr Opin Genet Dev. 2000 Feb;10 (1):94-9. doi: 10.1016/s0959-437x(99)00038-6.
- Sherr CJ. Divorcing ARF and p53: an unsettled case. Nat Rev Cancer. 2006 Sep;6(9):663-73. doi: 10.1038/nrc1954. Epub 2006 Aug 17.
- Sherr CJ. Tumor surveillance via the ARF-p53 pathway. Genes Dev. 1998 Oct 1;12(19):2984-91. doi: 10.1101/gad.12.19.2984.
- Shi G, Jin Y. Role of Oct4 in maintaining and regaining stem cell pluripotency. Stem Cell Res Ther. 2010 Dec 14;1(5):39. doi: 10.1186/scrt39.
- Shi G, Jin Y. Role of Oct4 in maintaining and regaining stem cell pluripotency. Stem Cell Res Ther. 2010 Dec 14;1(5):39. doi: 10.1186/scrt39.
- Shi G, Jin Y. Role of Oct4 in maintaining and regaining stem cell pluripotency. Stem Cell Res Ther. 2010 Dec 14;1(5):39. doi: 10.1186/scrt39.

- Shimizu T, Ishikawa T, Sugihara E, Kuninaka S, Miyamoto T, Mabuchi Y, Matsuzaki Y, Tsunoda T, Miya F, Morioka H, Nakayama R, Kobayashi E, Toyama Y, Kawai A, Ichikawa H, Hasegawa T, Okada S, Ito T, Ikeda Y, Suda T, Saya H. c-MYC overexpression with loss of Ink4a/Arf transforms bone marrow stromal cells into osteosarcoma accompanied by loss of adipogenesis. Oncogene. 2010 Oct 21;29(42):5687-99. doi: 10.1038/onc.2010.312. Epub 2010 Aug 2.
- Silva J, Domínguez G, Silva JM, García JM, Gallego I, Corbacho C, Provencio M, España P, Bonilla F. Analysis of genetic and epigenetic processes that influence p14ARF expression in breast cancer. Oncogene. 2001 Jul 27;20(33):4586-90. doi: 10.1038/sj.onc.1204617.
- Solozobova V, Blattner C. p53 in stem cells. World J Biol Chem. 2011 Sep 26;2(9):202-14. doi: 10.4331/wjbc.v2.i9.202.
- Stoffers DA, Zinkin NT, Stanojevic V, Clarke WL, Habener JF. Pancreatic agenesis attributable to a single nucleotide deletion in the human IPF1 gene coding sequence. Nat Genet. **1997** Jan;15(1):106-10. doi: 10.1038/ng0197-106.
- Stoffers DA, Zinkin NT, Stanojevic V, Clarke WL, Habener JF. Pancreatic agenesis attributable to a single nucleotide deletion in the human IPF1 gene coding sequence. Nat Genet. 1997 Jan;15(1):106-10. doi: 10.1038/ng0197-106.
- Stolt CC, Lommes P, Sock E, Chaboissier MC, Schedl A, Wegner M. The Sox9 transcription factor determines glial fate choice in the developing spinal cord. Genes Dev. 2003 Jul 1;17(13):1677-89. doi: 10.1101/gad.259003. PMID: 12842915;
- Stone S, Jiang P, Dayananth P, Tavtigian SV, Katcher H, Parry D, Peters G, Kamb A. Complex structure and regulation of the P16 (MTS1) locus. Cancer Res. 1995 Jul 15;55(14):2988-94.
- Stott FJ, Bates S, James MC, McConnell BB, Starborg M, Brookes S, Palmero I, Ryan K, Hara E, Vousden KH, Peters G. The alternative product from the human CDKN2A locus, p14(ARF), participates in a regulatory feedback loop with p53 and MDM2. EMBO J. 1998 Sep 1;17(17):5001-14. doi: 10.1093/emboj/17.17.5001.
- Sun Y, Jiang X, Chen S, Fernandes N, Price BD. A role for the Tip60 histone acetyltransferase in the acetylation and activation of ATM. Proc Natl Acad Sci U S A. 2005 Sep 13;102(37):13182-7. doi: 10.1073/pnas.0504211102. Epub 2005 Sep 2.
- Swafford DS, Middleton SK, Palmisano WA, Nikula KJ, Tesfaigzi J, Baylin SB, Herman JG, Belinsky SA. Frequent aberrant methylation of p16INK4a in primary rat lung tumors. Mol Cell Biol. 1997 Mar;17(3):1366-74. doi: 10.1128/MCB.17.3.1366.
- Tamm C, Pijuan Galitó S, Annerén C. A comparative study of protocols for mouse embryonic stem cell culturing. PLoS One. 2013 Dec 10;8(12):e81156. doi: 10.1371/journal.pone.0081156.

- Tanaka TS, Kunath T, Kimber WL, Jaradat SA, Stagg CA, Usuda M, Yokota T, Niwa H, Rossant J, Ko MS. Gene expression profiling of embryo-derived stem cells reveals candidate genes associated with pluripotency and lineage specificity. Genome Res. 2002 Dec;12(12):1921-8. doi: 10.1101/gr.670002.
- Tanase CP, Neagu AI, Necula LG, Mambet C, Enciu AM, Calenic B, Cruceru ML, Albulescu R. Cancer stem cells: involvement in pancreatic cancer pathogenesis and perspectives on cancer therapeutics. World J Gastroenterol. 2014 Aug 21;20(31):10790-801. doi: 10.3748/wjg.v20.i31.10790.
- Torres-Padilla ME, Chambers I. Transcription factor heterogeneity in pluripotent stem cells: a stochastic advantage. Development. 2014 Jun;141(11):2173-81. doi: 10.1242/dev.102624.
- Tschan MP, Federzoni EA, Haimovici A, Britschgi C, Moser BA, Jin J, Reddy VA, Sheeter DA, Fischer KM, Sun P, Torbett BE. Human DMTF1β antagonizes DMTF1α regulation of the p14(ARF) tumor suppressor and promotes cellular proliferation. Biochim Biophys Acta. 2015 Sep;1849(9):1198-208. doi: 10.1016/j.bbagrm.2015.07.009. Epub 2015 Jul 15.
- Tsujimoto H, Hagiwara A, Sugihara H, Hattori T, Yamagishi H. Promoter methylations of p16INK4a and p14ARF genes in early and advanced gastric cancer. Correlations of the modes of their occurrence with histologic type. Pathol Res Pract. 2002;198(12):785-94. doi: 10.1078/0344-0338-00337.
- Ulanet DB, Hanahan D. Loss of p19(Arf) facilitates the angiogenic switch and tumor initiation in a multi-stage cancer model via p53-dependent and independent mechanisms. PLoS One. 2010 Aug 27;5(8):e12454. doi: 10.1371/journal.pone.0012454.
- van Oosterwijk JG, Li C, Yang X, Opferman JT, Sherr CJ. Small mitochondrial Arf (smArf) protein corrects p53-independent developmental defects of Arf tumor suppressor-deficient mice. Proc Natl Acad Sci U S A. 2017 Jul 11;114(28):7420-7425. doi: 10.1073/pnas.1707292114. Epub 2017 Jun 26.
- van Oosterwijk JG, Li C, Yang X, Opferman JT, Sherr CJ. Small mitochondrial Arf (smArf) protein corrects p53-independent developmental defects of Arf tumor suppressor-deficient mice. Proc Natl Acad Sci U S A. 2017 Jul 11;114(28):7420-7425. doi: 10.1073/pnas.1707292114. Epub 2017 Jun 26.
- Vidal VP, Chaboissier MC, Lützkendorf S, Cotsarelis G, Mill P, Hui CC, Ortonne N, Ortonne JP, Schedl A. Sox9 is essential for outer root sheath differentiation and the formation of the hair stem cell compartment. Curr Biol. 2005 Aug 9;15(15):1340-51. doi: 10.1016/j.cub.2005.06.064.
- Villasenor A, Chong DC, Cleaver O. Biphasic Ngn3 expression in the developing pancreas. Dev Dyn. 2008 Nov;237(11):3270-9. doi: 10.1002/dvdy.21740.

- Villasenor A, Chong DC, Cleaver O. Biphasic Ngn3 expression in the developing pancreas. Dev Dyn. 2008 Nov;237(11):3270-9. doi: 10.1002/dvdy.21740.
- Vivo M, Fontana R, Ranieri M, Capasso G, Angrisano T, Pollice A, Calabrò V, La Mantia G. p14ARF interacts with the focal adhesion kinase and protects cells from anoikis. Oncogene. 2017 Aug 24;36(34):4913-4928. doi: 10.1038/onc.2017.104. Epub 2017 Apr 24.
- Vivo M, Ranieri M, Sansone F, Santoriello C, Calogero RA, Calabrò V, Pollice A, La Mantia G. Mimicking p14ARF phosphorylation influences its ability to restrain cell proliferation. PLoS One. 2013;8(1):e53631. doi: 10.1371/journal.pone.0053631. Epub 2013 Jan 7.
- Vonlanthen S, Heighway J, Tschan MP, Borner MM, Altermatt HJ, Kappeler A, Tobler A, Fey MF, Thatcher N, Yarbrough WG, Betticher DC. Expression of p16INK4a/p16alpha and p19Arf/p16beta is frequently altered in non-small cell lung cancer and correlates with p53 overexpression. Oncogene. 1998 Nov 26;17(21):2779-85. doi: 10.1038/sj.onc.1202501.
- Wang J, Walsh K. Resistance to apoptosis conferred by Cdk inhibitors during myocyte differentiation. Science. 1996 Jul 19;273(5273):359-61. doi: 10.1126/science.273.5273.359.
- Wang X, Sterr M, Burtscher I, Chen S, Hieronimus A, Machicao F, Staiger H, Häring HU, Lederer G, Meitinger T, Cernilogar FM, Schotta G, Irmler M, Beckers J, Hrabě de Angelis M, Ray M, Wright CVE, Bakhti M, Lickert H. Genome-wide analysis of PDX1 target genes in human pancreatic progenitors. Mol Metab. 2018 Mar;9:57-68. doi: 10.1016/j.molmet.2018.01.011. Epub 2018 Jan 31.
- Wang X, Sterr M, Burtscher I, Chen S, Hieronimus A, Machicao F, Staiger H, Häring HU, Lederer G, Meitinger T, Cernilogar FM, Schotta G, Irmler M, Beckers J, Hrabě de Angelis M, Ray M, Wright CVE, Bakhti M, Lickert H. Genome-wide analysis of PDX1 target genes in human pancreatic progenitors. Mol Metab. 2018 Mar;9:57-68. doi: 10.1016/j.molmet.2018.01.011. Epub 2018 Jan 31.
- Wang X, Zha M, Zhao X, Jiang P, Du W, Tam AY, Mei Y, Wu M. Siva1 inhibits p53 function by acting as an ARF E3 ubiquitin ligase. Nat Commun. 2013;4:1551. doi: 10.1038/ncomms2533.
- Warfel NA, El-Deiry WS. p21WAF1 and tumourigenesis: 20 years after. Curr Opin Oncol. 2013 Jan;25(1):52-8. doi: 10.1097/CCO.0b013e32835b639e.
- Weber HO, Samuel T, Rauch P, Funk JO. Human p14(ARF)-mediated cell cycle arrest strictly depends on intact p53 signaling pathways. Oncogene. 2002 May 9;21(20):3207-12. doi: 10.1038/sj.onc.1205429.
- Weber J, Öllinger R, Friedrich M, Ehmer U, Barenboim M, Steiger K, Heid I, Mueller S, Maresch R, Engleitner T, Gross N, Geumann U, Fu B, Segler A, Yuan D, Lange S, Strong A, de la Rosa J, Esposito I, Liu P, Cadiñanos

J, Vassiliou GS, Schmid RM, Schneider G, Unger K, Yang F, Braren R, Heikenwälder M, Varela I, Saur D, Bradley A, Rad R. CRISPR/Cas9 somatic multiplex-mutagenesis for high-throughput functional cancer genomics in mice. Proc Natl Acad Sci U S A. 2015 Nov 10;112(45):13982-7. doi: 10.1073/pnas.1512392112. Epub 2015 Oct 27.

- Weber JD, Jeffers JR, Rehg JE, Randle DH, Lozano G, Roussel MF, Sherr CJ, Zambetti GP. p53-independent functions of the p19(Arf) tumor suppressor. Genes Dev. 2000 Sep 15;14(18):2358-65. doi: 10.1101/gad.827300.
- Weber JD, Kuo ML, Bothner B, DiGiammarino EL, Kriwacki RW, Roussel MF, Sherr CJ. Cooperative signals governing ARF-mdm2 interaction and nucleolar localization of the complex. Mol Cell Biol. 2000 Apr;20(7):2517-28. doi: 10.1128/MCB.20.7.2517-2528.2000.
- Weber JD, Taylor LJ, Roussel MF, Sherr CJ, Bar-Sagi D. Nucleolar Arf sequesters Mdm2 and activates p53. Nat Cell Biol. 1999 May;1(1):20-6. doi: 10.1038/8991.
- Xiong Y, Hannon GJ, Zhang H, Casso D, Kobayashi R, Beach D. p21 is a universal inhibitor of cyclin kinases. Nature. 1993 Dec 16;366(6456):701-4. doi: 10.1038/366701a0.
- Xuan S, Borok MJ, Decker KJ, Battle MA, Duncan SA, Hale MA, Macdonald RJ, Sussel L. Pancreas-specific deletion of mouse Gata4 and Gata6 causes pancreatic agenesis. J Clin Invest. 2012 Oct;122(10):3516-28. doi: 10.1172/JCI63352. Epub 2012 Sep 24.
- Xuan S, Sussel L. GATA4 and GATA6 regulate pancreatic endoderm identity through inhibition of hedgehog signaling. Development. 2016 Mar 1;143(5):780-6. doi: 10.1242/dev.127217.
- Yarbrough WG, Bessho M, Zanation A, Bisi JE, Xiong Y. Human tumor suppressor ARF impedes S-phase progression independent of p53. Cancer Res. 2002 Feb 15;62(4):1171-7.
- Yi Y, Shepard A, Kittrell F, Mulac-Jericevic B, Medina D, Said TK. p19Arf determines the balance between normal cell proliferation rate and apoptosis during mammary gland development. Mol Biol Cell. 2004 May;15(5):2302-11. doi: 10.1091/mbc.e03-11-0785.
- Zakrzewski W, Dobrzyński M, Szymonowicz M, Rybak Z. Stem cells: past, present, and future. Stem Cell Res Ther. 2019 Feb 26;10(1):68. doi: 10.1186/s13287-019-1165-5.
- Zalzman M, Falco G, Sharova LV, Nishiyama A, Thomas M, Lee SL, Stagg CA, Hoang HG, Yang HT, Indig FE, Wersto RP, Ko MS. Zscan4 regulates telomere elongation and genomic stability in ES cells. Nature. 2010 Apr 8;464(7290):858-63. doi: 10.1038/nature08882. Epub 2010 Mar 24.
- Zezula J, Casaccia-Bonnefil P, Ezhevsky SA, Osterhout DJ, Levine JM, Dowdy SF, Chao MV, Koff A. p21cip1 is required for the differentiation of oligodendrocytes independently of cell cycle withdrawal. EMBO Rep. 2001 Jan;2(1):27-34. doi: 10.1093/embo-reports/kve008.

- Zhang S, Cui W. Sox2, a key factor in the regulation of pluripotency and neural differentiation. World J Stem Cells. 2014 Jul 26;6(3):305-11. doi: 10.4252/wjsc.v6.i3.305.
- Zhang Y, Xiong Y, Yarbrough WG. ARF promotes MDM2 degradation and stabilizes p53: ARF-INK4a locus deletion impairs both the Rb and p53 tumor suppression pathways. Cell. 1998 Mar 20;92(6):725-34. doi: 10.1016/s0092-8674(00)81401-4.
- Zheng Y, Zhao YD, Gibbons M, Abramova T, Chu PY, Ash JD, Cunningham JM, Skapek SX. Tgfbeta signaling directly induces Arf promoter remodeling by a mechanism involving Smads 2/3 and p38 MAPK. J Biol Chem. 2010 Nov 12;285(46):35654-64. doi: 10.1074/jbc.M110.128959. Epub 2010 Sep 8.
- Zhou D, Luo Y, Dingli D, Traulsen A. The invasion of de-differentiating cancer cells into hierarchical tissues. PLoS Comput Biol. 2019 Jul 1;15(7):e1007167. doi: 10.1371/journal.pcbi.1007167.
- Zhou Q, Law AC, Rajagopal J, Anderson WJ, Gray PA, Melton DA. A multipotent progenitor domain guides pancreatic organogenesis. Dev Cell. 2007 Jul;13(1):103-14. doi: 10.1016/j.devcel.2007.06.001.
- Zindy F, Eischen CM, Randle DH, Kamijo T, Cleveland JL, Sherr CJ, Roussel MF. Myc signaling via the ARF tumor suppressor regulates p53-dependent apoptosis and immortalization. Genes Dev. 1998 Aug 1;12(15):2424-33. doi: 10.1101/gad.12.15.2424.

APPENDIX

genes

MDPI

Article

Identification of *Cdk8* and *Cdkn2d* as New Prame-Target Genes in 2C-like Embryonic Stem Cells

Valeria Lucci [1,2,*], Elena De Marino [1], Daniela Tagliaferri [3], Stefano Amente [4], Alessandra Pollice [1], Viola Calabrò [1], Maria Vivo [5], Geppino Falco [1,2,3,†] and Tiziana Angrisano [1,*,†]

1 Department of Biology, University of Naples "Federico II", 80147 Naples, Italy
2 IEOS-CNR, Institute of Experimental Endocrinology and Oncology "G. Salvatore"—National Research Council, 80131 Naples, Italy
3 Biogem Scarl, Istituto di Ricerche Genetiche "Gaetano Salvatore", 83031 Ariano Irpino, Italy
4 Department of Molecular Medicine and Medical Biotechnology, University of Naples "Federico II", 80131 Naples, Italy
5 Department of Chemistry and Biology, University of Salerno, 84084 Fisciano, Italy
* Correspondence: valeria.lucci@unina.it (V.L.); tangrisa@unina.it (T.A.); Tel.: +39-081-679721 (T.A.)
† These authors contributed equally to this work.

Abstract: Embryonic stem cells (ESCs) present a characteristic pluripotency heterogeneity correspondent to specific metastates. We recently demonstrated that retinoic acid (RA) induces an increase in a specific 2C-like metastate marked by target genes specific to the two-cell embryo stage in preimplantation. Prame (Preferentially expressed antigen in melanoma) is one of the principal actors of the pluripotency stage with a specific role in RA responsiveness. Additionally, PRAME is overexpressed in a variety of cancers, but its molecular functions are poorly understood. To further investigate Prame's downstream targets, we used a chromatin immunoprecipitation sequencing (ChIP-seq) assay in RA-enriched 2C-like metastates and identified two specific target genes, *Cdk8* and *Cdkn2d*, bound by Prame. These two targets, involved in cancer dedifferentiation and pluripotency, have been further validated in RA-resistant ESCs. Here, we observed for the first time that Prame controls the *Cdk8* and *Cdkn2d* genes in ESCs after RA treatment, shedding light on the regulatory network behind the establishment of naïve pluripotency.

Keywords: PRAME; embryo stem cell; RA-resistant

Citation: Lucci, V.; De Marino, E.; Tagliaferri, D.; Amente, S.; Pollice, A.; Calabrò, V.; Vivo, M.; Falco, G.; Angrisano, T. Identification of *Cdk8* and *Cdkn2d* as New Prame-Target Genes in 2C-like Embryonic Stem Cells. *Genes* **2022**, *13*, 1745. https://doi.org/10.3390/genes13101745

Academic Editor: Allison D. Ebert

Received: 5 August 2022
Accepted: 23 September 2022
Published: 27 September 2022

1. Introduction

Prame, *Gm12794c* in mice, is a member of a multigene family present in humans and other mammals [1]; it is expressed in different cancers [2] and is associated with a novel stem cell molecular signature in the 2C-like metastate, characteristic of naïve pluripotency [3]. ESCs are characterized by different metastable subpopulations that fluctuate among different levels of pluripotency, defined as metastates. These metastates are marked by specific factors whose expression affects the state of cell pluripotency [4–6]. Occasionally, a metastable subpopulation may convert to a highly pluripotent metastate (2C-like) resembling the two-cell stage (2C) embryos, in which a rearrangement of chromatin induces a reprogramming of a transcription named zygotic genome activation (ZGA) [7].

Recently, it was demonstrated that RA enhances ESCs' metastate subpopulation, named Zscan4 metastate, marked by a specific 2C-like gene signature, including *Prame* and *Zscan4*, in which ESCs retain both self-renewal and pluripotency capability [8–10]. Correlated to this aspect, human PRAME overexpression has been demonstrated to block retinoic acid (RA)-mediated cell differentiation, cell growth arrest, and apoptotic death, suggesting that PRAME acts as an inhibitor of the retinoic acid receptor (RAR) [11–13]. Moreover, PRAME overexpression was found to promote leukemic cell proliferation and inhibit all-trans retinoic acid (ATRA)-induced myeloid differentiation [14] and in several

hematological malignancies characterized by the block of myeloid differentiation [15]. Indeed, the murine Prame counteracts RA-dependent differentiation. RA induces high levels of Prame, contributing to the overall DNA hypomethylation and global increase in H3K27 acetylation levels throughout the *Cdkn1a* transcriptional repression induced by the PCR2 complex [13]. The considerable heterogeneity among the different Prame isotypes made it challenging to determine their specific function, so the clinical relevance of Prame remains still unclear and prompted us to investigate whether Prame is a suitable ATRA-resistance therapeutic target. To better understand this aspect, we performed a Prame chromatin immunoprecipitation followed by sequencing (ChIP-seq). We found Prame-specific binding to *Cdk8* and *Cdkn2d* regulatory regions by this approach. We focused our attention on these two targets because of their involvement in cancer dedifferentiation and pluripotency.

Cdk8 is a cyclin-dependent kinase implicated in cellular homeostasis and developmental programming, and it has been shown to regulate several signaling pathways that are crucial regulators of both embryonic stem cell pluripotency and cancer [16].

On the other hand, Cdkn2d is a member of the INK4 family of cyclin-dependent kinase inhibitors that generally regulate the G1-to-S phase transition [17]; interestingly, *Cdkn2d* dissymmetric mRNA distribution was observed in the 2-cell stage in blastomeres [18].

Our ChIP-seq data were validated by chromatin immunoprecipitation and gene expression analysis in ES$^{pZscan4\text{-EME/Prame-FLAG}}$ transgenic cell line. Moreover, we used a second transgenic cell line, overexpressing Prame, to analyze the Prame -specific activity on *Cdk8* and *Cdkn2d* gene expression to maintain the pluripotent metastate in cells treated or not treated with RA.

2. Materials and Methods

2.1. Cell Culture

The pZscan4-Emerald cells, a gift from Dr. Minoru S.H.Ko, were transfected with the Prame-3xFlag vector (ES$^{pZscan4\text{-EME/Prame-FLAG}}$), generated in [13], and validated for pluripotency expression markers after RA treatment. It was necessary to use the FLAG-tag for Prame immunoprecipitation analysis as there is no available antibody against the murine isoform of the Prame studied.

ES$^{pZscan4\text{-EME/Prame-FLAG}}$ cells were cultured in gelatin-coated 6-well plates in a complete ES medium: DMEM (Sigma-Aldrich, St. Louis, MO, USA); 15% FBS (EuroClone, Italy); 1000 U/mL leukemia inhibitory factor (LIF) (ESGRO, Chemicon, SIGMA, Darmstad, Germany); 1 mM sodium pyruvate; 0.1 mM nonessential amino acids (NEAA), 2.0 mM L-glutamine (Invitrogen, Waltham, MA, USA), 0.1 mM β-mercaptoethanol, and 500 U/mL penicillin/streptomycin, 125 µg/mL G418, and 2.5 µg/mL Blasticidin (Sigma-Aldrich). ESCs were incubated at 37 °C with 5% CO_2. To enrich Zscan4-EME positive cells (EME+) expressing Emerald protein, the ES$^{pZscan4\text{-EME/PRAME-FLAG}}$ cells were treated with 1.5 µM RA for 4 days. EME+/NoFLAG, containing only *Zscan4* promoter fuser to Emerald protein, was used as a negative control in the immunoprecipitation assay with ant-FLAG antibodies.

The second ES cell line Prame inducible by tetracycline, ES^{Gm12794cp2Lox} was initially described and validated in [13], and in this study it is named ES^{Pramep2Lox}. Briefly, the coding sequence of *Prame* was amplified from an available plasmid and cloned into a p2Lox targeting vector. Cellular clones were grown with 275 µg/mL neomycin (Invitrogen), and an empty p2Lox vector stably transfected in ESCs was used as a negative control cell line.

ES^{Pramep2Lox} and p2Lox empty vector cell lines were cultured in DMEM (Invitrogen) supplemented with 15% ES-certified FBS (Invitrogen), 0.1 mM nonessential amino acids (Invitrogen), 1 mM sodium pyruvate (Invitrogen), 0.1 mM β-mercaptoethanol (Sigma-Aldrich), 50 U mL^{-1} penicillin/50 µg mL^{-1} streptomycin (Invitrogen), and 1000 U mL^{-1} LIF (Sigma-Aldrich). Clones were treated for 72 h in the absence or presence of 1.5 µg/mL doxycycline to induce transgene expression, followed by the presence or absence of RA 1.5 µM for 4 days.

Finally, an E14 ES transient knockdown of the *Prame* gene was generated. The *Prame* shRNA was transfected into a pLKO.1 vector (Addgene, Arsenal, UK) using AgeI and EcoRI restriction enzymes. All these passages were verified by sequence analysis. The ES cells were transfected with Lipofectamine Transfection Reagent (Invitrogen^{TM}) according to the manufacturer's instructions.

2.2. Flow Cytometry and Sorting of ESpZscan4-Em/Prame-FLAG Transgenic Cell Lines

1×10^6 cell line ES$^{pZscan4\text{-EME/Prame-FLAG}}$ was plated in p100 and treated with 1.5 µM all-trans RA for 4 days and the medium was changed every day. ES E14 cell lines, plated in ES medium and treated with RA, were used as a negative control.

Then, the cells were harvested by Trypsin (Invitrogen) and resuspended in a complete ES medium containing 25 mM HEPES buffer and by FACS-sorted according to the fluorescent intensity of Emerald into a complete ES medium containing HEPES and separated in EME+ (Zscan4/Emerald expressing) and EME-(Zscan4/Emerald not expressing) as performed in [19].

Cell sorting experiments were performed by the cell sorter FACSAria and analyzed through FACSDiva Software Version 6.1.3 (Becton Dickinson, Franklin Lakes, NJ, USA). Analysis of forward scatter (FSC) vs. side scatter (SSC) dot plots excluded dead cells and debris. Afterward, an FSC-Area vs. FSC-Height dot plot was used to identify single cells and exclude doublets. In all experiments, purity was higher than 95% of the desired cells.

2.3. Western Blot Analysis

Total proteins extracted from EME+ and EME− cells were analyzed by western blot as described in [20]. The antibodies used are as follows: mouse monoclonal antibody anti-FLAG M2 (Sigma Aldrich, Milan, Italy) and rabbit polyclonal anti-Gapdh (Santa Cruz Biotechnology, Heidelberg, Germany).

2.4. qPCR Analysis

For qPCR analysis of FACS-sorted cells, total RNA was collected immediately after sorting from EME+ and EME- cells by TRIzol (Invitrogen) as performed in [21]. The integrity of the RNA was assessed by denaturing agarose gel electrophoresis (presence of sharp 28S, 18S, and 5S bands) and spectrophotometry. A total of 1 µg of RNA of each sample was reverse transcribed with QuantiTect® Reverse Transcription (Qiagen, Germany, Europe) according to the manufacturer's instructions. qPCR analyses were performed using 20 ng cDNA per well in duplicate with SYBR green master mix (Applied Biosystems, Waltham, MA, USA) according to the manufacturer's instructions. Reactions were run on Applied Biosystem 7500 (Applied Biosystems). Fold induction was calculated and normalized with the DDCt method and considered the values of at least three independent experiments. The gene-specific primers are available in Table 1.

Table 1. List of genes and sequences of primers used for relative gene expression analysis by qPCR.

Gene	Sequence Fw (5′-3′)	Sequence Rv (5′-3′)	[1] Method
Cdkn2d	CCACCGGTATCCACTATGCT	GCACAGGACTAGTACCGGAG	qPRC
Cdk8	TCCAGTGGTTGTAACATTCTGGT	TTCTGCAAATATACACCCTATAGCC	qPRC
Prame	TGCTGCCAAATTCCTTTCTC	GAGAGTTGGCAGCGATTCAT	qPRC
Gapdh	AATGGTGAAGGTCGGTGTG	GAAGATGGTGATGGGCTTCC	qPRC
Cdkn2d	TCCTCATGCTGGTTCTGTGT	AGGAGGGAAAACAAGGGCTT	ChIP
Cdk8	TTAAATGAGACATGGGCGCG	GGAGTTTACCACCCGCTTTG	ChIP

[1] In the Method column, qPCR indicates the gene expression analysis, while primers used for ChIP assay are indicated in the Method column with ChIP.

2.5. ChIP Analysis

ChIP analysis was performed as previously described [22] using the EpiQuikTM chromatin immunoprecipitation kit from Epigentek Group Inc. (Brooklyn, NY, USA). Then, 2×10^6 cells sorted into EME+ and EME- were cross-linked in a fresh culture medium with 1% formaldehyde for 10 min, sonicated and used for each immunoprecipitation with 3 µg of antibodies. Immunoprecipitated DNA was used for massively parallel sequencing or analyzed on a real-time PCR machine (Applied Biosystem 7500), SYBR green master mix according to the manufacturer's instructions. Primer sequences are listed in Table 1.

2.6. ChIP-Sequencing, Mapping, and Peak Analysis

Prame immunoprecipitation was used as anti-FLAG antibody on cells EME+ and EME- using independent biological replicates. Single-end 50-bp libraries were prepared from Genomix4life.

The signal obtained by precipitation with the control EME- and input was subtracted from the signals obtained with the specific antibodies. Results are expressed as a percentage of the input, and calculations considered the values of at least two biological replicates. ChIP-seq libraries were prepared with 10 ng of ChIP (or Input) DNA with TruSeq ChIP Sample Prep Kit according to the manufacturer's instructions of Illumina sequencing. Before sequencing, libraries were quantified using Qubit (Invitrogen) and quality-controlled using Agilent's bioanalyzer. The basic steps are represented in the form of a flowchart in Figure 1.

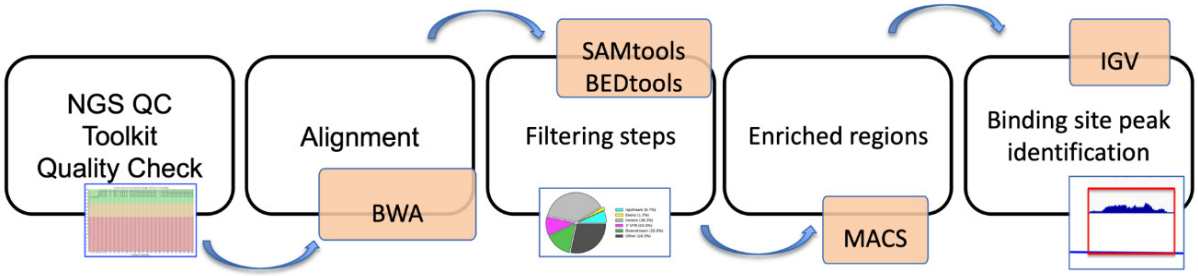

Figure 1. Flow chart for ChIP-seq analysis in RA-treated EME+ cells. The multiple steps involved in the analyses of ChIP_seq data are schematically displayed.

A 50 bp single-end sequencing was performed using Illumina HiSeq 2000 platform (Genomix4life S.R.L., Baronissi, Salerno, Italy) according to standard operating procedures. ChIP-seq reads were quality-checked with NGS QC Toolkit. Alignments were performed with BWA to the reference genome mm9 (mouse assembly July 2007 NCBI37). SAMtools [23] and BEDtools [24] were used for filtering steps and file format conversion. The peaks were identified from uniquely mapped reads without duplicates using MACS, and the *p*-value cutoff used for peak detection was 1×10^{-5}. ChIP-seq data were normalized on DNA Input and expressed as a log2 value. ChIP-seq peaks were annotated with PAVIS [25]. IGV genome browser was used for data visualization (Figure 1). To plot data of average profiles around prime target genes, specific site positions were retrieved from the mouse genome (mm9).

2.7. Statistical Analysis

Statistical significance between two or three groups was assessed with Student's *t*-test and or ANOVA test, respectively. Data are expressed as mean ± standard deviation (SD). All experiments were repeated at least three times. A p-value < 0.05 was considered statistically significant.

3. Results

3.1. RA induces Zscan4 Metastate and Prame Expression in ES$^{pZscan4\text{-}EME/PRAME\text{-}FLAG}$

To identify the Prame target genes, we used a transgenic ESCs line that simultaneously expresses FLAG-tagged Prame protein and Emerald downstream to the *Zscan4* promoter (ES$^{pZscan4\text{-}EME/Prame\text{-}FLAG}$), as described in Material Methods and previously validated for expression of pluripotent marker genes [13]. ES$^{pZscan4\text{-}EME/Prame\text{-}FLAG}$ cell line RA-treated was sorted for Emerald expression (or Zscan4 metastate), then immunoprecipitated with an anti-FLAG antibody and analyzed by next-generation sequencing (Figure 2A).

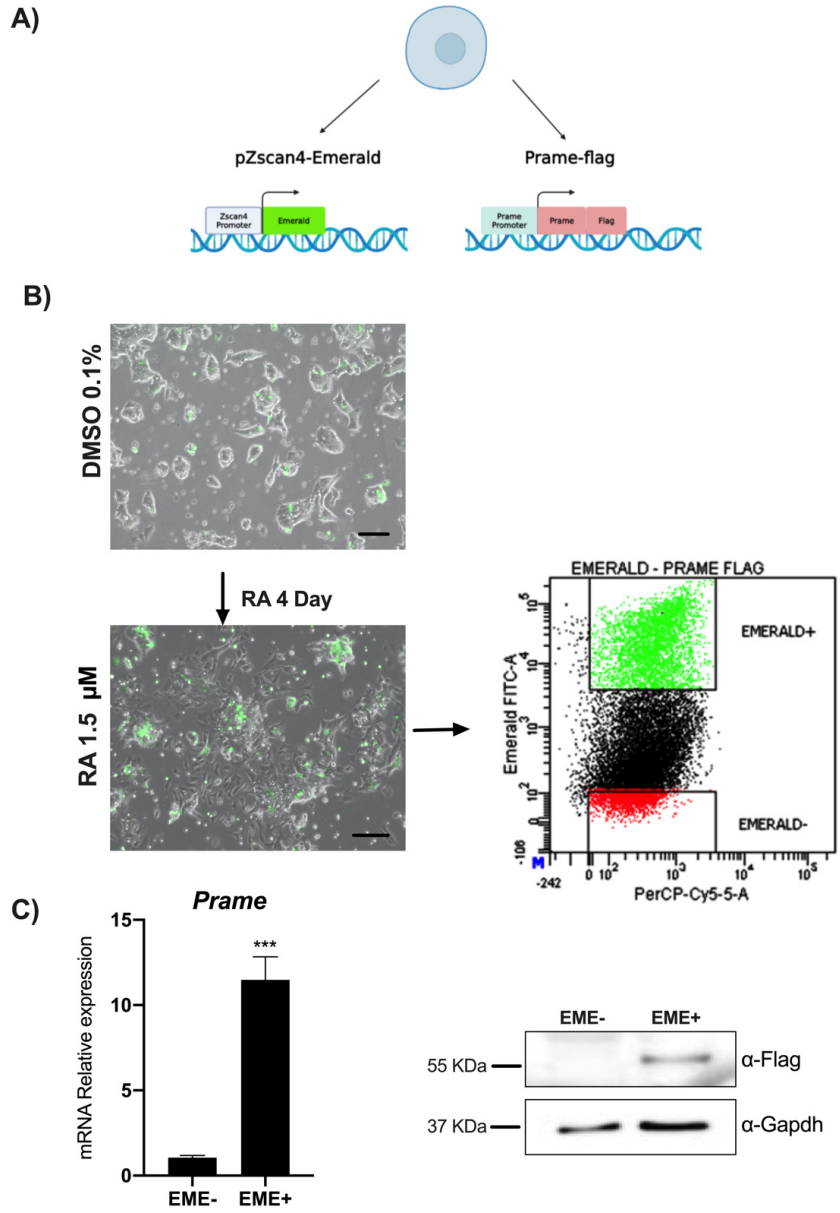

Figure 2. RA induces Zscan4-Metastate and Prame expression in *ES$^{pZscan4\text{-}EME/Prame\text{-}FLAG}$*. (**A**) Schematic representation of ES transgenic cells for pZscan-Emerald and PRAME-FLAG expression. (**B**) Zscan4 and Prame positive cells visualized by Emerald reporter. After four days of RA treatment. Cells were imaged using phase-contrast microscopy (scale bars, 100 nm). Flow cytometry evaluation (dot blot) in *ES$^{pZscan4\text{-}EME/PRAME\text{-}FLAG}$* cell lines of two subgroups, EME+ and EME-). (**C**) PRAME expression analysis for sorting validation by qPCR and western blot assays. Data are shown as mean ± SD from three independent experiments, normalized with Gapdh, and reported to the control (EME-). *** and $p < 0.001$.

To obtain an enriched EME+ cell population, ES$^{pZscan4\text{-}EME/Prame\text{-}FLAG}$ cells were cultured with 1.5 µM of RA for four days. Zscan4 induction was evaluated through fluorescence microscopy (Figure 2B) and FACS analysis to quantify Zscan4 expression; we analyzed the percentage of green cells (EME+) in ES$^{pZscan4\text{-}EME/Prame\text{-}FLAG}$ that increased to 21.8% after RA treatment (Figure 2C). In addition, we further confirmed the successful separation of Prame gene and protein expression in EME+ cells by western blot (Figure 2C). Finally, we performed a ChIP-seq analysis in EME+ cells.

3.2. Identification of Prame Target Genes by ChIP-Seq Analysis

To identify Prame target genes upon RA treatment, we collected 2 × 10^6 EME+ cells after sorting. In Figure S1A, we can see the distribution of Prame binding regions: upstream and downstream gene regions, 5′UTR and 3′UTR, introns in the form of a pie chart (Figure S1B). As shown in Figure S1B, binding is mainly found in regulatory regions (upstream, 3′-UTR and downstream gene regions).

The ChIP-seq analysis showed 15 specific genes significantly bound by Prame (*Cdk8*, *Cdkn2d*, *uc009gks.1*, *St6galnac1*, *Stard13*, *Mir26b*, *533042B09Rik*, *Gm15319*, *Gm3168*, *AK053193*, *Mir715*, *Zc3h7a*, *Filip1l*, *AK041614*, *and Gm10406*) and described in Table 2.

Table 2. Prame target genes identified by ChIP-seq analysis in EME+ cell lines.

Gene	Category	Chr	Description
Cdk8	Intron	5	Cell division protein kinase 8
Cdkn2d	Upstream, Downstream	9	Cyclin-dependent kinase 4 inhibitor D
uc009gks.1	Upstream, Intron, 3′UTR, Downstream	7	Hypothetical protein LOC72244
St6galnac1	Intron	11	α-N-Acetyl-galactosaminide
Stard13	Intron	5	stAR-related lipid transfer protein 13 isoform
Mir26b	Downstream	1	Mus musculus microRNA 26 b (Mir26b), microRNA
5330429B09Rik	Downstream	8	Subname: Full = putative uncharacterized protein
Gm15319	Intron	8	Testis-specific gene with ankyrin repeats
Gm3168	3′UTR	8	Subname: Full = Gag protein
AK053193	Downstream	10	Mus musculus 9,5 days embryo parthenogenote cDNA, RIKEN full
Mir715	Downstream	17	Mus musculus microRNA 715 (Mir715), microRNA
Zc3h7a	Intron	16	Zinc Finger CCCH-type containing 7A
Filip1l	Intron	16	Filamin A-interacting protein 1-like isoform 1
AK041614	Downstream	15	Mus musculus 3 days neonate thymus cDNA, RIKEN full-length enriched library
Gm10406	Intron	14	Alpha7-takusan

Among these, we chose *Cdk8* and *Cdkn2d* for further validation. Cdk8 is a cyclin-dependent kinase that maintains both tumors and embryonic stem cells in an undifferentiated state [16], while Cdkn2d (cyclin-dependent kinase inhibitor 2D) is a cell growth regulator that controls G1 cell cycle progression and results in dissymmetrically expressed cells in the 2-cell stage, thus, representing good targets of the pluripotency stage marked by Prame expression [14].

Figure 3A indicates the schematic position of primers used for ChIP analysis validation by qPCR on *Cdk8* and *Cdkn2d* enriched sequences after ChIP-seq.

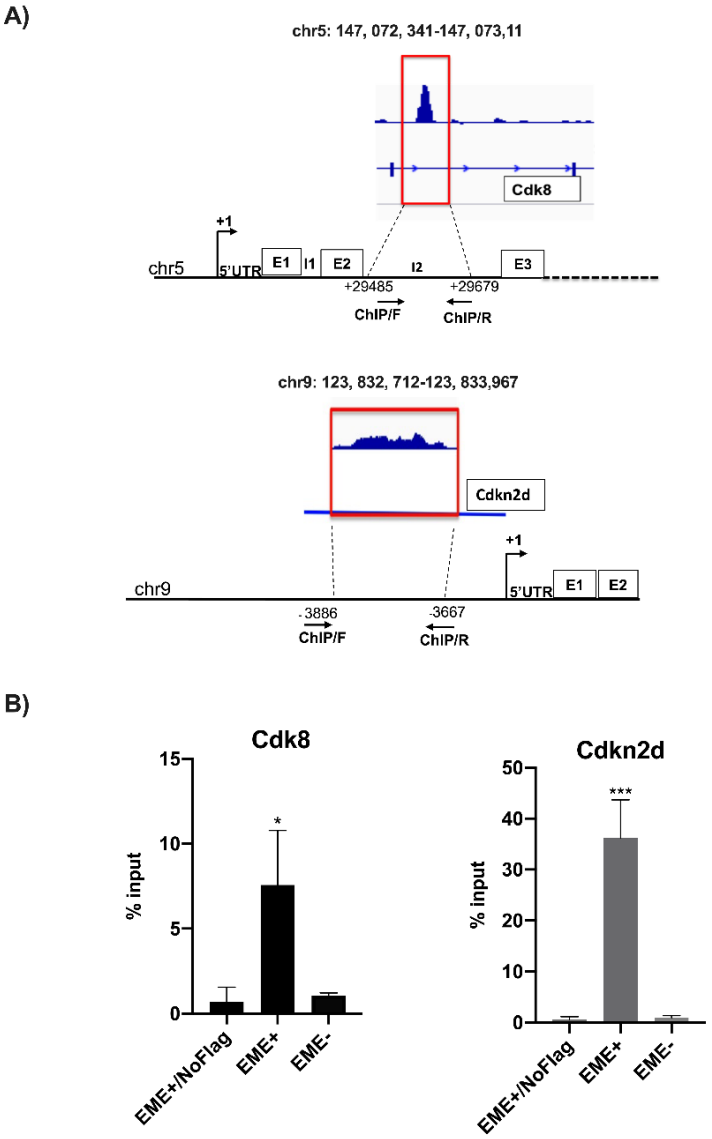

Figure 3. Prame-target gene identification by ChIP-seq analysis and ChIP assay for validation. (**A**) Schematic representations of *Cdk8* intron 2 and *Cdkn2d* upstream regions with enriched sequences, peaks were indicated on specific chromosome positions. (**B**) ChIP assay validation followed by qPCR analysis for Prame binding sites on *Cdk8* and *Cdk2d* gene sequences in EME+, EME, and EME+/NoFLAG cells (without Prame-FLAG) as the negative control. Data are shown as mean ± SD from three independent experiments, normalized with Gapdh, and reported to the control (EME-). *, $p < 0.05$; ***, and $p < 0.001$.

EME+ and EME- cells and EME+/NoFLAG DNA immunoprecipitated for Prame, with anti-FLAG antibody, was analyzed through qPCR for *Cdk8* and *Cdkn2d* enrichment to confirm data obtained by ChIP-seq. Data are calculated as the percentage of the input (Figure 3B). The EME+/NoFLAG cells were used as a negative control of immunoprecipitation.

3.3. RA Induces Cdk8 and Cdkn2d Expression

To understand how RA influences *Cdk8* and *Cdkn2d* expression, a qPCR analysis was performed in EME+ and in EME- cells (Figure 4A,B). The gene expression analysis showed a significant enhancement of *Cdk8* and *Cdkn2d* expression in EME+ cells compared to EME- (Figure 3). These data indicate that the Prame binding to Cdk8 and Cdkn2d genes increases their expression.

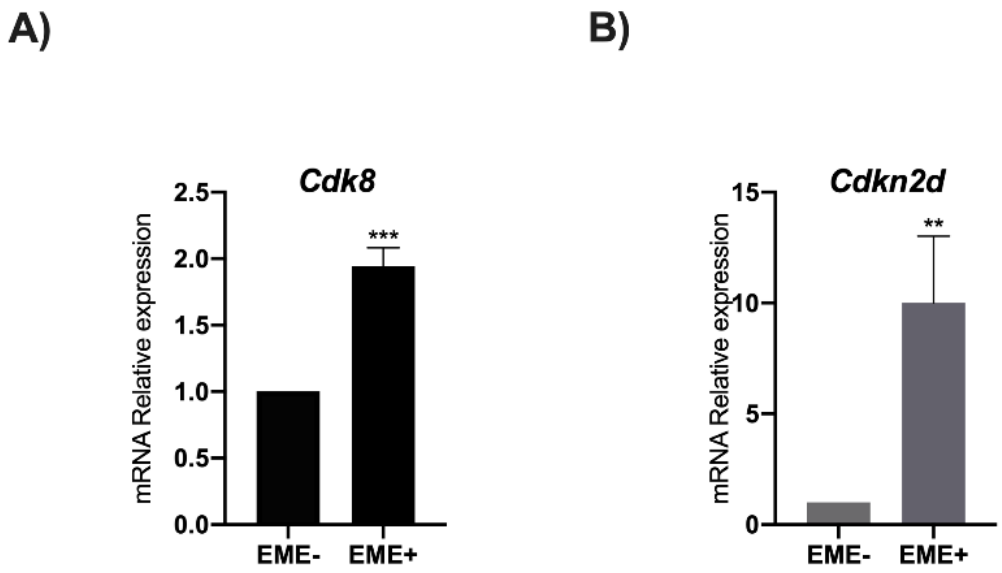

Figure 4. RA induces *Cdk8* and *Cdkn2d* gene expression in ESCs. (**A**) *Cdk8* and (**B**) *Cdkn2d* gene levels in EME+ cells after RA treatment. Data are shown as mean ± SD from three independent experiments, normalized with *Gapdh*, and reported to the control (EME-). **, $p < 0.01$ ***, and $p < 0.001$.

3.4. Prame Enhances Cdk8 and Cdkn2d Expression in ES^{Gm12794cp2Lox} Transgenic Cells

To understand whether Prame overexpression influences *Cdk8* and *Cdkn2d* gene expression in ES cells, an ES^{Pramep2Lox} cell line in which Prame expression is induced by doxycycline was employed [13]. The ESCs stably transfected with the inducible PRAME expressing construct were treated with doxycycline for 3 days (Figure 5A) and then with RA for 4 days. To validate Prame induction by doxycycline and then by RA treatment, both Prame and *Zscan4* gene expression were analyzed by qPCR (Figure 5B). The ES cell line p2Lox empty vector was used as a negative control for the Dox treatment. Our data shows a 5-fold higher *Prame* gene expression after the Dox treatment (Figure 5B), with cells maintaining a classic ESC pluripotent morphology as previously described [13]. *Zscan4* gene expression was observed after RA treatment, confirming the Zscan4 metastate induced by RA. Finally, we observed that *Cdk8* and *Cdkn2d* expressions were directly increased in ESCs overexpressing Prame without RA (Figure 5C). This data shows for the first time that Prame directly influences the expression of their target genes, also without RA treatment.

3.5. Prame Controls Cdk8 Expression

To shed light on the role of Prame in *Cdk8* and *Cdkn2d* gene regulation, transient inactivation of *Prame* was performed in E14 ES. The sh*Prame* vector and a sh-scrambled (sh-scr as a negative control) were transfected in ESCs for 24 h. *Prame* specific-shRNA mapped to the Exon2-coding region (Figure 6A). Total RNA was extracted from ES cells transfected with sh*Prame* and sh-scr. The qPCR analysis showed a significant reduction in *Cdk8* expression in ESCs upon *Prame* silencing compared to sh-scr cell control (Figure 6B), while *Cdkn2d* expression remains unaffected by *Prame* silencing (Figure 6B).

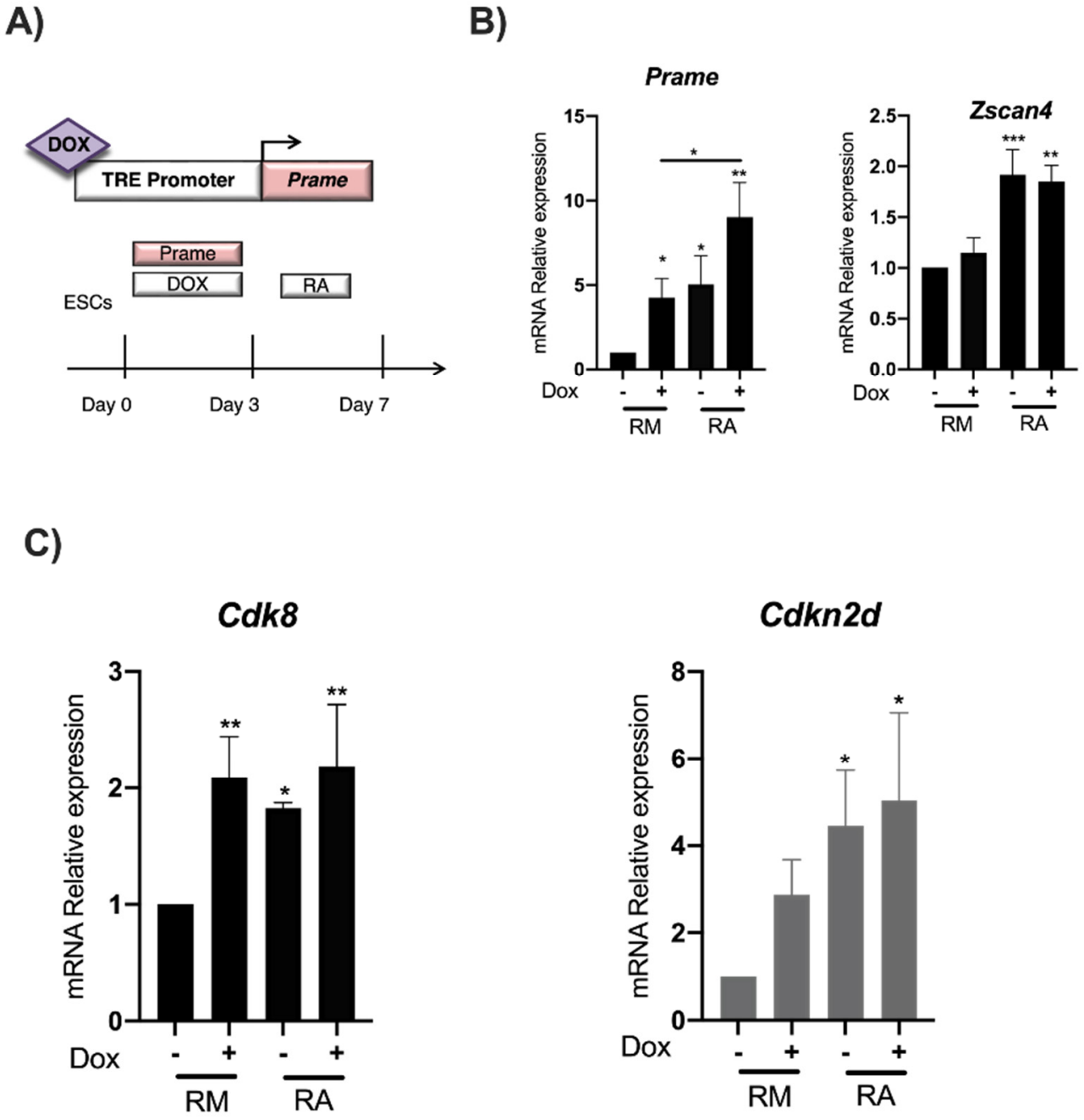

Figure 5. Prame overexpression influences *Cdk8* gene expression in ES cells. (**A**) Schematic representation of the minimal Dox-inducible promoter driving the expression of Prame in the $ES^{Gm12794cp2Lox}$ cell line. (**B**) A qPCR analysis showing relative Prame and *Zscan4* mRNA levels in $ES^{Gm12794cp2Lox}$ cells treated or not treated with Dox (1.5 μg/mL) for 72 h and then with RA (1.5 μM) for 4 days. (**C**) *Cdk8* gene expression, but not *Cdkn2d*, was induced directly by Prame overexpression in $ES^{Gm12794cp2Lox}$ cells. (RM is the regular medium without RA). Data are shown as mean ± SD from three independent experiments, normalized with *Gapdh*, and reported to the control (Dox-). *, $p < 0.05$; **, $p < 0.01$ ***, and $p < 0.001$.

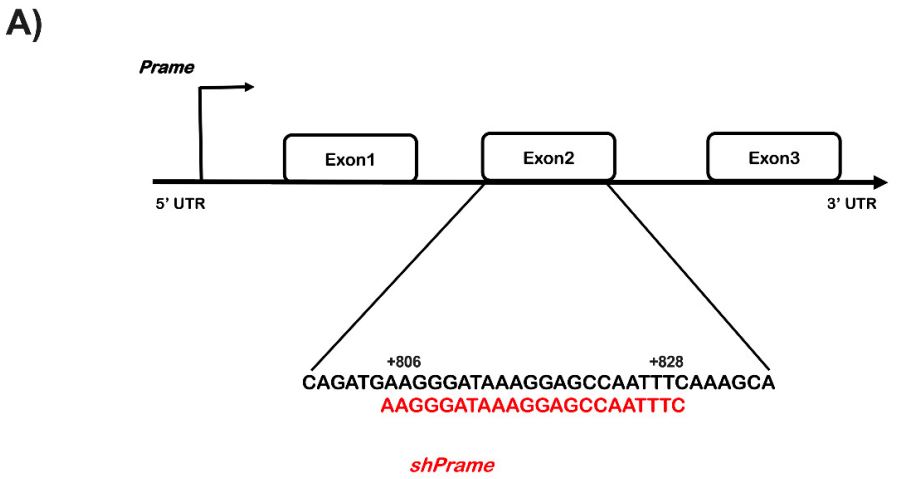

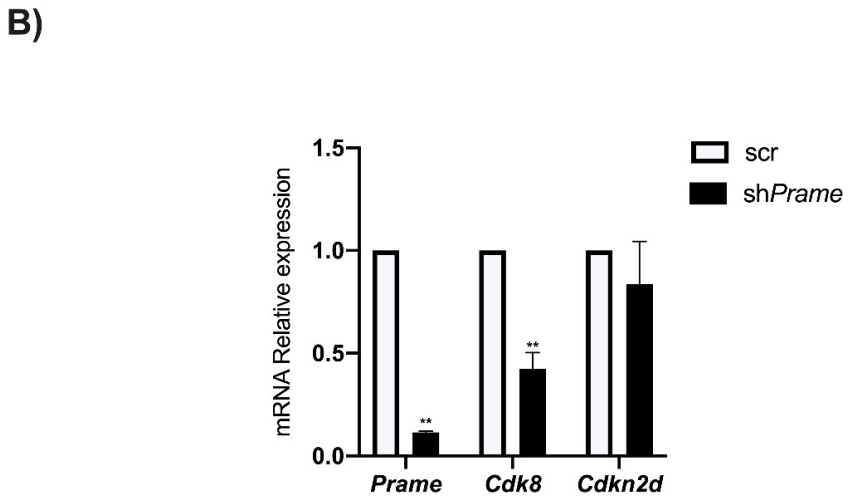

Figure 6. The *Prame knock-down* specifically affects *Cdk8* gene expression in ESCs. (**A**) Schematic representation of *shPrame* (sequence in red) localized in the second exon of *Prame* coding region at a distance indicated from TSS. (**B**) The ESC cells were transfected in transient for 24 h with *sh*Prame and scr (scrambled), the negative control. Data are shown as mean ± SD from three independent experiments, normalized with *Gapdh*, and reported with respect to the control. **, $p < 0.01$.

4. Discussion

The role of PRAME in human cancers is well established. PRAME is recruited in human cells to epigenetically and transcriptionally activate promoter regions bound by the nuclear transcription factor Y (NFY). This transcription factor is essential for early embryonic development [26] and has been implicated in the maintenance of the high proliferative capacity of ES cells [27] as well as in the inhibition of differentiation [28,29]. In addition, several studies indicated that Prame-like genes have roles in the early stages of spermatogenesis [30] and oogenesis [31], as well as in embryonic development and embryonic stem cells [32,33]. Moreover, Prame overexpression in E14 embryonic stem cells was reported to maintain a pluripotent state in the absence of the antidifferentiation factor LIF [13,34] and in ESCs that were RA-resistant [8].

Together, all these data are consistent with the notion that stem cells and neoplastic tissues share many properties, and several oncogenic pathways can also regulate self-renewal mechanisms in stem cells [35]. Therefore, the identification of Prame functions and targets indeed represents a step forward, not only in the cancer diagnostic approach but also in the therapeutic approach.

Here, we report, for the first time, two putative novel Prame targets in RA-treated ESCs. To better understand the regulatory network underpinning the establishment of naïve pluripotency marked by *Zscan4* and *Prame* genes in ESCs, we used $ES^{pZscan4}$-EME/Prame-FLAG transgenic cell lines, allowing us to immunoprecipitate Prame and its chromatin-bound fragments by using anti-FLAG antibodies. The Prame-bound sequences were characterized by ChIP-seq analysis. Among the putative Prame targets identified, we focused our attention on Cdk8, and Cdkn2d.

Cyclin-dependent kinases (CDKs) are key players in cell cycle regulation. Being involved in the regulation of cell cycle checkpoints, Cdk8, and Cdkn2d are involved in several cellular pathways, however, very little is known about their involvement in the establishment of RA-resistant Zscan4 metastate pluripotent cells. CDK8 was shown to maintain tumor dedifferentiation and embryonic stem cells pluripotency stage [16] drugs resistance in several cancer disease models [36,37]. Similar evidence was reported for Cdkn2d overexpression [38]. Concerning *Cdkn2d*, unlike *Cdk8*, we could not find any alteration in its expression upon Prame silencing. A possible explanation for this phenomenon is that Cdkn2d may be regulated by a higher expression level of Prame occurring under particular cell conditions.

Our data uncovered an important novel role of *Cdk8* and *Cdkn2d* expression in the Prame-dependent naïve pluripotent metastate. Remarkably, CDK inhibitors, such as CDK4/6 inhibitors, are already used in preclinical studies for cancer treatment [39]. In particular, CDK8 inhibitors have been used in acute myelogenous leukaemia and several other types of cancers, including breast cancer. Cancer cells treated with CDK8 inhibitors responded with decreased cell viability and increased apoptosis [40,41]. However, the function of Cdk8 and Cdkn2d may be cell-context dependent. Therefore, it will be necessary to deeply investigate the protein expression and the molecular and epigenetic mechanisms underlying Prame-induced Cdk8 and Cdkn2d activation in ESCs to identify the tumor specificity of anti-Cdk8 or anti-Cdkn2d pharmacological compounds affecting cancer cells mimicking the PRAME-marked stage of cell pluripotency.

5. Conclusions

In our work, we identified, for the first time, *Cdk8* and *Cdkn2d* as new Prame -target genes through a ChIP-seq analysis specific to ESCs enriched in Prame expression after RA treatment.

The identification of new targets for Prame in ESCs represents a milestone in the field of ESC therapy, specifically for CSC drug delivery. Our data opens a new window on the study of CSC therapies, RA-resistant. In the future, it will be necessary to use drugs and combinations of these in cancers marked by *Cdk8* and *Cdkn2d* expression.

Supplementary Materials: The following supporting information can be downloaded at: https://www.mdpi.com/article/10.3390/genes13101745/s1, Figure S1: The enriched regions after anti-FLAG antibody immunoprecipitation.

Author Contributions: Conceptualization, T.A. and G.F.; methodology, V.L. and D.T.; sequencing analysis, S.A.; data validation E.D.M.; investigation, G.F. and A.P.; data curation, T.A.; writing—original draft preparation, T.A.; writing—review and editing, M.V. and V.C.; supervision, G.F.; funding acquisition, G.F., T.A. and A.P. All authors have read and agreed to the published version of the manuscript.

Funding: The research was supported by STAR Linea 1, 2014 (University of Naples Federico II) to G.F. and FRA_2021 to A.P. and T.A.

Institutional Review Board Statement: Not applicable.

Informed Consent Statement: Not applicable.

Data Availability Statement: Not applicable.

Conflicts of Interest: The authors have declared that no competing interest exist.

References

1. Madissoon, E.; Töhönen, V.; Vesterlund, L.; Katayama, S.; Unneberg, P.; Inzunza, J.; Hovatta, O.; Kere, J. Differences in gene expression between mouse and human for dynamically regulated genes in early embryo. *PLoS ONE* **2014**, *9*, 102949. [CrossRef]
2. Li, J.; Yin, J.; Zhong, J.; Yang, Z.; Tang, A.; Li, S. Clinicopathological and Prognostic Significance of PRAME Overexpression in Human Cancer: A Meta-Analysis. *Biomed. Res. Int.* **2020**, *2020*, 8828579. [CrossRef] [PubMed]
3. Graf, U.; Casanova, E.A.; Wyck, S.; Dalcher, D.; Gatti, M.; Vollenweider, E.; Okoniewski, M.J.; Weber, F.A.; Patel, S.S.; Schmid, M.W.; et al. Pramel7 mediates ground-state pluripotency through proteasomal-epigenetic combined pathways. *Nat. Cell Biol.* **2017**, *19*, 763–773. [CrossRef] [PubMed]
4. Amano, T.; Hirata, T.; Falco, G.; Monti, M.; Sharova, L.V.; Amano, M.; Sheer, S.; Hoang, H.G.; Piao, Y.; Stagg, C.A.; et al. Zscan4 restores the developmental potency of embryonic stem cells. *Nat. Commun.* **2013**, *4*, 1966. [CrossRef] [PubMed]
5. Natale, C.F.; Angrisano, T.; Pistelli, L.; Falco, G.; Calabrò, V.; Netti, P.A.; Ventre, M. Topographic Cues Impact on Embryonic Stem Cell Zscan4-Metastate. *Front. Bioeng. Biotechnol.* **2020**, *8*, 178. [CrossRef]
6. Falco, G.; Lee, S.M.; Stanghellini, I.; Bassey, U.C.; Hamatani, T.; Ko, M.S.H. Zscan4: A novel gene expressed exclusively in late 2-cell embryos and embryonic stem cells. *Dev. Biol.* **2007**, *307*, 539–550. [CrossRef]
7. Dahl, J.A.; Jung, I.; Aanes, H.; Greggains, G.D.; Manaf, A.; Lerdrup, M.; Li, G.; Kuan, S.; Li, B.; Lee, A.Y.; et al. Broad histone H3K4me3 domains in mouse oocytes modulate maternal-to-zygotic transition. *Nature* **2016**, *537*, 548–552. [CrossRef]
8. Tagliaferri, D.; De Angelis, M.T.; Russo, N.A.; Marotta, M.; Ceccarelli, M.; Del Vecchio, L.; De Felice, M.; Falco, G. Retinoic Acid Specifically Enhances Embryonic Stem Cell Metastate Marked by Zscan4. *PLoS ONE* **2016**, *11*, 0147683. [CrossRef]
9. Cerulo, L.; Tagliaferri, D.; Marotta, P.; Zoppoli, P.; Russo, F.; Mazio, C.; De Felice, M.; Ceccarelli, M.; Falco, G. Identification of a novel gene signature of ES cells self-renewal fluctuation through system-wide analysis. *PLoS ONE* **2014**, *9*, 83235.
10. Macfarlan, T.S.; Gifford, W.D.; Driscoll, S.; Lettieri, K.; Rowe, H.M.; Bonanomi, D.; Firth, A.; Singer, O.; Trono, D.; Pfaff, S.L.; et al. Embryonic stem cell potency fluctuates with endogenous retrovirus activity. *Nature* **2012**, *487*, 57–63. [CrossRef]
11. Epping, M.T.; Wang, L.; Edel, M.J.; Carlée, L.; Hernandez, M.; Bernards, R. The human tumor antigen PRAME is a dominant repressor of retinoic acid receptor signaling. *Cell* **2005**, *122*, 835–847. [CrossRef] [PubMed]
12. Epping, M.T.; Wang, L.; Plumb, J.A.; Lieb, M.; Gronemeyer, H.; Brown, R.; Bernards, R. A functional genetic screen identifies retinoic acid signaling as a target of histone deacetylase inhibitors. *Proc. Natl. Acad. Sci. USA* **2007**, *104*, 17777–17782. [CrossRef] [PubMed]
13. Napolitano, G.; Tagliaferri, D.; Fusco, S.; Cirillo, C.; De Martino, I.; Addeo, M.; Mazzone, P.; Russo, N.A.; Natale, F.; Cardoso, M.C.; et al. A novel member of Prame family, Gm12794c, counteracts retinoic acid differentiation through the methyltransferase activity of PRC2. *Cell Death Differ.* **2020**, *27*, 345–362. [CrossRef] [PubMed]
14. Oehler, V.G.; Guthrie, K.A.; Cummings, C.L.; Sabo, K.; Wood, B.L.; Gooley, T.; Yang, T.; Epping, M.T.; Shou, Y.; Pogoso-va-Agadjanyan, E.; et al. The preferentially expressed antigen in melanoma (PRAME) inhibits myeloid differentiation in normal hematopoietic and leukemic progenitor cells. *Blood* **2009**, *114*, 3299–3308. [CrossRef] [PubMed]
15. Wadelin, F.; Fulton, J.; McEwan, P.A.; Spriggs, K.A.; Emsley, J.; Heery, D.M. Leucine-rich repeat protein PRAME: Expression, potential functions and clinical implications for leukaemia. *Mol. Cancer* **2010**, *9*, 226. [CrossRef] [PubMed]
16. Adler, A.S.; McCleland, M.L.; Truong, T.; Lau, S.; Modrusan, Z.; Soukup, T.M.; Roose-Girma, M.; Blackwood, E.M.; Firestein, R. CDK8 maintains tumor dedifferentiation and embryonic stem cell pluripotency. *Cancer Res.* **2012**, *72*, 2129–2139. [CrossRef]
17. Kim, W.Y.; Sharpless, N.E. The regulation of INK4/ARF in cancer and aging. *Cell* **2006**, *127*, 265–275. [CrossRef]
18. Sun, J.; Zhang, Y.; Yin, B.; Li, J.; Liu, G.; Xu, W.; Tang, S. Differential expression of Axin1, Cdc25c and Cdkn2d mRNA in 2-cell stage mouse blastomeres. *Zygote* **2012**, *20*, 305–310. [CrossRef]
19. Troiano, A.; Pacelli, C.; Ruggieri, V.; Scrima, R.; Addeo, M.; Agriesti, F.; Lucci, V.; Cavaliere, G.; Mollica, M.P.; Caterino, M. ZSCAN4+ mouse embryonic stem cells have an oxidative and flexible metabolic profile. *EMBO Rep.* **2020**, *21*, 48942. [CrossRef]
20. Vivo, M.; Fontana, R.; Ranieri, M.; Capasso, G.; Angrisano, T.; Pollice, A.; Calabrò, V.; La Mantia, G. p14ARF interacts with the focal adhesion kinase and protects cells from anoikis. *Oncogene* **2017**, *36*, 4913–4928. [CrossRef] [PubMed]
21. Montano, E.; Pollice, A.; Lucci, V.; Falco, G.; Affinito, O.; La Mantia, G.; Vivo, M.; Angrisano, T. Pancreatic Progenitor Commitment Is Marked by an Increase in Ink4a/Arf Expression. *Biomolecules* **2021**, *11*, 1124. [CrossRef] [PubMed]
22. Angrisano, T.; Pero, R.; Brancaccio, M.; Coretti, L.; Florio, E.; Pezone, A.; Calabrò, V.; Falco, G.; Keller, S.; Lembo, F.; et al. Cyclical DNA Methylation and Histone Changes Are Induced by LPS to Activate COX-2 in Human Intestinal Epithelial Cells. *PLoS ONE* **2016**, *11*, 0156671. [CrossRef] [PubMed]
23. Li, H.; Durbin, R. Fast and accurate short read alignment with Burrows-Wheeler transform. *Bioinformatics* **2009**, *25*, 1754–1760. [CrossRef] [PubMed]
24. Quinlan, A.R.; Hall, I.M. BEDTools: A flexible suite of utilities for comparing genomic features. *Bioinformatics* **2010**, *26*, 841–842. [CrossRef]
25. Huang, W.; Loganantharaj, R.; Schroeder, B.; Fargo, D.; Li, L. PAVIS: A tool for peak annotation and visualization. *Bioinformatics* **2013**, *29*, 3097–3099. [CrossRef]
26. Bhattacharya, A.; Deng, J.M.; Zhang, Z.; Behringer, R.; De Crombrugghe, B.; Maity, S.N. The B subunit of the CCAAT box binding transcription factor complex (CBF/NF-Y) is essential for early mouse development and cell proliferation. *Cancer Res.* **2003**, *63*, 8167–8172.

27. Grskovic, M.; Chaivorapol, C.; Gaspar-Maia, A.; Li, H.; Ramalho-Santos, M. Systematic identification of cis-regulatory sequences active in mouse and human embryonic stem cells. *PLoS ONE* **2007**, *3*, 145. [CrossRef]
28. Gurtner, A.; Manni, I.; Fuschi, P.; Mantovani, R.; Guadagni, F.; Sacchi, A.; Piaggio, G. Requirement for down-regulation of the CCAAT-binding activity of the NF-Y transcription factor during skeletal muscle differentiation. *Mol. Biol. Cell* **2003**, *14*, 2706–2715. [CrossRef]
29. Costessi, A.; Mahrour, N.; Tijchon, E.; Stunnenberg, R.; Stoel, M.A.; Jansen, P.W.; Sela, D.; Martin-Brown, S.; Washburn, M.P.; Florens, L.; et al. The tumor antigen PRAME is a subunit of a Cul2 ubiquitin ligase and associates with active NFY promoters. *EMBO J.* **2011**, *30*, 3786–3798. [CrossRef]
30. Wang, P.J.; McCarrey, J.R.; Yang, F.; Page, D.C. An abundance of X-linked genes expressed in spermatogonia. *Nat. Genet.* **2001**, *27*, 422–426. [CrossRef]
31. Dadé, S.; Callebaut, I.; Mermillod, P.; Monget, P. Identification of a new expanding family of genes characterized by atypical LRR domains. Localization of a cluster preferentially expressed in oocyte. *FEBS Lett.* **2003**, *555*, 533–538. [CrossRef]
32. Bortvin, A.; Eggan, K.; Skaletsky, H.; Akutsu, H.; Berry, D.L.; Yanagimachi, R.; Page, D.C.; Jaenisch, R. Incomplete reactivation of Oct4-related genes in mouse embryos cloned from somatic nuclei. *Development* **2003**, *130*, 1673–1680. [CrossRef] [PubMed]
33. Cazzato, G.; Mangialardi, K.; Falcicchio, G.; Colagrande, A.; Ingravallo, G.; Arezzo, F.; Giliberti, G.; Trilli, I.; Loizzi, V.; Lettini, T.; et al. Preferentially Expressed Antigen in Melanoma (PRAME) and Human Malignant Melanoma: A Retrospective Study. *Genes* **2022**, *13*, 545. [CrossRef] [PubMed]
34. Cinelli, P.; Casanova, E.A.; Uhlig, S.; Lochmatter, P.; Matsuda, T.; Yokota, T.; Rülicke, T.; Ledermann, B.; Bürki, K. Expression profiling in transgenic FVB/N embryonic stem cells overexpressing STAT3. *BMC Dev. Biol.* **2008**, *8*, 57. [CrossRef]
35. Reya, T.; Morrison, S.J.; Clarke, M.F.; Weissman, I.L. Stem cells, cancer, and cancer stem cells. *Nature* **2001**, *414*, 105–111. [CrossRef] [PubMed]
36. Menzl, I.; Zhang, T.; Berger-Becvar, A.; Grausenburger, R.; Heller, G.; Prchal-Murphy, M.; Edlinger, L.; Knab, M.V.; Uras, I.Z.; Grundschober, E.; et al. A kinase-independent role for CDK8 in BCR-ABL1+ leukemia. *Nat. Commun.* **2019**, *10*, 4741. [CrossRef]
37. Sharko, A.C.; Lim, C.K.; McDermott, M.S.J.; Hennes, C.; Philavong, K.P.; Aiken, T.; Tatarskiy, V.V.; Roninson, I.B.; Broude, E.V. The Inhibition of CDK8/19 Mediator Kinases Prevents the Development of Resistance to EGFR-Targeting Drugs. *Cells* **2021**, *10*, 144. [CrossRef]
38. Antonova, O.; Rukova, B.; Mladenov, B.; Rangelov, S.; Hammoudeh, Z.; Nesheva, D.; Staneva, R.; Spasova, V.; Grigorov, E.; Hadjidekova, S.; et al. Expression profiling of muscle-invasive and non-invasive bladder tumors for biomarkers identification related to drug resistance, sensitivity, and tumor progression. *Biotechnol. Biotechnol. Equip.* **2020**, *34*, 506–514. [CrossRef]
39. Thoma, O.M.; Neurath, M.F.; Waldner, M.J. Cyclin-Dependent Kinase Inhibitors and Their Therapeutic Potential in Colorectal Cancer Treatment. *Front. Pharm.* **2021**, *12*, 757120. [CrossRef]
40. Spear, J.M.; Lu, Z.; Russu, W.A. Pharmacological Inhibition of CDK8 in Triple-Negative Breast Cancer Cell Line MDA-MB-468 Increases E2F1 Protein, Induces Phosphorylation of STAT3 and Apoptosis. *Molecules* **2020**, *25*, 5728. [CrossRef]
41. Xi, M.; Chen, T.; Wu, C.; Gao, X.; Wu, Y.; Luo, X.; Du, K.; Yu, L.; Cai, T.; Shen, R.; et al. CDK8 as a therapeutic target for cancers and recent developments in discovery of CDK8 inhibitors. *Eur. J. Med. Chem.* **2019**, *164*, 77–91. [CrossRef] [PubMed]

genes

MDPI

Article

Integrated Bioinformatics Analysis Reveals Novel miRNA as Biomarkers Associated with Preeclampsia

Mariarita Brancaccio [1,*], Caterina Giachino [2], Assunta Maria Iazzetta [2], Antonio Cordone [2], Elena De Marino [2], Ornella Affinito [1], Maria Vivo [3], Viola Calabrò [2], Alessandra Pollice [2] and Tiziana Angrisano [2,*]

[1] Department of Molecular Medicine and Medical Biotechnology, University of Naples Federico II, 80131 Naples, Italy
[2] Department of Biology, University of Naples Federico II, 80126 Naples, Italy
[3] Department of Chemistry and Biology, University of Salerno, 84084 Fisciano, Italy
* Correspondence: brancacciomariarita2@gmail.com (M.B.); tangrisa@unina.it (T.A.); Tel.: +39-33-93121924 (M.B.); +39-34-94670474 (T.A.)

Abstract: Preeclampsia is a leading cause of perinatal maternal-foetal mortality and morbidity. This study aims to identify the key microRNAs (miRNA) in preeclampsia and uncover their potential functions. We downloaded the miRNA expression profile of GSE119799 for plasma and GSE177049 for the placenta. Each dataset consisted of five patients (PE) and five controls (N). From a technical point of view, we analysed the counts per million (CPM) for both datasets, highlighting 358 miRNAs in common, 78 unique for plasma and 298 unique for placenta. At the same time, we performed an expression differential analysis ($|\log FC| \geq 1$ and FDR ≤ 0.05) to evaluate the biological impact of the miRNAs. This approach allowed us to highlight 321 miRNAs in common between plasma and placenta, within which four were upregulated in plasma. Furthermore, the same analysis revealed five miRNAs expressed exclusively in plasma; these were also upregulated. In conclusion, the in-depth bioinformatics analysis conducted during our study will allow us, on the one hand, to verify the targets of each of the nine identified miRNAs; on the other hand, to use them both as new non-invasive biomarkers and as therapeutic targets for the development of *personalised* treatments.

Keywords: bioinformatics; preeclampsia; microRNA; biomarkers; epigenetic; therapeutic targets

Citation: Brancaccio, M.; Giachino, C.; Iazzetta, A.M.; Cordone, A.; De Marino, E.; Affinito, O.; Vivo, M.; Calabrò, V.; Pollice, A.; Angrisano, T. Integrated Bioinformatics Analysis Reveals Novel miRNA as Biomarkers Associated with Preeclampsia. *Genes* **2022**, *13*, 1781. https://doi.org/10.3390/genes13101781

Academic Editor: Björn Voß

Received: 28 July 2022
Accepted: 27 September 2022
Published: 2 October 2022

1. Introduction

It has been reported that, in countries with advanced economies, 10–20% of pregnancy is affected by some form of hypertension [1]. The exact incidence of preeclampsia (PE) is not known, but it is believed that it can be around 5–8% [2]. Preeclampsia also represents the basis of 15–20% of maternal mortality cases [3] and constitutes one of the leading causes of perinatal mortality and morbidity [4]. It is usually diagnosed based on the de novo onset of hypertension and proteinuria [5]. The lack of reliable methods for early detection limits the opportunities for prevention, diagnosis and timely treatment.

MicroRNAs (miRNAs) are small endogenous single-stranded non-coding RNA molecules found in the transcriptome of plants, animals and some DNA viruses [6–8]. These are polymers encoded by eukaryotic nuclear DNA about 20–22 nucleotides long and are mainly active in the regulation of gene expression at the transcriptional and post-transcriptional levels [6–8]. The miRNAs are incorporated into the RNA-induced silencing complex (RISC) and induce gene silencing by overlapping with complementary sequences present on target messenger RNA (mRNA) molecules [6–8]. In addition, it is known that miRNAs are responsible for the epigenetic regulation of several molecules [9]. This link leads to translation repression or degradation of the target molecule [6–8].

A lot of evidence regarding the role of miRNAs in preeclampsia has been accumulated in the last 10 years [10]. Differentially expressed miRNAs are characteristic of both mild

and severe PE [10]. In many cases, they target signalling pathway-related genes that result in altered processes directly involved in PE [10].

High-throughput platforms such as Next Generation Sequencing technology (NGS) are increasingly popular for miRNA and gene expression analysis in PE. For example, Mavreli and collaborators use an NGS approach, highlighting that miR-23b-5p and miR-99b-5p are downregulated in plasma of PE compared to controls [11]. In the same work, the authors highlighted that the targets of these microRNAs were associated with glycometabolism and the immune response involved in the pathogenesis of PE [11].

On the other hand, Vashukova and co-authors, using Ion Tor-rent next-generation sequencing technology, identified a total of 22 miRNAs that included 16 miRNAs previously known to be associated with PE and six novel miRNAs [12]. Among the six new miRNAs, four were upregulated (miR-518a, miR-527, miR-518e and miR-4532) and two were downregulated (miR-98 and miR-135b) in PE placentas compared to controls [12].

The results currently reported in the literature suggest that PE is associated with specific alterations in the expression pattern of placental miRNAs.

We decided to compare miRNAs expressed between plasma and placenta for the following reasons. First of all, the placenta is a deciduous, and therefore temporary, organ that forms in the uterus during pregnancy. The placenta is responsible for nourishing, protecting and supporting fetal growth. The placenta is common to the pregnant woman and the fetus; a part of it has maternal origins (constituted by the modified or deciduous uterine endometrium), while the remainder has fetal origins (formed by the chorionic villi). Therefore, the placenta represents the fetus's roots in the mother's soil. Secondarily, plasma is the liquid component of the blood, in which the corpuscular elements (red blood cells, white blood cells and platelets) are suspended. Finally, the mother's immune system during pregnancy must be tolerant of the fetus during gestosis; to do this at the plasma level, chemokines, miRNAs, and cytokines that do not allow premature abortions are released.

Consequently, the identification of common biomarkers can be of help in PE monitoring.

In light of this, our work aimed to compare, through a bioinformatics approach, the gene expression profile of miRNAs coming from two databases. The databases used were GSE119799 for plasma [11] and GSE177049 for the placenta to discover the miRNAs and key genes that contribute to the pathology of PE and thus provide new insights into potential biomarkers for prognosis and therapeutic strategies of PE.

2. Materials and Methods

2.1. Data Collection and Processing

The following miRNA datasets were downloaded from the Gene Expression Omnibus: GSE177049 containing miRNA data from ten placental samples (n = 5 control (N); n = 5 patient with preeclampsia (PE)) and GSE119799 [11] containing miRNA data from ten plasma samples (n = 5 control (N); n = 5 patients with preeclampsia (PE)).

For placental samples, only processed expression data (CPM) for 794 miRNAs were available and obtained as described in https://www.ncbi.nlm.nih.gov/geo/query/acc.cgi?acc=GSE177049 (accessed on 27 July 2022). Briefly, miRDeep2 is a software package for identification of novel and known miRNAs in deep sequencing data; therefore, it was used to quantify the expression level of known mature miRNAs curated in the human miRBase database. The miRNA-seq was analysed by R/Bioconductor package Edge R [13], which employs a negative binomial generalised linear model with likelihood ratio test (glmLRT) to compare the miRNAs expression level between two conditions. Only those miRNAs (n = 656) expressed at counts per million (CPM) above 0.5 in at least 90% of the samples.

For plasma samples, raw counts were available for 4483 miRNAs, out of them 1753 were novel miRNAs and 2730 known miRNAs. Out of them, to best compare plasma and placental samples, we filtered out the novel miRNAs, and we retained only those known miRNAs (n = 436) expressed at counts per million (CPM) above 0.5 in at least 90% of the samples After a TMM normalisation, differential expression was assessed with glmLRT method implemented in R/Bioconductor package Edge R [13].

For both datasets, only miRNAs genes with $|\log FC| \geq 1$ and an adjusted *p*-value (FDR) ≤ 0.05 were defined as differentially expressed.

Venn diagram to show overlapping and specific miRNAs was performed by R package VennDiagram.

Heatmap was performed by R package gplots. The count-per-million (CPM) at log2 scale, denoted as logCPM, was computed for visualisation of miRNA abundance in heatmap-clustering analysis.

2.2. Prediction of miRNAs' Targets

To identify the targets of the collected miRNAs, we used three different tools: (1) miRDB, an online database for the prediction of the miRNA targets [14,15]; (2) RNA22 version 2.0, software for miRNA target predictions [16], and TargetScan 8.0, a web server of miRNA target predictions [17–22].

We first searched for targets in miRDB using 60–100 as a range for the Target Score [14,15]. The targets identified with miRDB were then analysed in RNA22 version 2.0 using the following filters: base pair min value = 12, folding energy max value (Kcal/mol) = −12 and *p*-value < 0.05. Lastly, only the targets identified in RNA22 version 2.0 were validated in TargetScan 8.0 taking the total context ++ score as the prediction truthfulness values [18].

2.3. Functional Enrichment Analysis

Functional enrichment analysis of target genes was performed by using Kyoto Encyclopedia of Genes and Genomes (KEGG) database implemented in miRNet 2.0 [23]. Statistical significance was evaluated by the hypergeometric test. Only pathways with FDR ≤ 0.05 were considered as significative.

3. Results

3.1. The Plasma and Placental miRNoma Landscape in Preeclampsia

miRNoma landscape in preeclampsia was analysed in two public datasets: GSE119799 for plasma [11] and GSE177049 for the placenta. After appropriate filtering and normalisation procedures, we obtained a total 656 miRNAs in placenta and 436 in plasma (see Section 2 for details). As shown in Venn diagram, 358 miRNAs were in common between placenta and plasma while the remaining were specific of each tissue (see Figure 1).

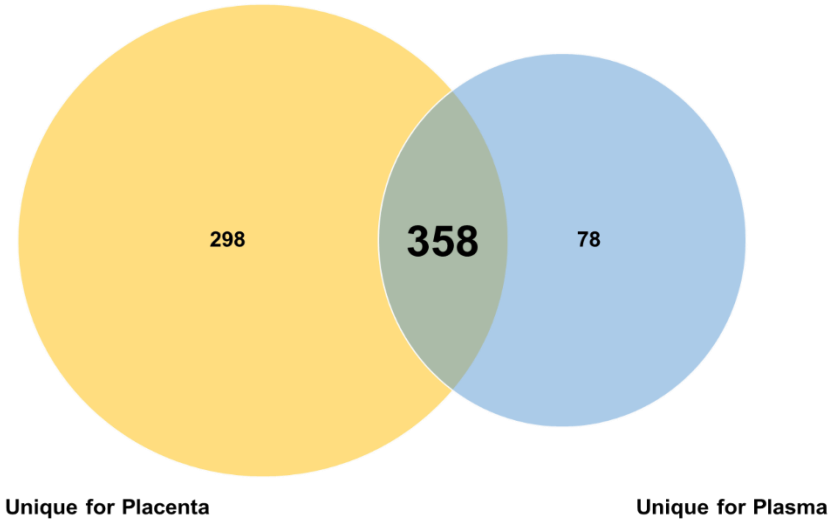

Figure 1. Venn diagram of overlapping and specific miRNAs in plasma and placenta.

3.2. Comparison of miRNAs Expression Profiles in a Woman with PE

To clarify the role of miRNAs in PE, we have focused on 358 miRNAs in common between placenta and plasma.

Focusing on plasma, among these 358 miRNAs, we extracted four differentially expressed miRNAs ($|\log FC| \geq 1$ and FDR ≤ 0.05). All of them were upregulated in comparison with the control (Figure 2). The same miRNAs resulted in being non-differentially expressed between control and preeclampsia patients in placenta. A comparison of the expression levels of these four common miRNAs in plasma and placenta is reported in Figure 3.

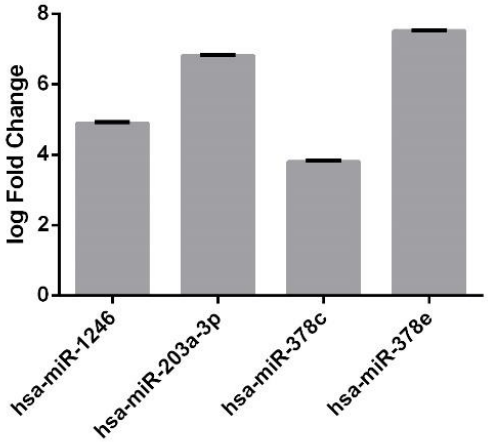

Figure 2. Differentially Expressed miRNAs in common between plasma and placenta. Barplot shows the upregulated miRNAs expression levels in plasma. The expression levels are expressed as log Fold Change (log2FC).

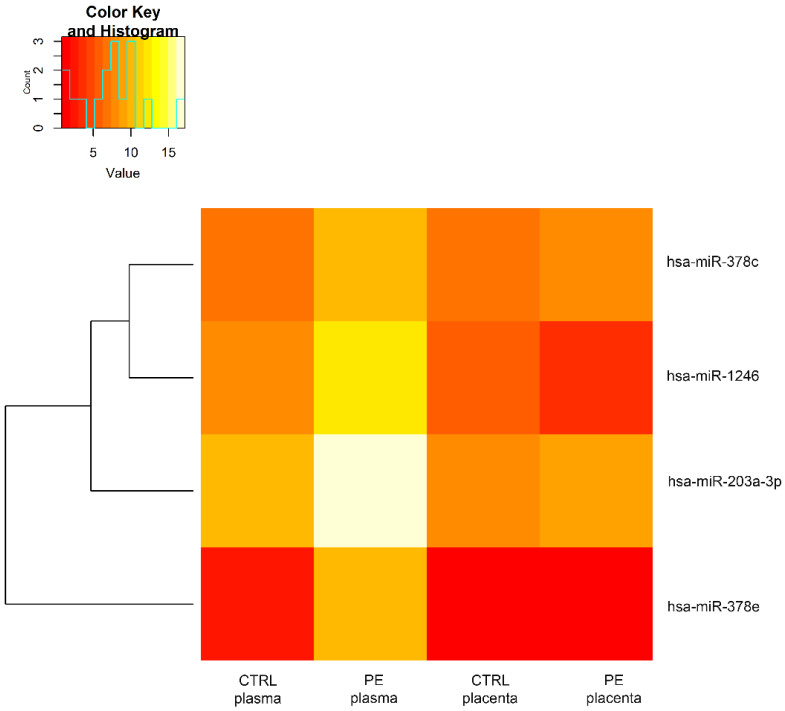

Figure 3. Heatmap: common miRNAs expression profiles in plasma and placenta. Heatmap shows the expression levels of each common miRNA in plasma and placenta tissues. The expression level of each miRNA (rows) was averaged within the pre-classified group (column). Values are expressed as log2CPM.

Furthermore, we also evaluated the expression levels of plasma-specific miRNAs. We found five plasma-specific differentially expressed miRNAs, all of them upregulated with respect to normal samples (Figure 4).

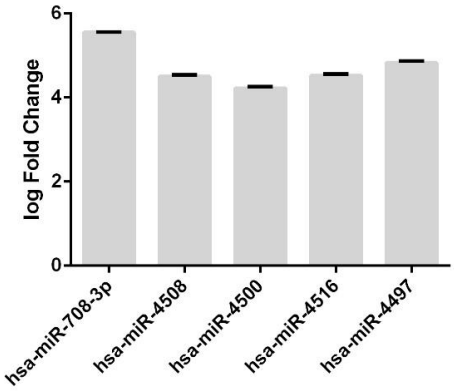

Figure 4. Differentially Expressed of plasma-specific miRNAs. Barplot shows the upregulated unique miRNAs in plasma. The expression levels are expressed as log Fold Change (log2FC).

3.3. Annotation of miRNAs Involved in the Pathogenesis of Preeclampsia and Their Targets

To investigate the role of the 4 miRNAs found in common between plasma and placenta, we carried out a systematic analysis identifying the targets and the role of these miRNAs in the pathogenesis of preeclampsia (see Table 1).

Table 1. Role and target of miRNAs in common between plasma and placenta in preeclampsia.

miRNA	Target	References
hsa-mir-1246	• interacts with NRF2 promotes the differentiation of the syncytiotrophoblast • modulates Jarid2 in human trophoblast differentiation • modulates p53, PI3K/AKT, mTOR in glioblastoma	[24,25]
hsa-mir-203a-3p	• plays an anti-inflammatory role in PE pregnant women by downregulating the IL24 level • isolated in plasma exosomes of women with PE	[26–28]
hsa-mir-378c	• upregulated in the first trimester of pregnancy in women with PE • may lead to the downregulation of genes involved in the HIF-1/VEGF signaling pathway, adversely affecting angiogenesis, implantation and embryo development, and participates in abortion process.	[29,30]
hsa-mir-378e	• expressed in the endometrium	[31]

The same type of analysis was performed for the 5 miRNAs unique to plasma (see Table 2).

Table 2. Role and target of upregulated miRNAs in preeclampsia unique for plasma.

miRNA	Target	References
hsa-miR-708-3p	• Downregulated in breast cancer, Inhibits metastases through Neuronatin • may represent a potential therapeutic target via the ADAM17-GATA/STAT3 axis in idiopathic pulmonary fibrosis	[32,33]

Table 2. *Cont.*

miRNA	Target	References
hsa-miR-4508	• upregulated in rheumatoid arthritis; is a therapeutic target of the same pathology • upregulated in hepatic cancer cells (HepG2)	[34,35]
hsa-miR-4500	• isolated in plasma exosomes of women with PE • is epigenetically downregulated in colorectal cancer and functions as a novel tumor suppressor by regulating HMGA2 • Inhibits Migration, Invasion, and Angiogenesis of Breast Cancer Cells via RRM2-Dependent MAPK Signaling Pathway	[28,36,37]
hsa-miR-4516	• potential biomarker for early diagnosis of dust-induced pulmonary fibrosis • plays a role in PUVA-induced apoptosis through the downregulation of STAT3/CDK6/UBE2N in keratinocytes • downregulated in psoriasis inhibits keratinocyte motility by targeting fibronectin/integrin α9 signalling • Biomarker of Premature Ovarian Insufficiency • altered in preterm births	[38–42]
hsa-miR-4497	• tumor suppressor in laryngeal squamous cell carcinoma via negatively modulation the GBX2 • increases the expression and secretion of TNFα induced by LPS in mothers with type 1 diabetes contain • upregulated in placentas with selective intrauterine growth restriction	[43–45]

Following this analysis, we have shown that 1 (hsa-mir-378e) of the 4 miRNAs identified had never been reported as biomarkers for preeclampsia or diseases related to it, but as a marker of pathologies linked to the endometrium.

On the other hand, for the remaining 3 (hsa-mir-1246, hsa-mir-203a-3p and hsa-mir-378c), the targets that were activated and/or repressed during the pathophysiology of preeclampsia were also noted (see Table 1). As reported in Table 1, most of the targets appear to be involved in the process of placentation and inflammation.

Among these 5 miRNA, 2 (hsa-miR-708-3p and hsa-miR-4508) are not known as possible miRNA involved in the pathophysiology of preeclampsia, but disorders such as cancer and autoimmune diseases are found (Table 2). Instead, the other 3 miRNAs (hsa-miR-4500, hsa-miR-4516 and hsa-miR-4497) have been found in processes that may occur during preeclampsia such as intrauterine growth retardation or preterm birth (Table 2).

3.4. Analysis of the Predicted miRNA Targets

To shed light on the role of the 3 unidentified miRNAs (hsa-mir-378e, hsa-miR-708-3p and hsa-miR-4508) using bioinformatics analysis that did not have known targets to the pathophysiological process of preeclampsia, we predicted through miRDB using 60–100 as a range for the Target Score [14–22].

Following this analysis, we identified 310 targets for hsa-mir-378e, 457 targets for hsa-miR-708-3p and 125 targets for hsa-miR-4508 (Figure 5 and Table S1). After that, we merged the obtained results with RNA22 version 2.0 using the following filters: base pair min value = 12, folding energy max value (Kcal/mol) = −12 and p-value < 0.05. In this case, 57 common targets for hsa-mir-378e, 2 common targets for hsa-miR-708-3p and 15 common targets for hsa-miR-4508 were found (Figure 5 and Table S2).

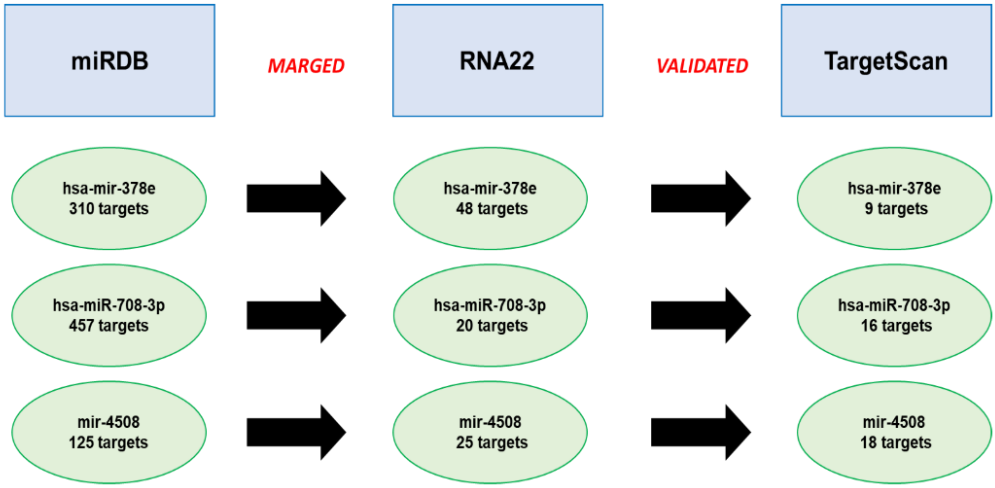

Figure 5. Predicted targets for preeclampsia miRNAs. The overlapping target genes were predicted thanks to the online analysis tools: miRDB, RNA22 and TargetScan; in miRDB using 60–100 as a range for the Target Score; in the RNA22 version 2.0 using the following filters: base pair min value = 12, folding energy max value (Kcal/mol) = −12 and p-value < 0.05. In TargetScan 8.0, take the total context ++ score as the prediction truthfulness value.

Finally, to validate the identified targets, we used TargetScan 8.0, taking the total context ++ score as the prediction truthfulness values [18] (Table S3). In particular, we highlighted 41 targets for hsa-mir-378e, 2 targets for hsa-miR-708-3p and 13 targets for hsa-miR-4508 (see Figure 5 and Table S3).

3.5. Functional Enrichment Analysis

To better investigate functional pathways where target genes are involved, we performed an enrichment analysis by using a KEGG database implemented in miRNet 2.0 [23] (Figure 6). Interestingly, we found three pathways potentially associated with preeclampsia: MAPK signalling pathway (FDR = 0.006), TGF-β signalling pathway (FDR = 0.011), Insulin signalling pathway (FDR = 0.020) and VEGF signalling pathway (FDR = 0.031) (Figure 6).

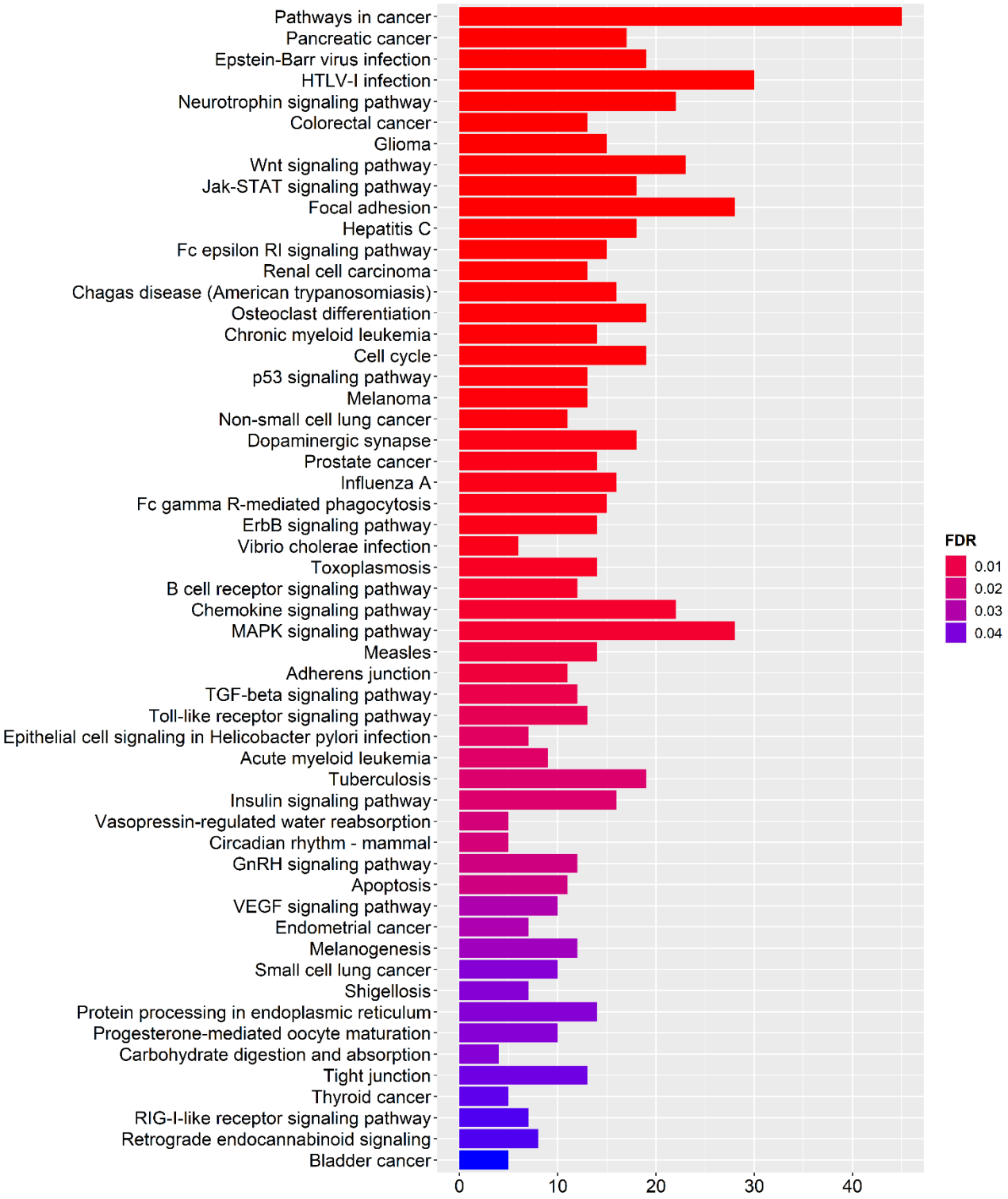

Figure 6. Pathway Enrichment Analysis. The *y*-axis represents the enriched KEGG items; the *x*-axis shows the gene count. The color of each bar represents enrichment significance. Only pathways with FDR $\leq$ are considered as statistically significant.

4. Discussion

PE is a multisystem disorder specific to pregnancy, and a deficiency in our knowledge of the exact aetiology and pathogenesis of this human disorder restricts the ability to treat this disease [46]. Therefore, the identification of molecular targets to build a panel of

biomarkers involved in the pathophysiology of PE is crucial to develop more effective diagnostic and therapeutic strategies.

At the same time, it is now known that miRNAs play a fundamental role as next-generation biomarkers [47–56]. The miRNAs being measurable through biological fluids and regulating numerous cellular targets represent "the gold standard of biomarkers" in pathologies in which a rapid prognosis and constant monitoring are required [47–56].

In light of this, our study focused on identifying miRNAs that can be used as biomarkers in preeclampsia.

First of all, through deep bioinformatics analysis, we have identified the miRNAs in common with the placenta and plasma. The search for stable miRNAs in the two tissues mainly involved in the pathophysiology of preeclampsia aims to employ these miRNAs as specific and sensitive biomarkers. Indeed, the biomarkers used in diagnosing and monitoring multifactorial disorders must be peculiar [47–56].

We then focused our attention on up and down miRNAs regulated between the placenta and plasma. In particular, the placenta and the foetus are connected by the umbilical cord; the placenta represents the sustenance system of the foetus because it functions as an exchange point between maternal and foetal blood.

Recently, Chang and co-workers showed that placental miRNA trafficking mainly to the maternal circulation and that maternal miRNA could transit to the placenta and even into the foetal compartment. These findings define an extraordinary miRNA-based non-hormonal means of communication between the placenta and the foetus-maternal compartments [57]. Consequently, the trafficking between maternal and foetal blood is of fundamental importance for monitoring both the state of health of the mother and the foetus [52]; therefore, the identification of stable miRNAs in common between the placenta and the blood helps monitor PE and the correct development of the foetus.

Furthermore, it is now known that placental cell disorders are closely associated with adverse pregnancy outcomes and the manifestation of PE. At the same time, numerous miRNAs have been found in the human placenta and growing evidence is revealing their role as protagonists in regulating placental cell behaviours. Indeed, recent studies indicate that placenta-derived miRNAs can be released into the maternal circulation by encapsulating them in exosomes and potentially targeting various maternal cells [58].

In our case of the 4 miRNAs in common between placenta and plasma that we highlighted, 3 (hsa-mir-1246, hsa-mir-203a-3p and hsa-mir-378c) were known actors in the pathophysiology of PE [24–30]; instead, the other 1 (hsa-mir-378e) has never been indicated as a possible biomarker of PE.

In addition, the targets prediction analysis of hsa-mir-378e allowed us to highlight two interesting targets that appear to be involved in the pathophysiology of PE: insulin-like growth factor-1 (IGF-1) and mitogen-activated protein kinase 1 (MAPK-1) [59–63].

Plasma IGF-1 levels are known to correlate with the severity of preeclampsia [59–62]. In fact, in the study conducted by Ingec and collaborators [60], IGF-1 and insulin-like growth factor binding protein-1 (IGFBP-1) were measured in groups with different degrees of PE (20 mild pre-eclamptic, 20 severe pre-eclamptic, 20 eclamptic patients and 20 healthy pregnant women in the third trimester) [60].

The authors pointed out on IGF-1 levels were lower in pre-eclamptic and eclamptic patients than in controls, while IGFBP-1 had an opposite trend [60].

The deficiency of IGF-1 could cause harm to the foetus; in fact, Halhali and co-authors [62] have shown that, in women suffering from preeclampsia, there is a decrease in IGF-1 levels also in the cord blood, influencing the growth of the foetus [62].

On the other hand, it is known that impaired trophoblast invasion partly modulated by abnormal MAPK1/ERK2 signalling played important roles in the pathological process of preeclampsia [63].

At the same time, within the 5 miRNAs unique to plasmas, we have brought to light 2 miRNAs (hsa-mir-708-3p and hsa-mir-4508) which do not appear to be noted as actors of PE [32–35].

For hsa-mir-708-3p, we have identified 16 targets, but of particular importance is the fibroblast growth factor receptor 2 (FGFR2). In fact, recent studies have shown that specific mutations of FGFR2 can be the substrate for the emergence of PE [64]. Furthermore, it has been shown that the methylation status of FGFR2 influences the phenomenon of placentation and especially sex-specific preterm births [65].

In addition, for hsa-mir-4508, we have identified 18 targets; among these, of particular importance is solute carrier family 43, member 3 (SLC43A3) and solute carrier family 12 (potassium/chloride transporter), and member 4 (SLC12A4), both involved in the regulation of prolactin levels in the amniotic fluid and therefore responsible for foetal development [66].

Finally, during functional enrichment analysis, on the one hand, we confirmed two signalling pathways that emerged during the search for specific targets: MAPK and Insulin signalling pathway [59–63]; on the other hand, we have shed light on two other extremely interesting signalling pathways for preeclampsia: TGF-β and VEGF [67,68].

Normal human pregnancy depends on the physiological transformation of spiral arteries by invasive trophoblasts. Preeclampsia is associated with impaired trophoblast invasion and spiral artery transformation. Recent studies have suggested that TGF-β is overexpressed in the placenta of PE patients and that this may be responsible for failed trophoblast invasion [67].

Moreover, there is additional experimental evidence that supports the hypothesis that interference with VEGF/PlGF signalling could mediate endothelial dysfunction in preeclampsia. VEGF is important in the stabilisation of endothelial cells in mature blood vessels. VEGF is particularly important in the health of the fenestrated and sinusoidal endothelium found in the renal glomerulus, brain, and liver organs severely affected in preeclampsia. VEGF is highly expressed by glomerular podocytes, and VEGF receptors are present in glomerular endothelial cells [68].

The meticulous bioinformatic analysis and target prediction of miRNAs not yet known as protagonists of the pathophysiological process of PE have allowed us to shed light on new biomarkers that could also represent new therapeutic targets for new therapies. Having highlighted nine upregulated miRNAs in plasma, four of which are also expressed in the placenta, can help in the development of rapid and non-invasive tests to monitor preeclampsia during gestation without having to wait for birth to be able to access tests on the placenta and/or on the foetus.

5. Conclusions

The data shown here confirm that miRNAs play a fundamental role in the pathophysiology of preeclampsia [69]. In addition, the in-depth bioinformatics analysis carried out on the validation of new targets allowed us to unearth new biomarkers. In conclusion, our study allowed us to lay the foundations for the development of a panel of biomarkers that can be used both as prognostic factors and as monitoring factors for both pathology and any drug therapies.

Supplementary Materials: The following supporting information can be downloaded at: https://www.mdpi.com/article/10.3390/genes13101781/s1, Table S1: Supplementary 1_miRDB; Table S2: Supplementary 2_RNA22 and Table S3: Supplementary 3_TargetScanHuman.

Author Contributions: Conceptualisation, M.B. and T.A.; methodology, C.G., A.M.I., A.C., E.D.M. and O.A.; software, M.B., O.A. and T.A.; validation, M.B., O.A. and T.A.; formal analysis, M.B., C.G., A.M.I., A.C., E.D.M., O.A. and T.A.; investigation, C.G., A.M.I., A.C. and E.D.M.; data curation, M.B., C.G., A.M.I., A.C., E.D.M., O.A. and T.A.; writing—original draft preparation, M.B., O.A. and T.A.; writing—review and editing, M.B., O.A., M.V., V.C., A.P. and T.A.; visualisation, M.B. and T.A.; supervision, M.B. and T.A. All authors have read and agreed to the published version of the manuscript.

Funding: This research received no external funding.

Institutional Review Board Statement: Not applicable.

Informed Consent Statement: Not applicable.

Data Availability Statement: Not applicable.

Conflicts of Interest: The authors declare no conflict of interest.

References

1. Budde, U.; Schneppenheim, R. Von Willebrand factors and von Willebrand disease. *Rev. Clin. Exp. Hematol.* **2001**, *5*, 335–368. [CrossRef] [PubMed]
2. Horan, J.T.; Francis, C.W. Fibrin degradation products, fibrin monomer and soluble fibrin in disseminated intravascular coagulation. *Semin. Thromb. Hemost.* **2001**, *27*, 657–666. [CrossRef] [PubMed]
3. Szpera-Gozdziewicz, A.; Breborowicz, G.H. Endothelial dysfunction in the pathogenesis of pre-eclampsia. *Front. Biosci.-Landmark* **2014**, *19*, 734–746. [CrossRef] [PubMed]
4. Hodgins, S. Pre-eclampsia as Underlying Cause for Perinatal Deaths: Time for Action. *Glob. Health Sci. Pract.* **2015**, *3*, 525–527. [CrossRef]
5. Wagner, L.K. Diagnosis and management of preeclampsia. *Am. Fam. Physician* **2004**, *70*, 2317–2324. [PubMed]
6. Ambros, V. The functions of animal microRNAs. *Nature* **2004**, *431*, 350–355. [PubMed]
7. Bartel, D.P. MicroRNAs: Genomics, biogenesis, mechanism, and function. *Cell* **2004**, *116*, 281–297. [CrossRef]
8. Bartel, D.P. MicroRNAs: Target recognition and regulatory functions. *Cell* **2009**, *136*, 215–233. [CrossRef]
9. Petrillo, F.; Iervolino, A.; Angrisano, T.; Jelen, S.; Costanzo, V.; D'Acierno, M.; Cheng, L.; Wu, Q.; Guerriero, I.; Mazzarella, M.C.; et al. Dysregulation of Principal Cell miRNAs Facilitates Epigenetic Regulation of AQP2 and Results in Nephrogenic Diabetes Insipidus. *J. Am. Soc. Nephrol.* **2021**, *32*, 1339–1354. [CrossRef]
10. Skalis, G.; Katsi, V.; Miliou, A.; Georgiopoulos, G.; Papazachou, O.; Vamvakou, G.; Nihoyannopoulos, P.; Tousoulis, D.; Makris, T. MicroRNAs in Preeclampsia. *Microrna* **2019**, *8*, 28–35.
11. Mavreli, D.; Lykoudi, A.; Lambrou, G.; Papaioannou, G.; Vrachnis, N.; Kalantaridou, S.; Papantoniou, N.; Koliale, A. Deep Sequencing Identified Dysregulated Circulating MicroRNAs in Late Onset Preeclampsia. *In Vivo* **2020**, *34*, 2317–2324. [CrossRef]
12. Vashukova, E.S.; Glotov, A.S.; Fedotov, P.V.; Efimova, O.A.; Pakin, V.S.; Mozgovaya, E.V.; Pendina, A.A.; Tikhonov, A.V.; Koltsova, A.S.; Baranov, V.S. Placental microRNA expression in pregnancies complicated by superimposed pre-eclampsia on chronic hypertension. *Mol. Med. Rep.* **2016**, *14*, 22–32. [CrossRef]
13. Robinson, M.D.; McCarthy, D.J.; Smyth, G.K. edgeR: A Bioconductor package for differential expression analysis of digital gene expression data. *Bioinformatics* **2010**, *26*, 139–140. [CrossRef]
14. Chen, Y.; Wang, X. miRDB: An online database for prediction of functional microRNA targets. *Nucleic Acids Res.* **2020**, *48*, D127–D131. [CrossRef] [PubMed]
15. Liu, W.; Wang, X. Prediction of functional microRNA targets by integrative modeling of microRNA binding and target expression data. *Genome Biol.* **2019**, *22*, 18. [CrossRef]
16. Miranda, K.C.; Huynh, T.; Tay, Y.; Ang, Y.; Tam, W.; Thomson, A.M.; Lim, B.; Rigoutsos, I. A pattern-based method for the identification of MicroRNA binding sites and their corresponding heteroduplexes. *Cell* **2006**, *126*, 1203–1217. [CrossRef] [PubMed]
17. McGeary, S.E.; Lin, K.S.; Shi, C.Y.; Pham, T.M.; Bisaria, N.; Kelley, G.M.; Bartel, D.P. The biochemical basis of microRNA targeting efficacy. *Science* **2019**, *20*, 1741. [CrossRef] [PubMed]
18. Agarwal, V.; Bell, G.W.; Nam, J.; Bartel, D.P. Predicting effective microRNA target sites in mammalian mRNAs. *eLife* **2015**, *4*, 05005. [CrossRef]
19. García, D.M.; Baek, D.; Shin, C.; Bell, G.W.; Grimson, A.; Bartel, D.P. Weak Seed-Pairing Stability and High Target-Site Abundance Decrease the Proficiency of lsy-6 and Other miRNAs. *Nat. Struct. Mol. Biol.* **2011**, *8*, 1139–1146. [CrossRef]
20. Friedman, R.C.; Farh, K.K.; Burge, C.B.; Bartel, D.P. Most Mammalian mRNAs Are Conserved Targets of MicroRNAs. *Genome Res.* **2009**, *19*, 92–105. [CrossRef] [PubMed]
21. Grimson, A.; Farh, K.K.; Johnsto, W.K.; Garrett-Engele, P.; Lim, L.P.; Bartel, D.P. MicroRNA Targeting Specificity in Mammals: Determinants beyond Seed Pairing. *Mol. Cell* **2007**, *27*, 91–105. [CrossRef] [PubMed]
22. Lewis, B.P.; Burge, C.B.; Bartel, D.P. Conserved Seed Pairing, Often Flanked by Adenosines, Indicates that Thousands of Human Genes are MicroRNA Targets. *Cell* **2005**, *120*, 15–20. [CrossRef] [PubMed]
23. Chang, L.; Zhou, G.; Soufan, O.; Xia, J. miRNet 2.0—Network-based visual analytics for miRNA functional analysis and systems biology. *Nucl. Acids Res.* **2020**, *48*, W244–W251. [CrossRef]
24. Muralimanoharan, S.; Kwak, Y.T.; Mendelson, C.R. Redox-Sensitive Transcription Factor NRF2 Enhances Trophoblast Differentiation via Induction of miR-1246 and Aromatase. *Endocrinology* **2018**, *159*, 2022–2033. [CrossRef]
25. de Los Santos-Jiménez, J.; Campos-Sandoval, J.A.; Márquez-Torres, C.; Urbano-Polo, N.; Brøndegaard, D.; Martín-Rufián, M.; Lobo, C.; Peñalver, A.; Gómez-García, M.C.; Martín-Campos, J.; et al. Glutaminase isoforms expression switches microRNA levels and oxidative status in glioblastoma cells. *J. Biomed. Sci.* **2021**, *28*, 14. [CrossRef]
26. Ma, H.Y.; Cu, W.; Sun, Y.H.; Chen, X. MiRNA-203a-3p inhibits inflammatory response in preeclampsia through regulating IL24. *Eur. Rev. Med. Pharmacol. Sci.* **2020**, *24*, 5223–5230.
27. Chen, Z.; Zhang, W.; Wu, M.; Huang, H.; Zou, L.; Luo, Q. Pathogenic mechanisms of preeclampsia with severe features implied by the plasma exosomal mirna profile. *Bioengineered* **2021**, *12*, 9140–9149. [CrossRef]

28. Menon, R.; Debnath, C.; Lai, A.; Guanzon, D.; Bhatnagar, S.; Kshetrapal, P.K.; Sheller-Miller, S.; Salomon, C. ù Circulating Exosomal miRNA Profile During Term and Preterm Birth Pregnancies: A Longitudinal Study. *Endocrinology* **2019**, *160*, 249–275. [CrossRef]
29. Gu, Y.; Sun, J.; Groome, L.J.; Wang, Y. Differential miRNA expression profiles between the first and third trimester human placentas. *Am. J. Physiol. Endocrinol. Metab.* **2013**, *304*, E836–E843. [CrossRef] [PubMed]
30. Tian, Q.X.; Xia, S.H.; Wu, Y.H.; Zhang, J.H.; Wang, L.Y.; Zhu, W.P. Comprehensive analysis of the differential expression profile of microRNAs in missed abortion. *Kaohsiung J. Med. Sci.* **2020**, *36*, 114–121. [CrossRef]
31. Chen, P.; Li, T.; Guo, Y.; Jia, L.; Wang, Y.; Fang, C. Construction of Circulating MicroRNAs-Based Non-invasive Prediction Models of Recurrent Implantation Failure by Network Analysis. *Front. Genet.* **2021**, *12*, 712150. [CrossRef] [PubMed]
32. Kasiappan, R.; Rajarajan, D. Role of MicroRNA Regulation in Obesity-Associated Breast Cancer: Nutritional Perspectives. *Adv. Nutr.* **2017**, *8*, 868–888. [CrossRef] [PubMed]
33. Liu, B.; Li, R.; Zhang, J.; Meng, C.; Zhang, J.; Song, X.; Lv, C. MicroRNA-708-3p as a potential therapeutic target via the ADAM17-GATA/STAT3 axis in idiopathic pulmonary fibrosis. *Exp. Mol. Med.* **2018**, *50*, e465. [CrossRef] [PubMed]
34. Hayakawa, K.; Kawasaki, M.; Hirai, T.; Yoshida, Y.; Tsushima, H.; Fujishiro, M.; Ikeda, K.; Morimoto, S.; Takamori, K.; Sekigawa, I. MicroRNA-766-3p Contributes to Anti-Inflammatory Responses through the Indirect Inhibition of NF-κB Signaling. *Int. J. Mol. Sci.* **2019**, *20*, 809. [CrossRef] [PubMed]
35. Li, L.; Cheng, Y.; Lin, L.; Liu, Z.; Du, S.; Ma, L.; Li, J.; Peng, Z.; Yan, J. Global Analysis of miRNA Signature Differentially Expressed in Insulin-resistant Human Hepatocellular Carcinoma Cell Line. *Int. J. Med. Sci.* **2020**, *17*, 664–677. [CrossRef]
36. Yu, F.Y.; Tu, Y.; Deng, Y.; Guo, C.; Ning, J.; Zhu, Y.; Lv, X.; Ye, H. MiR-4500 is epigenetically downregulated in colorectal cancer and functions as a novel tumor suppressor by regulating HMGA2. *Cancer Biol. Ther.* **2016**, *17*, 1149–1157. [CrossRef]
37. Li, S.; Mai, H.; Zhu, Y.; Li, G.; Sun, J.; Li, G.; Liang, B.; Chen, S. MicroRNA-4500 Inhibits Migration, Invasion, and Angiogenesis of Breast Cancer Cells via RRM2-Dependent MAPK Signaling Pathway. *Mol. Ther. Nucleic Acids* **2020**, *21*, 278–289. [CrossRef]
38. Huang, R.; Yu, T.; Li, Y.; Hu, J. Upregulated has-miR-4516 as a potential biomarker for early diagnosis of dust-induced pulmonary fibrosis in patients with pneumoconiosis. *Toxicol. Res.* **2018**, *7*, 415–422. [CrossRef]
39. Chowdhari, S.; Saini, N. hsa-miR-4516 mediated downregulation of STAT3/CDK6/UBE2N plays a role in PUVA induced apoptosis in keratinocytes. *J. Cell Physiol.* **2014**, *229*, 1630–1638. [CrossRef]
40. Chowdhari, S.; Sardana, K.; Saini, N. miR-4516, a microRNA downregulated in psoriasis inhibits keratinocyte motility by targeting fibronectin/integrin α9 signaling. *Biochim. Biophys. Acta Mol. Basis Dis.* **2017**, *1863*, 3142–3152. [CrossRef]
41. Umair, Z.; Baek, M.O.; Song, J.; An, S.; Chon, S.J.; Yoon, M.S. MicroRNA-4516 in Urinary Exosomes as a Biomarker of Premature Ovarian Insufficiency. *Cells* **2022**, *11*, 2797. [CrossRef] [PubMed]
42. Yang, H.; Ma, Q.; Wang, Y.; Tang, Z. Clinical application of exosomes and circulating microRNAs in the diagnosis of pregnancy complications and foetal abnormalities. *J. Transl. Med.* **2020**, *18*, 32. [CrossRef] [PubMed]
43. Chen, X.; Zhang, L.; Tang, S. MicroRNA-4497 functions as a tumor suppressor in laryngeal squamous cell carcinoma via negatively modulation the GBX2. *Auris Nasus Larynx* **2019**, *46*, 106–113. [CrossRef] [PubMed]
44. Mirza, A.H.; Kaur, S.; Nielsen, L.B.; Størling, J.; Yarani, R.; Roursgaard, M.; Mathiesen, E.R.; Damm, P.; Svare, J.; Mortensen, H.B.; et al. Breast Milk-Derived Extracellular Vesicles Enriched in Exosomes from Mothers with Type 1 Diabetes Contain Aberrant Levels of microRNAs. *Front. Immunol.* **2019**, *10*, 2543. [CrossRef]
45. Wen, H.; Chen, L.; He, J.; Lin, J. MicroRNA expression profiles and networks in placentas complicated with selective intrauterine growth restriction. *Mol. Med. Rep.* **2017**, *16*, 6650–6673. [CrossRef]
46. Gathiram, P.; Moodley, J. Pre-eclampsia: Its pathogenesis and pathophysiolgy. *Cardiovasc. J. Afr.* **2016**, *27*, 71–78. [CrossRef]
47. Lin, Z.; Chen, Y.; Lin, Y.; Lin, H.; Li, H.; Su, X.; Fang, Z.; Wang, J.; Wei, Q.; Teng, J.; et al. Potential miRNA biomarkers for the diagnosis and prognosis of esophageal cancer detected by a novel absolute quantitative RT-qPCR method. *Sci. Rep.* **2020**, *10*, 20065. [CrossRef]
48. Buhagiar, A.; Seria, E.; Borg, M.; Borg, J.; Ayers, D. Overview of microRNAs as liquid biopsy biomarkers for colorectal cancer sub-type profiling and chemoresistance. *Cancer Drug Resist* **2021**, *4*, 934–945. [CrossRef]
49. Ragozzino, E.; Brancaccio, M.; Di Costanzo, A.; Scalabrì, F.; Andolfi, G.; Wanderlingh, L.G.; Patriarca, E.J.; Minchiotti, G.; Altamura, S.; Summa, V.; et al. 6-Bromoindirubin-3′-oxime intercepts GSK3 signaling to promote and enhance skeletal muscle differentiation affecting miR-206 expression in mice. *Sci. Rep.* **2019**, *9*, 18091. [CrossRef]
50. Tribolet, L.; Kerr, E.; Cowled, C.; Bean, A.G.D.; Stewart, C.R.; Dearnley, M.; Farr, R.J. MicroRNA Biomarkers for Infectious Diseases: From Basic Research to Biosensing. *Front. Microbiol.* **2020**, *11*, 1197. [CrossRef] [PubMed]
51. Brancaccio, M.; Natale, F.; Falco, G.; Angrisano, T. Cell-Free DNA Methylation: The New Frontiers of Pancreatic Cancer Biomarkers' Discovery. *Genes* **2019**, *11*, 14. [CrossRef]
52. Brancaccio, M.; Mennitti, C.; Calvanese, M.; Gentile, A.; Musto, R.; Gaudiello, G.; Scamardella, G.; Terracciano, D.; Frisso, G.; Pero, R.; et al. Diagnostic and Therapeutic Potential for HNP-1, HBD-1 and HBD-4 in Pregnant Women with COVID-19. *Int. J. Mol. Sci.* **2022**, *23*, 3450. [CrossRef]
53. Pero, R.; Brancaccio, M.; Mennitti, C.; Gentile, L.; Franco, A.; Laneri, S.; De Biasi, M.G.; Pagliuca, C.; Colicchio, R.; Salvatore, P.; et al. HNP-1 and HBD-1 as Biomarkers for the Immune Systems of Elite Basketball Athletes. *Antibiotics* **2020**, *9*, 306. [CrossRef] [PubMed]

54. Lake, J.; Storm, C.S.; Makarious, M.B.; Bandres-Ciga, S. Genetic and Transcriptomic Biomarkers in Neurodegenerative Diseases: Current Situation and the Road Ahead. *Cells* **2021**, *10*, 1030. [CrossRef] [PubMed]
55. Zhao, E.; Xie, H.; Zhang, Y. Predicting Diagnostic Gene Biomarkers Associated with Immune Infiltration in Patients with Acute Myocardial Infarction. *Front. Cardiovasc. Med.* **2020**, *7*, 586871. [CrossRef]
56. Ruggieri, V.; Russi, S.; Zoppoli, P.; La Rocca, F.; Angrisano, T.; Falco, G.; Calice, G.; Laurino, S. The Role of MicroRNAs in the Regulation of Gastric Cancer Stem Cells: A Meta-Analysis of the Current Status. *J. Clin. Med.* **2019**, *8*, 639. [CrossRef]
57. Chang, G.; Mouillet, J.F.; Mishima, T.; Chu, T.; Sadovsky, E.; Coyne, C.B.; Parks, W.T.; Surti, U.; Sadovsky, Y. Expression and trafficking of placental microRNAs at the feto-maternal interface. *FASEB J.* **2017**, *31*, 2760–2770. [CrossRef]
58. Xu, P.; Ma, Y.; Wu, H.; Wang, Y.L. Placenta-Derived MicroRNAs in the Pathophysiology of Human Pregnancy. *Front. Cell Dev. Biol.* **2021**, *9*, 646326. [CrossRef] [PubMed]
59. Liao, S.; Vickers, M.H.; Taylor, R.S.; Jones, B.; Fraser, M.; McCowan, L.M.E.; Baker, P.N.; Perry, J.K. Maternal serum IGF-1, IGFBP-1 and 3, and placental growth hormone at 20weeks' gestation in pregnancies complicated by preeclampsia. *Pregnancy Hypertens* **2017**, *10*, 149–154. [CrossRef] [PubMed]
60. Ingec, M.; Gursoy, H.G.; Yildiz, L.; Kumtepe, Y.; Kadanali, S. Serum levels of insulin, IGF-1, and IGFBP-1 in pre-eclampsia and eclampsia. *Int. J. Gynaecol. Obstet.* **2004**, *84*, 214–219. [CrossRef]
61. Vatten, L.J.; Nilsen, T.I.; Juul, A.; Jeansson, S.; Jenum, P.A.; Eskild, A. Changes in circulating level of IGF-I and IGF-binding protein-1 from the first to second trimester as predictors of preeclampsia. *Eur. J. Endocrinol.* **2008**, *158*, 101–105. [CrossRef] [PubMed]
62. Halhali, A.; Tovar, A.R.; Torres, N.; Bourges, H.; Garabedian, M.; Larrea, F. Preeclampsia is associated with low circulating levels of insulin-like growth factor I and 1,25-dihydroxyvitamin D in maternal and umbilical cord compartments. *J. Clin. Endocrinol. Metab.* **2000**, *85*, 1828–1833. [PubMed]
63. Wang, Y.; Cheng, K.; Zhou, W.; Liu, H.; Yang, T.; Hou, P.; Li, X. miR-141-5p regulate ATF2 via effecting MAPK1/ERK2 signaling to promote preeclampsia. *Biomed. Pharmacother.* **2019**, *115*, 108953. [CrossRef] [PubMed]
64. Marwa, B.A.; Raguema, N.; Zitouni, H.; Feten, H.B.; Olfa, K.; Elfeleh, R.; Almawi, W.; Mahjoub, T. FGF1 and FGF2 mutations in preeclampsia and related features. *Placenta* **2016**, *43*, 81–85. [CrossRef] [PubMed]
65. Tian, F.Y.; Wang, X.M.; Xie, C.; Zhao, B.; Niu, Z.; Fan, L.; Hivert, M.F.; Chen, W.Q. Placental surface area mediates the association between FGFR2 methylation in placenta and full-term low birth weight in girls. *Clin. Epigenet.* **2018**, *22*, 39. [CrossRef] [PubMed]
66. Andersen, J.R.; Weber, T. Correlations between PRL and chloride, sodium, potassium and calcium in amniotic fluid. *Acta Obstet. Gynecol. Scand.* **1985**, *64*, 227–229. [CrossRef]
67. Lyall, F.; Simpson, H.; Bulmer, J.N.; Barber, A.; Robson, S.C. Transforming growth factor-β expression in human placenta and placental bed in third trimester normal pregnancy, preeclampsia, and fetal growth restriction. *Am. J. Pathol.* **2001**, *159*, 1827–1838. [CrossRef]
68. Maynard, S.E.; Karumanchi, S.A. Angiogenic factors and preeclampsia. *Semin. Nephrol.* **2011**, *31*, 33–46. [CrossRef]
69. Cirkovic, A.; Stanisavljevic, D.; Milin-Lazovic, J.; Rajovic, N.; Pavlovic, V.; Milicevic, O.; Savic, M.; Kostic Peric, J.; Aleksic, N.; Milic, N.; et al. Preeclamptic Women Have Disrupted Placental microRNA Expression at the Time of Preeclampsia Diagnosis: Meta-Analysis. *Front. Bioeng. Biotechnol.* **2021**, *9*, 782845. [CrossRef]